The Braincase Anatomy of the Late Cretaceous Dinosaur *Alioramus* (Theropoda: Tyrannosauroidea)

Author(s): Gabe S. Bever , Stephen L. Brusatte , Thomas D. Carr , Xing Xu , Amy M. Balanoff , Mark A. Norell

Source: Bulletin of the American Museum of Natural History, 376(1):1-72. 2013.
Published By: American Museum of Natural History
DOI: http://dx.doi.org/10.1206/810.1
URL: http://www.bioone.org/doi/full/10.1206/810.1

THE BRAINCASE ANATOMY OF THE LATE CRETACEOUS DINOSAUR *ALIORAMUS* (THEROPODA: TYRANNOSAUROIDEA)

GABE S. BEVER
Department of Anatomy, New York Institute of Technology, College of Osteopathic Medicine, Old Westbury, NY
Division of Paleontology, American Museum of Natural History, New York, NY

STEPHEN L. BRUSATTE
Division of Paleontology, American Museum of Natural History, New York, NY
Department of Earth and Environmental Sciences, Columbia University, New York, NY

THOMAS D. CARR
Department of Biology, Carthage College, Kenosha, WI

XING XU
Institute of Vertebrate Paleontology and Paleoanthropology, Beijing, China

AMY M. BALANOFF
Division of Paleontology
American Museum of Natural History, New York, NY

MARK A. NORELL
Division of Paleontology, American Museum of Natural History, New York, NY

Department of Earth and Environmental Sciences, Columbia University, New York, NY

BULLETIN OF THE AMERICAN MUSEUM OF NATURAL HISTORY
Number 376, 72 pp., 36 figures
Issued March 15, 2013

 ISSN 0003-0090

ABSTRACT

The late Cretaceous tyrannosaurid *Alioramus altai* is known from a single specimen whose articulated braincase exhibits a nearly unique combination of preservational quality, subadult stage of growth, and morphological complexity. We use a detailed physical preparation combined with high-resolution computed tomography to provide an expanded description of this braincase that includes details of the neurocranium and its dermal roof, pneumatic recesses and sinuses, cranial endocast, and inner ear cavities. A few notable features include a highly developed rostral tympanic recess marked by three pneumatic fenestrae, a highly pneumatic paroccipital process with both rostral and caudal pneumatic foramina, a prootic fossa housing external foramina for the trigeminal and facial nerves, a well-developed superficial lamina of the prootic, an expanded vestibular cavity, and an osseous labyrinth that is plesiomorphic in appearance. These observations, set within the currently available comparative context, elucidate numerous neuroanatomical transformations within Tyrannosauroidea and clarify where more data and work are needed. We expand the discussion for the 21 characters from the neurocranium utilized in a recent revision of tyrannosauroid phylogeny, including a listing of which tyrannosauroid taxa can be scored for the primitive and derived states of each character.

INTRODUCTION

The large-bodied theropod dinosaur *Alioramus* has long been a mysterious taxon, as it was established based on a single, incomplete, and generally poorly preserved specimen from the Late Cretaceous of Mongolia (the holotype of *A. remotus*: Kurzanov, 1976). Recently, the discovery of a second specimen, a remarkably preserved skeleton collected by the 2001 joint American Museum–Mongolian Academy of Science expedition to the Gobi Desert and established as the holotype of a new species (*A. altai*), has helped clarify the anatomy and phylogenetic position of *Alioramus* (IGM 100/1844; Brusatte et al., 2009). Phylogenetic assessment of the well-preserved, but not yet fully grown, skeleton indicates that *Alioramus* is nested within the derived Tyrannosauridae, the familiar theropod group containing *Tyrannosaurus* and its closest relatives, but outside the subclade defined by the colossal forms *Daspletosaurus torosus*, *Tarbosaurus bataar*, and *T. rex* (Brusatte et al., 2009, 2010a, 2010c, 2012; fig. 1). The preservational quality of IGM 100/1844, combined with its relatively young ontogenetic age and hypothesized phylogenetic position, emphasizes the potential of this specimen for informing patterns of growth, development, and evolution within Tyrannosauroidea, a broader group that includes the derived tyrannosaurids and their closest smaller-bodied relatives and is now known to have had a complex evolutionary history lasting over 100 million years (see Brusatte et al., 2010a).

The holotype of *Alioramus altai* recently formed the centerpiece of a major revision of tyrannosauroid anatomy (Brusatte et al., 2012), which in turn revealed a wealth of new character data that was central to an inclusive new analysis of tyrannosauroid phylogeny (Brusatte et al., 2010a). As part of this monographic effort, nearly all elements constituting IGM 100/1844 were individually described and figured. The only major skeletal component excluded as a point of focus in this work was the braincase. The braincase of IGM 100/1844 (figs. 2–7) is nearly complete and was briefly described and figured in Brusatte et al. (2009), including a digital reconstruction of its endocranial cavity. A cast of all major endocranial spaces was figured in Brusatte et al. (2010a) but without an accompanying description. More recently, a short but detailed description was published that focused solely on endocranial features bearing directly on phylogenetic transformations within Tyrannosauroidea or that inform the early evolutionary history of avian neuroanatomy (Bever et al., 2011). Our purpose here is to narrow the descriptive gap currently separating the braincase of IGM 100/1844 from what is available for the remainder of its preserved skeleton. This effort will make IGM 100/1844 one of the most thoroughly described specimens within a group whose neuroanatomy is becoming increasingly well understood (e.g., Brochu,

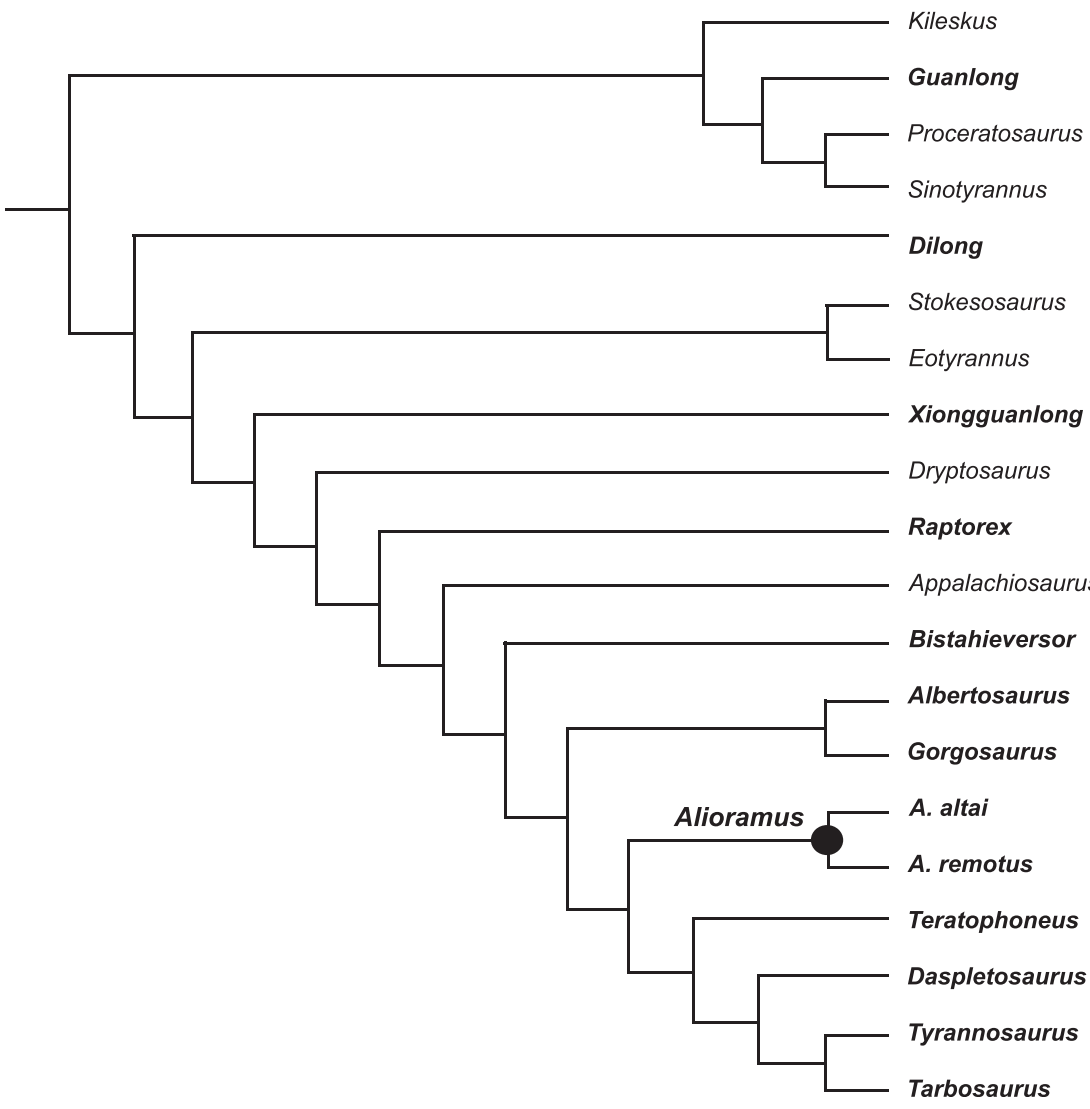

Fig. 1. The relationships of *Alioramus altai* within Tyrannosauroidea based on the phylogenetic analyses of Brusatte et al. (2010a, 2012). The majority of comparative observations in this study are restricted to those taxa represented in bold type.

2000, 2003; Witmer and Ridgely, 2009, 2010; Bever et al., 2011; Tsuihiji et al., 2011) and whose contribution to our understanding of dinosaur biology is rapidly increasing (Brusatte et al., 2010a).

In addition, we take this opportunity to discuss in greater detail the braincase characters determined by Brusatte et al. (2010a) to be phylogenetically informative within Tyrannosauroidea. This includes detailing what tyrannosauroid taxa can currently be scored for the derived and primitive states of each character, which will hopefully facilitate future efforts to expand the influence that braincase anatomy has on our understanding of tyrannosauroid relationships.

MATERIALS AND METHODS

The holotype of *Alioramus altai* (IGM 100/1844) was collected at Tsaagan Khushuu, Nemegt Formation (Maastrichtian), Mongolia.

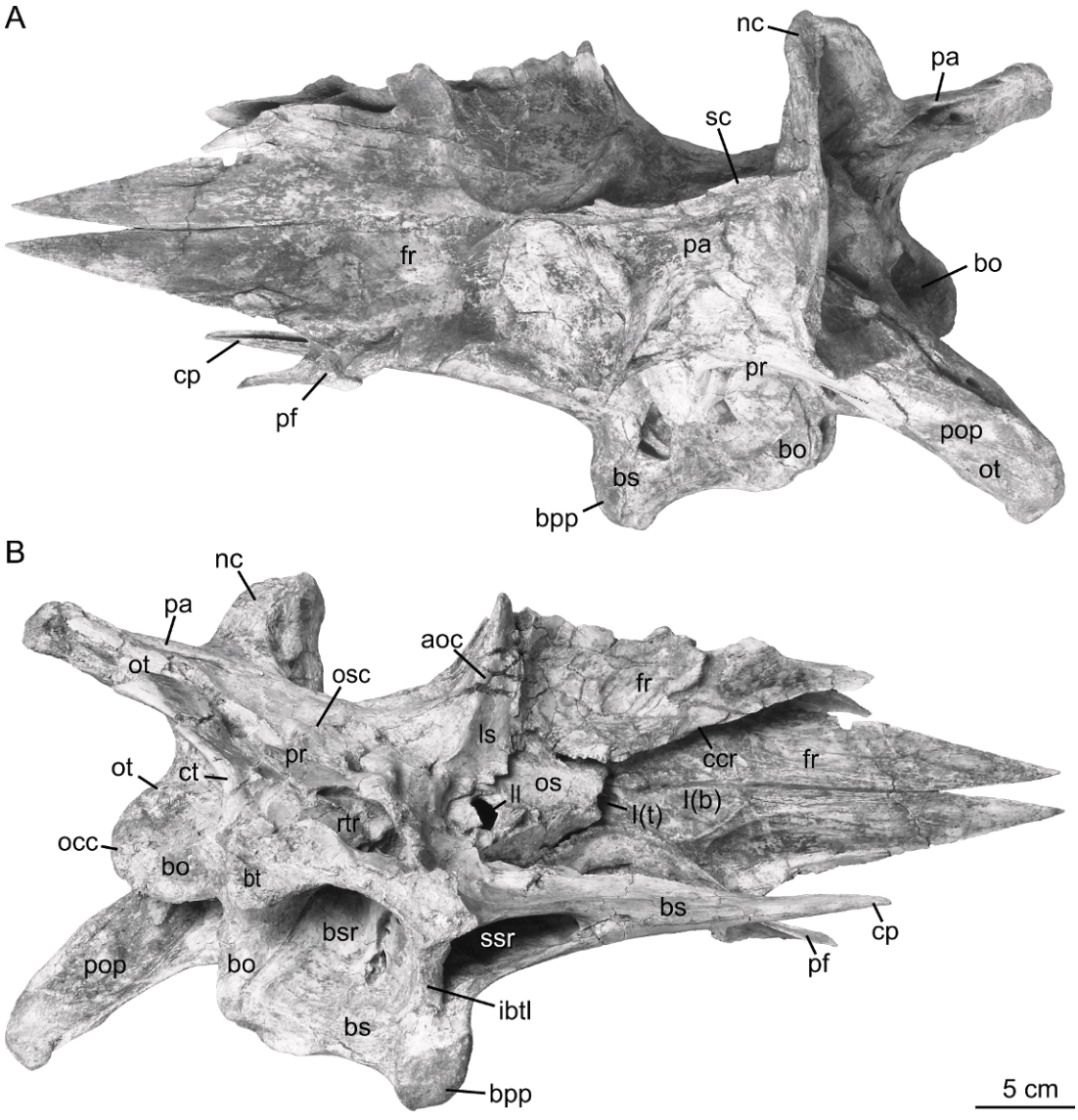

Fig. 2. Dorsal (**A**) and ventral (**B**) views of the articulated braincase of *Alioramus altai* (IGM 100/1844). See appendix 1 for anatomical abbreviations.

It is estimated to represent a nine-year-old late juvenile/subadult based on the number of lines of arrested growth (Brusatte et al., 2009). Amy Davidson (AMNH) physically prepared the specimen using airscribes, needles, and wooden tools. The specimen was consolidated with Butvar® B-76 (Monsanto Company), a terpolymer of vinyl butyral, vinyl alcohol, and vinyl acetate monomers. Joins were made with Paraloid® B-72 (Rohm and Haas Company), an ethyl methacrylate and methyl acrylate copolymer. Complete preparation records are held in the Division of Paleontology database.

The braincase was scanned at the University of Texas High-Resolution X-ray Computed Tomography Facility, Austin. Scanning occurred along the sagittal axis using a

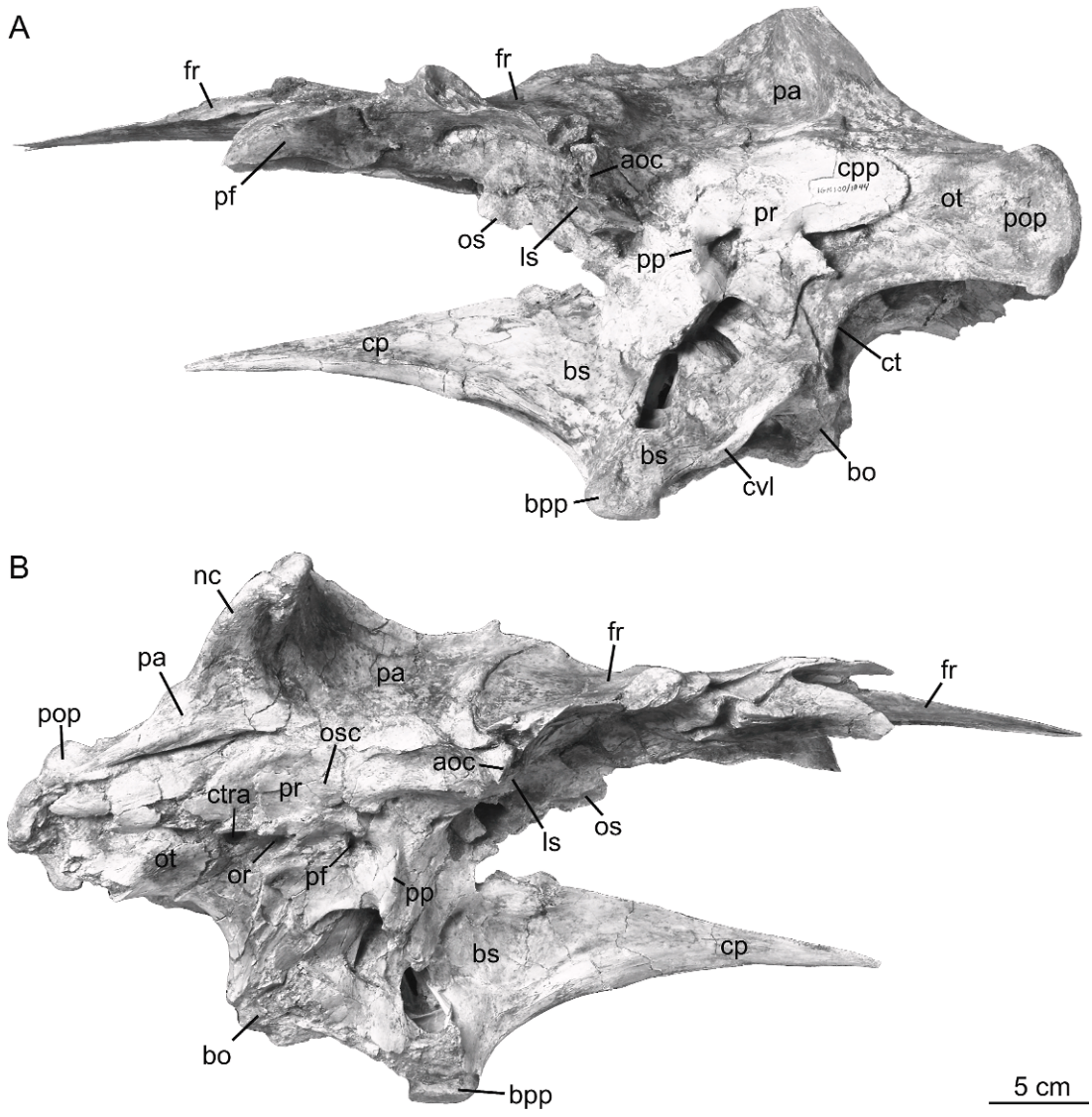

Fig. 3. Left lateral (**A**) and right lateral (**B**) views of the articulated braincase of *Alioramus altai* (IGM 100/1844). See appendix 1 for anatomical abbreviations.

voltage of 450 kV and amperage of 3 mA. A total of 431 slices were recovered at an image resolution of 1,024 × 1,024 pixels. The slice thickness and interslice spacing are both 0.25 mm with a reconstructed field of view of 301.6 mm. Reslicing of the data along the horizontal and coronal axes and all digital segmentation was performed using VG StudioMax 1.2.1. Individual segmentations of the endocranial cavity, cranial nerve canals, canals housing the neurocranial vasculature, and the pneumatic cavities investing the braincase were performed using the volumetric rendering program VG StudioMax 2.0.1. This software was also employed to construct a variety of 3D movies viewable at the Digital Morphology website (www.digimorph.org/specimens/Alioramus_altai). Any uncited comparative observations are based on our examination of the following specimens (see

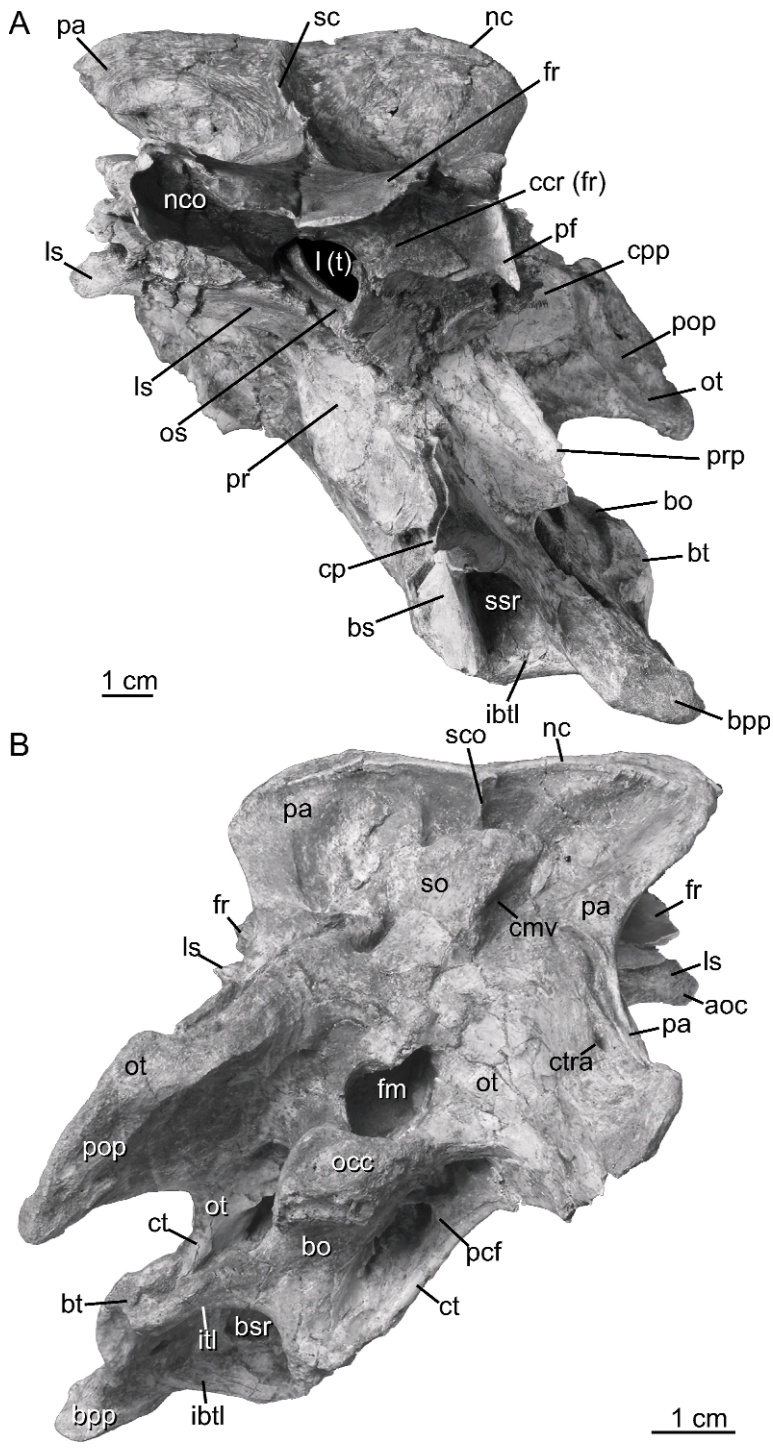

Fig. 4. Rostral (**A**) and caudal (**B**) views of the articulated braincase of *Alioramus altai* (IGM 100/1844). See appendix 1 for anatomical abbreviations.

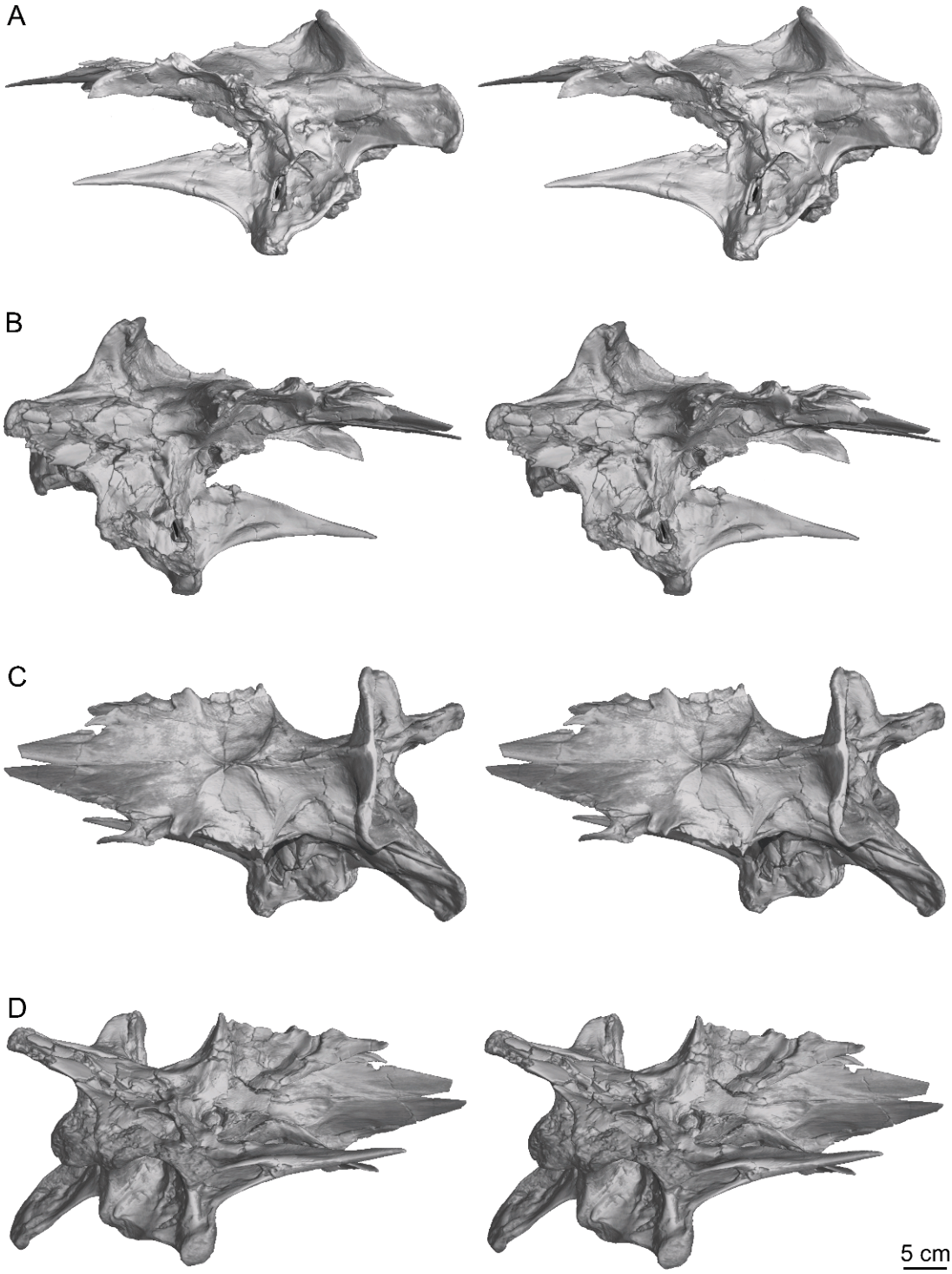

Fig. 5. Stereopairs of the articulated braincase of *Alioramus altai* (IGM 100/1844) in left lateral (**A**), right lateral (**B**), dorsal (**C**), and ventral (**D**) views. Images are reconstructed from CT data.

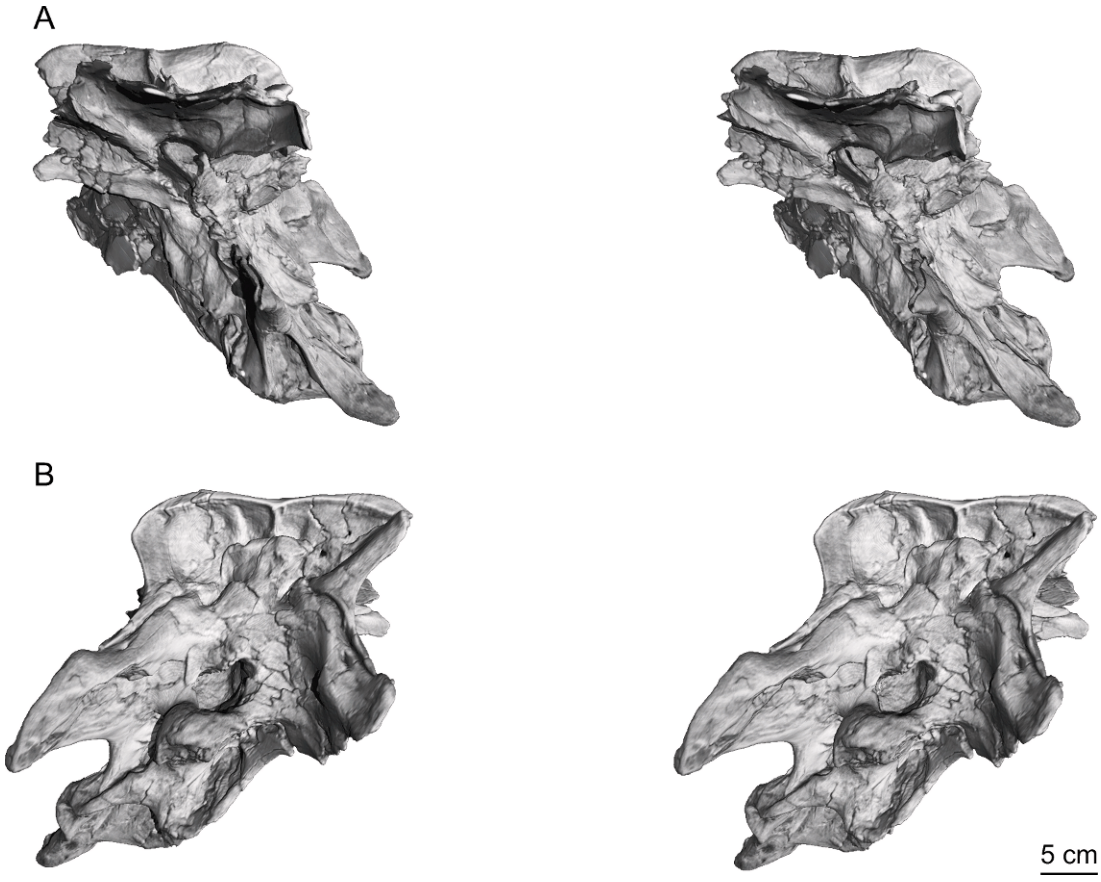

Fig. 6. Stereopairs of the articulated braincase of *Alioramus altai* (IGM 100/1844) in rostral (**A**) and caudal (**B**) views. Images are reconstructed from CT data.

appendix 1 for Institutional Abbreviations): *Albertosaurus* (CMN 5600; TMP 1981.010.0001), *Alioramus* (PIN 3141/1), *Bistahieversor* (NMMNH P-25049), *Daspletosaurus* (CMN 8506; FMNH PR308; TMP 1985.062.0001, 1994.143.0001, 2001.036.0001), *Dilong* (IVPP V14243), *Gorgosaurus* (AMNH FARB 5336, 5664; ROM 1247, 1422; TMP 1986.144.0001), *Guanlong* (IVPP V14531), *Raptorex* (LH PV18, a young specimen described as a distinct taxon by Sereno et al. [2009], but that may be a juvenile of a previously known taxon [Fowler et al., 2011]), *Tarbosaurus* (ZPAL MgD-I/3, MgD-I/4, MgD-I/38, MgD-107/7), *Teratophoneus* (BYU 8120/9396), and *Tyrannosaurus* (AMNH FARB 5027, 5029, 5117; CMNH 7541; DDM 35; FMNH PR2081; RSM 2523.8).

DESCRIPTION

General Comments

The braincase of IGM 100/1844 is well preserved and complete, with nearly all expected neurocranial and dermatocranial elements present and in articulation (figs. 2–7). The only exception is the ethmoid complex (mes- and sphenethmoids), which is missing in IGM 100/1844 but present as an ossified structure in *T. rex* (FMNH PR2081; Brochu, 2002). A scar on the ventral surface of the frontal marks the point of contact with the ethmoid ring and establishes that at least a cartilaginous complex was present. The neurocranium exhibits some clockwise distortion along the long axis of the skull (figs. 2, 4). This is largely independent of

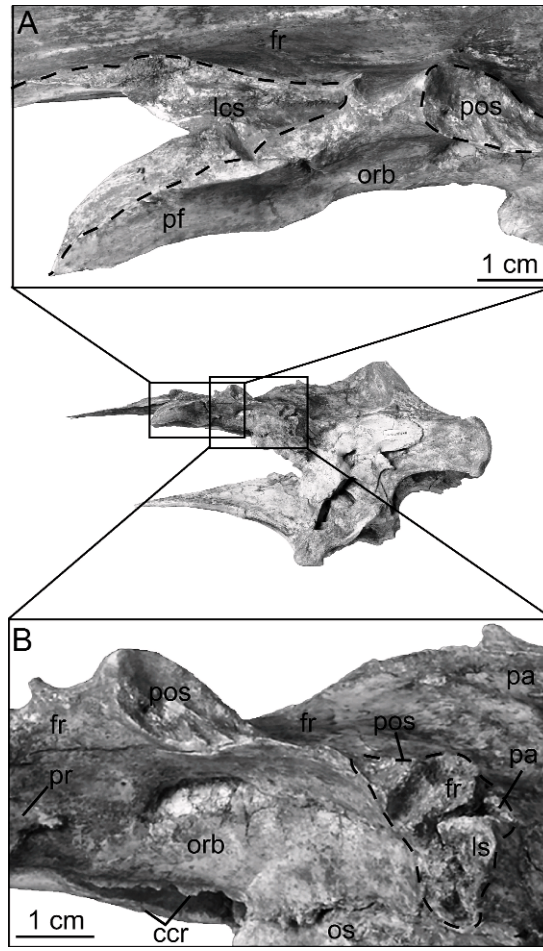

Fig. 7. The dorsal rim of the left orbit in *Alioramus altai* (IGM 100/1844) in dorsolateral (**A**) and left lateral (**B**) views. See appendix 1 for anatomical abbreviations.

the overlying dermal roof, presumably because these two cranial partitions had yet to tightly suture. Additionally, most individual braincase bones remain unfused (or only loosely fused with each other) with clearly visible and thus traceable margins. The distortion complicates the interpretation of internal structures on the left side of the braincase. External structures are better preserved on the left side, whereas the right side was eroded in the field. The resulting damage is most notable ventrally, where the right basipterygoid process and much of the osseous web linking that process with the basal tuber is missing.

Dermal Roof

Frontal: The left and right frontals are unfused along their entire length. Together, they are much longer rostrocaudally (140 mm, measured between the caudalmost point of the frontoparietal suture and the rostralmost point of the frontal bone) than wide mediolaterally (95 mm at the widest point). Much of their rostral length was covered by the nasal in life, such that the exposed frontal was approximately 80 mm long. The width-to-length ratio (1.2) is slightly less than that of other, more mature, tyrannosaurid specimens (e.g., 1.1, *T. rex*; RSM 2523.8; e.g.,

Brochu, 2003; Currie, 2003; Hurum and Sabath, 2003), but it is slightly larger than that of a juvenile specimen of *Tarbosaurus* (0.77; taken from Tsuihiji et al., 2011: fig. 5). These observations are consistent with the hypothesis that tyrannosaurid frontals widen with postnatal growth (Carr, 1999; Currie, 2003; Carr and Williamson, 2004)—an ontogenetic trajectory present in many, if not most, amniote clades, at least for the postorbial region of the frontal (e.g., Abdala et al., 2001; Bever, 2008; Bhullar, 2012). Basal tyrannosauroids, such as *Dilong paradoxus* (Xu et al., 2004), also have long frontals, suggesting that widening of the rostral cranial vault may be both an ontogenetic and phylogenetic trend within Tyrannosauroidea.

The frontal narrows in width rostrally before separating into two triangular prongs for articulation with the nasals. These prongs are remarkably thin (less than 1 mm in dorsoventral thickness) and their dorsal surfaces are covered with a series of fine lineations trending rostrocaudally, which mark the nasal overlap of the frontal. The rostral end of each nasal prong is broken, obscuring further details of the frontonasal suture, whose shape is often employed as a systematic character to differentiate tyrannosaurids (Russell, 1970; Brochu, 2003; Carr and Williamson, 2010). As in other tyrannosaurids, two prongs extend from the frontal to join the nasal; in contrast, multiple short prongs are seen in the large tyrannosauroid *Bistahieversor sealeyi*. The dorsal surface of the frontal is smooth and slightly concave between the nasal prongs, whereas it is flat between the lacrimal and postorbital articulations. A concave surface between the nasal prongs is also seen in *Raptorex kriegsteini* and adult *T. rex*; in contrast, the surface is flat in juvenile *T. rex* (CMNH 7541, DDM 35) and in subadult *Gorgosaurus libratus* (ROM 1247).

An ovoid facet in the dorsolateral surface of the frontal, immediately rostral to the orbital rim, accepts a deep peg from the caudal ramus of the lacrimal (figs. 7A, 8A). This surface faces rostrolaterally and is continuous rostroventrally with a shallow fossa on the lateral surface of the prefrontal. A raised rim delineates the frontal and prefrontal contributions to this surface. On the prefrontal, the frontal socket is deepest caudally, where it faces entirely rostrally, and it is concealed in lateral view by the orbital rim. More rostrally, the socket is exposed laterally, deeper dorsoventrally, and less inset into the frontal medially. At its rostral extent the articular surface abruptly thins dorsoventrally and fades into the thin lateral surface of the nasal prong. The prefrontal forms most of the lacrimal articulation in this region.

The frontal articulation with the postorbital is a long (47 mm), rostrodorsally trending surface, which is well preserved on the left side and comprised of three general regions (fig. 7B). Rostrally, an ovoid, cuplike surface (the "postorbital buttress") faces laterally and slightly ventrally and is scoured by a series of sharp ridges that secured the articulation. Caudal to the buttress, the frontal thins, forming a platelike shelf that fits into a deep groove in the postorbital. A smooth, 7 mm wide margin on the dorsal surface of the frontal indicates the postorbital overlapped the frontal as is seen in other tyrannosaurids (Currie, 2003). A newly discovered nontyrannosaurid tyrannosauroid from the Early Cretaceous of Liaoning reveals that some derived features in this region, including postorbital overlap of the frontal and postorbital-lacrimal contact, have a wider distribution (Xu et al., 2012). Caudal to the shelf is a rugose, capitate process that joins with the capitate process of the laterosphenoid and a thin peg from the parietal to fit into a smooth, concave socket on the medial surface of the postorbital.

Regional differentiation of the postorbital suture also is present in *Albertosaurus sarcophogus* (Currie, 2003), *Alioramus remotus* (PIN 3141/1), *Bistahieversor* (NMMNH P-25049), *Daspletosaurus* (CMN 8506), *Gorgosaurus* (ROM 1247), *Teratophoneus currei* (BYU 8120/9396). *Tarbosaurus* (Hurum and Sabath, 2003: fig. 17) and *Tyrannosaurus* (AMNH FARB 5117; Osborn, 1912: fig. 7) have the same morphology as juveniles and subadults, but as adults they exhibit a modified condition that superficially resembles a single, deep, rectangular surface. Therefore, unless this postnatal transformation is a derived feature of an exclusive

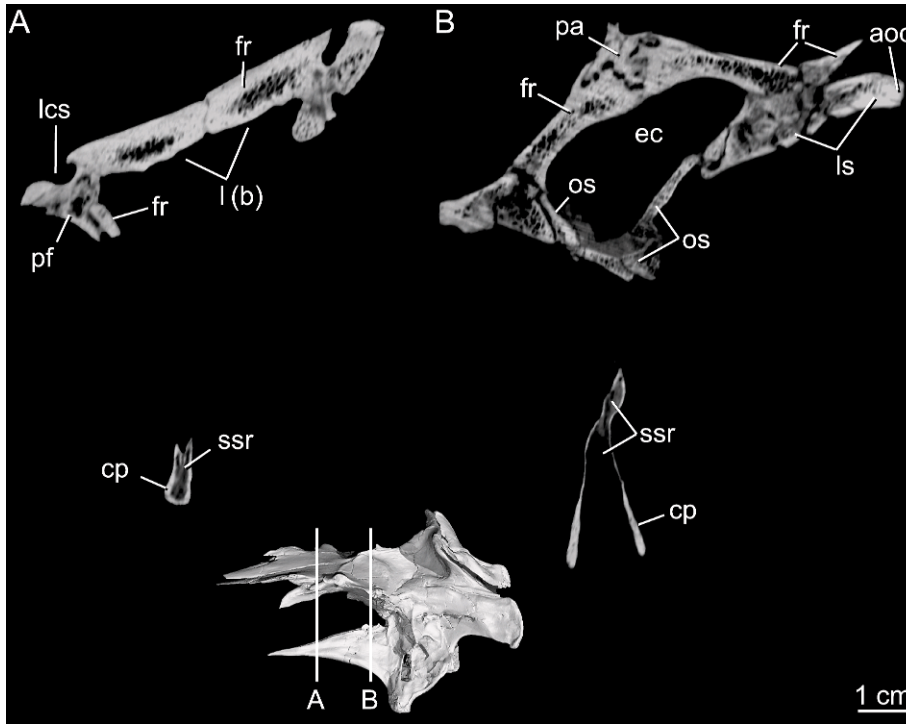

Fig. 8. Coronal slices through the braincase of *Alioramus altai* (IGM 100/1844) showing the olfactory region of the nasal cavity (**A**) and the rostral portion of the endocranial cavity. See appendix 1 for anatomical abbreviations.

Tarbosaurus and *Tyrannosaurus* clade, the condition in IGM 100/1844 reflects its immature status and larger, more mature *Alioramus* specimens should express the condition found in adult *Tarbosaurus* and *Tyrannosaurus*. The frontal contribution to the orbital rim takes the form of a 10 mm long concave notch (fig. 7A) that is comparable to the reduced contribution found in many tyrannosaurids (Brochu, 2003; Currie, 2003; Hurum and Sabath, 2003). Lateral postorbital-lacrimal contact often excludes the frontal from the orbital rim in large tyrannosaurid individuals (Hurum and Sabath, 2003; Currie, 2003).

The frontal contacts the parietal along a broad, caudally convex suture that is unfused (fig. 8B) and lacks the associated foramina described in some tyrannosaurids (e.g., *Teratophoneus*; BYU 8120/9396). This suture is raised, but not to the degree seen in *Tyrannosaurus* and *Tarbosaurus* (Brochu, 2003; Currie, 2003; Hurum and Sabath, 2003). The opposing parietals together form a distinct sagittal crest that extends onto the frontals, where it almost immediately bifurcates to delineate the rostromedial margins of extensive supratemporal fossae (35 mm rostrocaudal length and 42 mm mediolateral width at their midpoint). The dorsally raised caudal region of the frontals is most similar to that in *Albertosaurus* (Currie, 2003), *Gorgosaurus* (ROM 1247), and *Alioramus remotus* (PIN 3141/1), but it is less extensive than in *Daspletosaurus* (Currie, 2003: fig. 20), *Tarbosaurus* (ZPAL MgD-I/4; Hurum and Sabath, 2003), *Teratophoneus* (BYU 8120/9396), and *Tyrannosaurus* (AMNH FARB 5117; Brochu, 2003). In these latter taxa, the raised region comprises up to a quarter of frontal length. The supratemporal fossae nearly meet along the midline, being separated only by the sagittal crest, as in most tyrannosaurids (Brochu, 2003; Currie, 2003;

Holtz, 2004) (but see Tsuihiji et al., 2011). In contrast, the fossae of *Dilong paradoxus* and *Guanlong wucaii* (Xu et al., 2004, 2006) are widely separated by a broad, flat midline region of the frontals.

The ventral surface of the frontal roofs both the orbit and the forebrain portion of the endocranial cavity. These two regions are separated by a thick, rugose crest (= crista cranii of Ali et al., 2008), which continues rostrally as the sharp ventral surface of the prefrontal (see above). The endocranial region is hourglass shaped and marked by pronounced depressions for the olfactory bulbs that are delimited by a raised ethmoid scar (fig. 9). The conjoined olfactory depressions are large (36 mm long and 30 mm wide) and lie directly outside the olfactory fenestra formed by the frontals and parietals dorsally, the crista cranii laterally, and the orbitosphenoids ventrally. A deep fossa rostrolateral to these depressions and housed within the frontal, prefrontal, and lacrimal represents the caudal end of the olfactory region of the nasal cavity and would have been lined with olfactory epithelium (Witmer and Ridgely, 2009). The olfactory bulbs, previously thought to fill this fossa (e.g., Horner and Dobb, 1997; Brochu, 2000, 2003), were restricted to the region of the midline scars (Ali et al., 2008; Zelenitsky et al., 2009). The presence of vomeronasal organs within this space (Saveliev and Alifanov, 2007) is an unjustified inference for tyrannosaurs or any crown archosaur (Witmer and Ridgely, 2010). There is no evidence of the bony laminae that descend from the frontal as olfactory turbinates in the juvenile tyrannosaurid skull CMNH 7951 (Witmer and Ridgely, 2010). The interdigitating, horizontal articulation between the frontal and the underlying laterosphenoid is clearly visible in CT (figs. 9, 10A).

PREFRONTAL: The small prefrontal is a triradiate element, 60 mm long rostrocaudally at its maximum dimension. Its cuplike shape forms the lateral and dorsal roof of the deep olfactory fossa. The prefrontal is divided into two dorsal and one ventral processes. The medial dorsal process is thin, flat, and extends rostrally for 50 mm to underlie the nasal prong of the frontal. A small length of this process extends lateral to the frontal (on the right side, left side is broken) forming the only exposure of the prefrontal on the skull roof; this prong likely inserted into the nasal. A prefrontal-nasal contact is present in *Albertosaurus* (Currie, 2003: fig. 2), *Bistahieversor* (NMMNH P-27469), *Gorgosaurus* (ROM 1247), *Daspletosaurus* (CMN 8506), *Teratophoneus* (BYU 8120/9396), *Tarbosaurus* (Tsuihiji et al., 2011: fig. 5A), and *Tyrannosaurus* (Brochu, 2003: fig. 20) but absent in *Guanlong*. The lateral dorsal process is a short (40 mm), triangular projection extending rostrally and containing a dorsolaterally facing, smooth, inset surface that accepted the lacrimal. In dorsal view, the divergence of the lateral and medial dorsal processes creates an acute angle filled by the lacrimal. The third process (tapering ventral process of Currie, 2003) is often less than 1 mm thick and projects ventrally from the lateral dorsal process. It is the rostral continuation of the crista cranii of the frontal, and it forms the rostral portion of the orbital margin and dorsolateral surface of the olfactory fossa.

The presence of a prefrontal has long been an uncertainty debated among tyrannosaurid workers (Osborn, 1912; Russell, 1970; Bakker et al, 1988; see review in Brochu, 2003). This is not surprising, considering the variable external exposure of the prefrontal and its possible fusion to surrounding bones (Brochu, 2003; Currie, 2003). IGM 100/1844 clearly has a paired, unfused prefrontal in agreement with other well-preserved tyrannosaurid skulls (e.g., Brochu, 2003; Currie, 2003; Hurum and Sabath, 2003; Tsuihiji et al., 2011). The cuplike, triradiate shape and reduced ventral process makes the prefrontal of IGM 100/1844 similar to that of *Tyrannosaurus* (AMNH FARB 5117; Osborn, 1912; Brochu, 2003: fig. 20). The prefrontal of *Tarbosaurus* is dorsoventrally deeper, rostrocaudally shorter, and exhibits a greater separation of the lateral, dorsal, and ventral processes (Hurum and Sabath, 2003: fig. 8). It also sends a long ventral process along the medial side of the ventral ramus of the lacrimal that is clearly lacking in IGM 100/1844 and *Tyrannosaurus*. In lateral view, this condition is clearly visible in other tyrannosaurids, including *Daspletosaurus* (FMNH PR308). The prefrontal of IGM

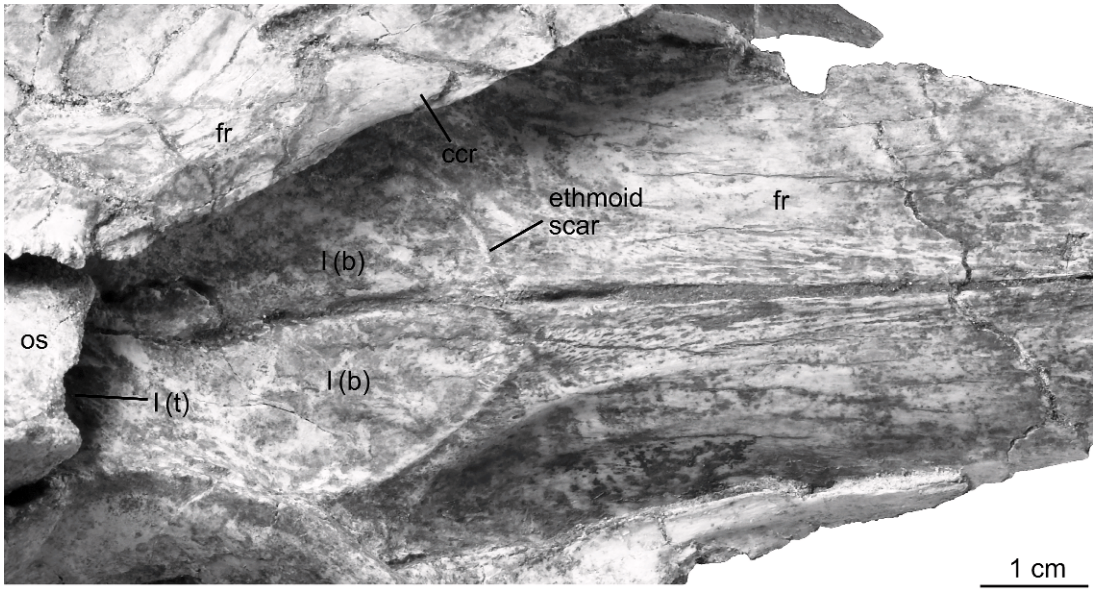

Fig. 9. Ventral view of the olfactory region of the nasal cavity in *Alioramus altai* (IGM 100/1844). The circular ethmoid scar marks the articulation of the unpreserved ethmoid complex. It also delineates the lateral extent of the olfactory (I) bulbs. See appendix 1 for anatomical abbreviations.

100/1844 and *Tyrannosaurus* overall is a longer, lower bone than in *Tarbosaurus*. The relatively large prefrontal of *Guanlong* is well exposed on the skull roof as a half-oval-shaped element that contributes broadly to the dorsal rim of the orbit. It also projects and extends for more than half the length of the ventral ramus of the lacrimal to form most of the rostral margin of the orbit. A small, subtriangular prefrontal is present in *Dilong* (Xu et al., 2004: 680), lying at the anterolateral edge of the frontal, just posterior and slightly medial to the lacrimal. Although difficult to see, its presence is indicated in both the holotype and a referred specimen (IVPP v14242). It is unclear what role variable, possibly age-related, fusion has on the perceived distribution of the prefrontal within Theropoda.

PARIETAL: The left and right parietals are fused (fig. 10), as in *Albertosaurus* (TMP 1981.010.0001), *Bistahieversor* (NMMNH P-27469), *Daspletosaurus* (CMN 8506), *Gorgosaurus* (ROM 1247), *Tyrannosaurus* (Brochu, 2003), and *Tarbosaurus* (Hurum and Sabath, 2003; Tsuihiji et al., 2011), with an hourglass-shaped dorsal surface whose midpoint constriction is formed by the supratemporal fossae (fig. 3). The conjoined parietals are 78 mm long rostrocaudally, 93 mm wide at their rostrolateral contacts with the frontals, 35 mm wide at their midlength, and 98 mm wide at the nuchal crest. The parietals contact the frontals rostrodorsally, postorbitals rostrolaterally, laterosphenoids rostroventrally, prootic and otoccipital ventrolaterally, and the supraoccipital caudally. As in other tyrannosauroids (Brochu, 2003; Currie, 2003; Hurum and Sabath, 2003; Xu et al., 2006), the rostroventral tip of the parietal lies between the capitate processes of the laterosphenoid and frontal and participates in a rugose peg that articulates with the postorbital (figs. 7A, 11). The laterosphenoid overlaps the parietal ventrolaterally along a dorsally convex suture immediately behind the parietal-postorbital contact. The parietal abuts the prootic and otoccipital across a long, straight, unfused suture. Lateral to this suture, the parietal received the squamosal along a triangular, rugose scar. Thus, the parietal separates the medial portion of the squamosal from the paroccipital process, as in *Tyrannosaurus* (Brochu, 2003). A finger-like caudolateral extension of the parietal extends along the dorsal margin of the

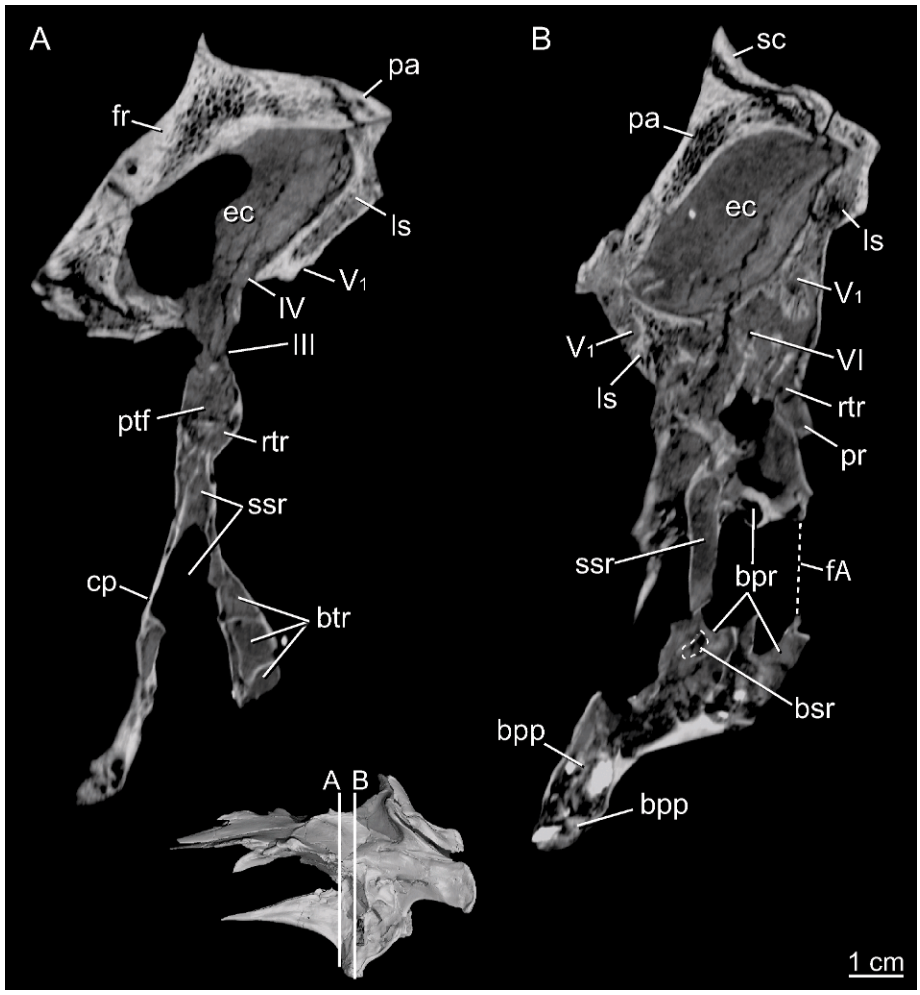

Fig. 10. Coronal slices through the braincase of *Alioramus altai* (IGM 100/1844). The slices expose the supratemporal fossa (A and B), caudal end of the cultriform process (**A**) and right basipterygoid process (**B**). See appendix 1 for anatomical abbreviations.

paroccipital process before terminating 10 mm short of its distal end (figs. 2–4). The parietal and frontal share a broad contact within the supratemporal fossa, as described above. The supraoccipital overlaps the parietal on the occipital surface. Despite forming intimate contacts with the highly pneumatized prootic, otoccipital, and supraoccipital, the parietal, as in other tyrannosaurids (Witmer and Ridgely, 2009), is apneumatic. This condition is also seen in *Bistahieversor* (NMMNH P-25049).

On the dorsal surface, the sagittal crest is only 2 mm wide mediolaterally and thus it only narrowly separates the right and left supratemporal fossae (fig. 2A). This condition is shared with most other tyrannosauroids (Brochu, 2003; Currie, 2003; Hurum and Sabath, 2003), including *Bistahieversor* (NMMNH P-27469) and *Dilong* (Xu et al., 2004), whereas in *Guanlong* (Xu et al., 2006) a broad, flat midline region of the parietals separates the fossae. The dorsal edge of the sagittal crest in IGM 100/1844 is concave in lateral view (fig. 3). This condition is also seen in *Bistahieversor* (NMMNH P-27469), *Daspletosaurus* (FMNH PR308), *Gorgosaurus* (ROM 1247), *Tarbosaurus* (ZPAL

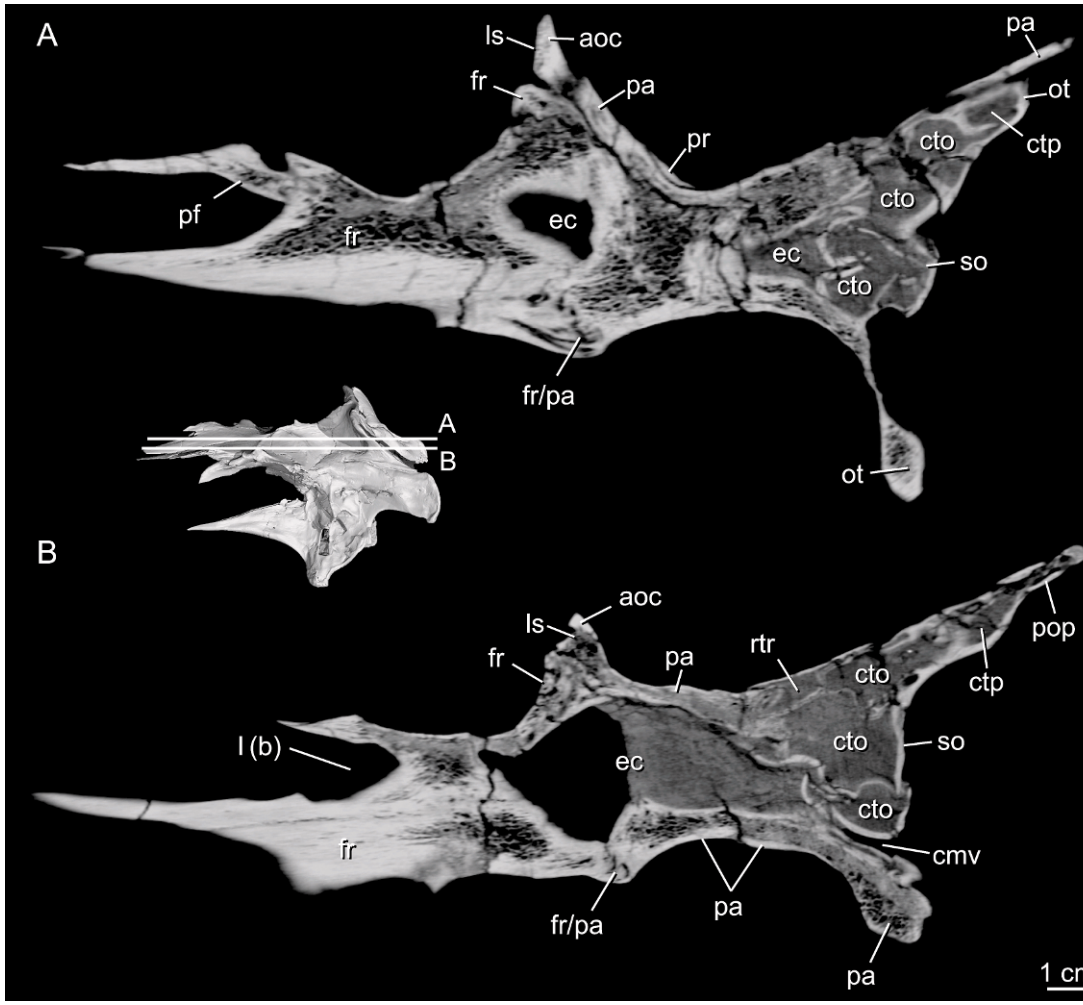

Fig. 11. Horizontal slices through the dermal roof and dorsal portion of the neurocranium of *Alioramus altai* (IGM 100/1844). See appendix 1 for anatomical abbreviations.

MgD-I/38), and *Tyrannosaurus* (AMNH FARB 5117). A broken flake of bone at the rostral end of the crest appears to represent a discrete, triangular process that forms a rostral apex in other tyrannosaurids (Brochu, 2003). A peak is also seen in adult *Bistahieversor* (NMMNH P-27469), where it is tall, and in subadult *Gorgosaurus* (ROM 1247), where it is low. *Guanlong* and *Dilong* possess two parasagittal crests, which is either a synapomorphy uniting these taxa or, more likely based on the well-supported phylogenetic relationships positing *Guanlong* and *Dilong* as successive sister taxa to more derived tyrannosauroids (Brusatte et al., 2010a), reflects the plesiomorphic tyrannosauroid condition. The parasagittal crests of *Dilong* differ from those of *Guanlong* in that they abut one another and are short.

The paired nuchal (transverse) crests, one on each side of the caudal margin of the parietal, are confluent rostromedially with the sagittal crest where they form the caudomedial corners of the supratemporal fossae (figs. 2, 4). A dorsal shelf of the parietal, which autapomorphically roofs this corner of the fossa in *Guanlong* (Xu et al., 2006), is not present. The conjoined nuchal crest is pronounced and contributes to an expanded occipital plate (fig. 4B). This

contribution is 40 mm deep dorsoventrally (taken approximately midway between the sagittal midline and the lateral margin of the nuchal crest—where the nuchal crest forms an apex along its dorsal margin) and rises 12 mm above the supraoccipital, but the crest is still more than twice as wide as it is deep. The contrasting and apparently derived condition in which the depth of the crest is more than half its width characterizes adult *Tarbosaurus*, *Tyrannosaurus*, and *Daspletosaurus* (Currie et al., 2003), and seemingly *Alioramus remotus*. This distinction often is held as phylogenetically informative (Holtz, 2001; Currie et al., 2003; Holtz et al., 2004), although crest proportions change considerably during postnatal growth (Carr, 1999; Tsuihiji et al., 2011) and their relationship to overall size remains unclear. The occipital (caudal) surface of the nuchal crest is deeply concave on either side of the supraoccipital, with numerous subpockets within each concavity. The concave caudal surface is also seen in *Daspletosaurus* (TMP 2001.036.0001), *Gorgosaurus* (ROM 1247), *Tarbosaurus* (ZPAL MgD-I/4), and *Tyrannosaurus* (AMNH FARB 5117). The individual crests have a convex dorsal margin that join at the midline to form a small, concave notch (fig. 4). This condition has been described as ''winglike tabs'' (Brochu, 2003: 26) and ''symmetric alae'' (Hurum and Sabath, 2003: 181) and is shared with other tyrannosaurids. A small but distinct crest extends onto the occipital surface of the parietal as a dorsal continuation of the sagittal crest of the supraoccipital (see below). This ridge is also seen in *Gorgosaurus* (ROM 1247), *Tarbosaurus* (ZPAL MgD-I/4), and *Tyrannosaurus* (AMNH FARB 5027). This crest may reflect the presence of a mammalianlike nuchal ligament (Sampson and Witmer, 2007).

Neurocranium

Supraoccipital: The supraoccipital is slightly crushed and sheared, but its basic external dimensions on the occipital plate are clear (fig. 4). It is 55 mm tall dorsoventrally, 6 mm wide mediolaterally at the foramen magnum, and 35 mm wide at its dorsal apex (its widest point). Its occipital surface slopes caudoventrally and thus faces caudodorsally. This condition is also seen in *Gorgosaurus* (ROM 1247), *Tarbosaurus* (ZPAL MgD-I/3), and *Tyrannosaurus* (AMNH FARB 5117). The supraoccipital contacts the parietal dorsally and laterally and the otoccipital (fused exoccipital-opisthotic) ventrolaterally. The supraoccipital narrowly contributes to the dorsal rim of the foramen magnum, as in all other tyrannosaurids (Brochu, 2003; Currie, 2003; Hurum and Sabath, 2003). This is not the wide contribution found in many other coelurosaurian and non-coelurosaurian theropods (e.g., Currie, 1985, 1995; Currie and Zhao, 1993; Makovicky and Norell, 1998; Allain, 2002; Rauhut, 2004; Sampson and Witmer, 2007). A midline contact of the otoccipitals that negates a supraoccipital contribution to the foramen magnum characterizes *Dilong* and *Guanlong* (Xu et al., 2004, 2006) and was considered a derived feature of tyrannosauroids by Holtz (2001). Thus, a reduced supraoccipital contribution to the foramen magnum is a derived feature of tyrannosauroids, but whether the ancestral tyrannosauroid expressed the condition found in IGM 100/1844 or that of *Guanlong* and *Dilong* remains unclear.

A thick, dorsoventrally trending, sagittal crest divides the occipital surface of the supraoccipital into left and right halves. The mediolateral width of this ridge increases dorsally, but the ridge does not form a bulbous prominence as in the large-bodied carcharodontosaurids (Coria and Currie, 2002; Brusatte and Sereno, 2008). The ridge is sharpest and most pronounced ventrally, immediately above the foramen magnum. This may be an artifact of crushing, but if biologically real, it is an autapomorphy of *Alioramus altai* among tyrannosauroids. In *Albertosaurus* (Currie et al., 2003), *Daspletosaurus* (Currie et al., 2003), *Gorgosaurus* (AMNH FARB 5336), *Tarbosaurus* (ZPAL MgD-I/3), and *Tyrannosaurus* (AMNH FARB 5117) the ridge is absent (Currie et al., 2003). Intraspecific variation in the presence/absence and strength of the ridge is present in ornithomimosaurs (Makovicky and Norell, 1998; Kobayashi and Barsbold, 2005) and may characterize early coelurosaurs.

The supraoccipital falls approximately 10 mm short of the dorsal margin of the

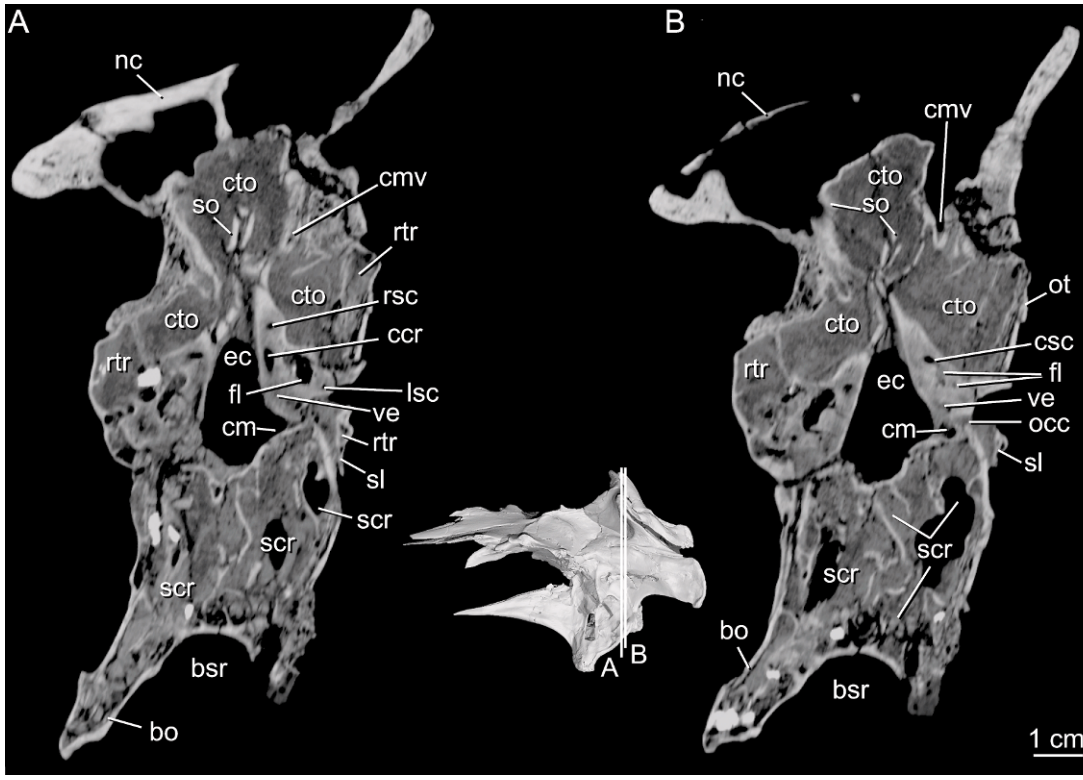

Fig. 12. Coronal slices through the braincase of *Alioramus altai* (IGM 100/1844). The slices transect the nuchal crest and inner ear region. See appendix 1 for anatomical abbreviations.

parietal nuchal crest, such that the height of the crest above the supraoccipital is less than half the height of the supraoccipital (above the foramen magnum). In contrast, the height of the crest above the supraoccipital is slightly more than half the height of the supraoccipital in *Gorgosaurus* (ROM 1247) and *Daspletosaurus* (TMP 2001.036.0001), and in large specimens of *Tarbosaurus* (Hurum and Sabath, 2003) and *Tyrannosaurus* (Brochu, 2003), the nuchal crest is twice the height, or greater, than the supraoccipital. The height of the nuchal crest, relative to the supraoccipital, is thus shortest in IGM 100/1844 among known tyrannosaurids. The supraoccipital and parietal in *Guanlong* extend to the same level dorsally.

A paired foramen transmitting the caudal middle cerebral vein opens onto the occipital surface at the junction of the supraoccipital, otoccipital, and parietal (Witmer and Ridgely, 2009). The associated canals lie completely within the supraoccipital, but they extend for most of their length near the supraoccipital-parietal suture (figs. 11B, 12), which houses these canals in other tyrannosaurids (Witmer and Ridgely, 2009). The canals originate in the hindbrain region of the endocranial cavity and mark the caudal extent of the transverse sinus. The parietal participates in a second penetration of the occipital plate that begins in the dural space above the midbrain rostral to, but in approximately the same mediolateral plane as, the internal foramen of the caudal middle cerebral vein. The associated canal is thin, irregular in shape, and penetrates the occipital plate within the parietal-supraoccipital suture dorsal to the external foramen of the caudal middle cerebral nerve (fig. 13). The canal may have been a bilaterally symmetrical structure, although its left counterpart is not visible (possibly as an artifact of scanning and/or postmortem distortion). The canal

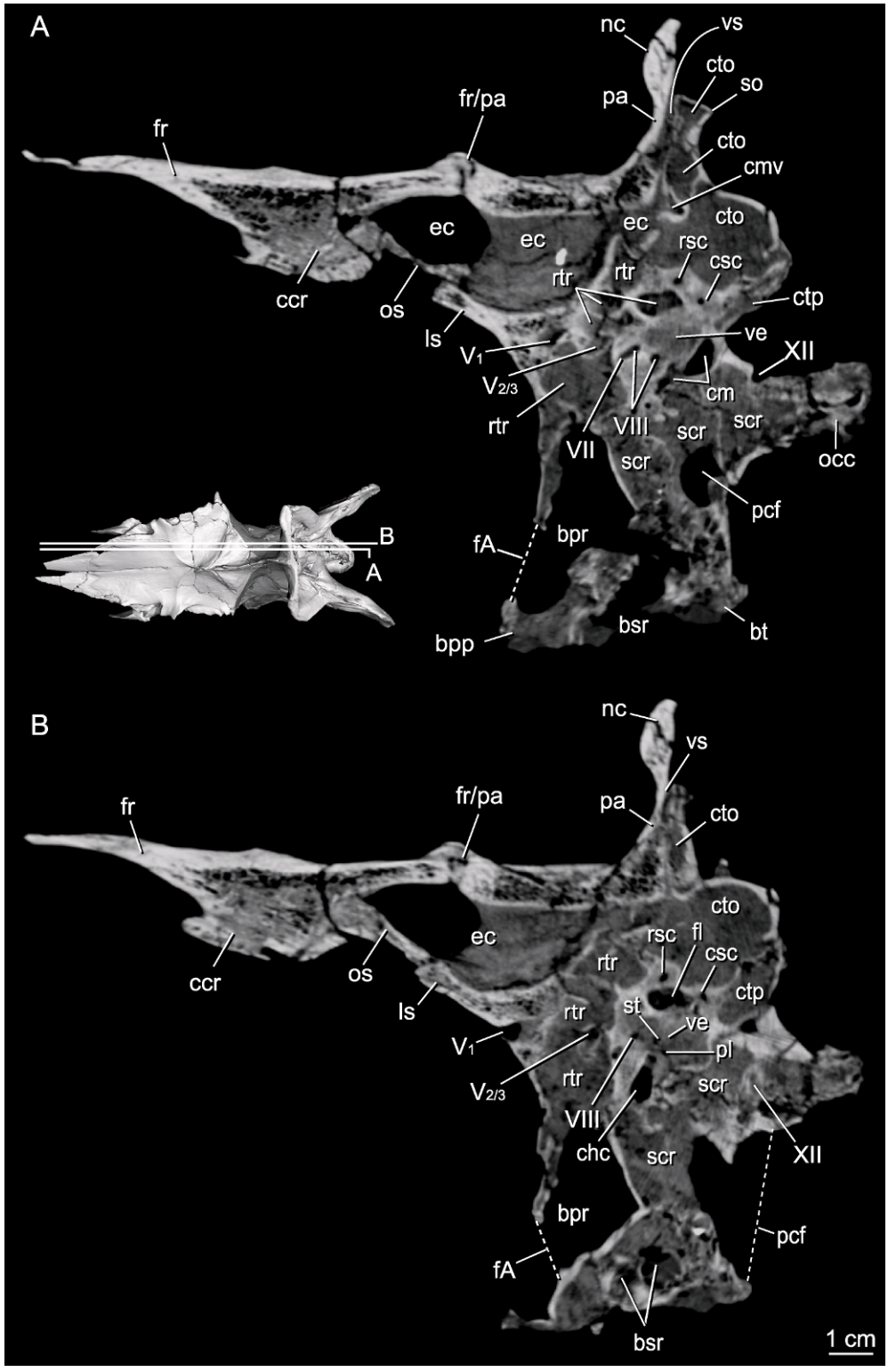

Fig. 13. Sagittal slices through the braincase of *Alioramus altai* (IGM 100/1844). See appendix 1 for anatomical abbreviations.

correlates in position and general morphology with the ''vascular structure'' identified on the endocast of *Tyrannosaurus* (FMNH PR2081; Brochu, 2000).

The supraoccipital in *Tarbosaurus* (Hurum and Sabath, 2003: fig. 17) and *Tyrannosaurus* (AMNH FARB 5117; Brochu, 2003: fig. 5) bifurcates dorsally into two fingerlike processes. Currie (2003) implies these ''knoblike'' structures are present in all tyrannosaurids, but they are absent in IGM 100/1844. This may reflect the young ontogenetic age of the specimen, as the processes appear late in the postnatal development of *Tyrannosaurus* (Carr, 1999). The dorsal margin of the supraoccipital is gently convex as in juvenile tyrannosaurids (Carr, 1999), *Guanlong* and *Dilong*, non-coelurosaurian tetanurans (e.g., Madsen, 1976; Currie and Zhao, 1993), and most coelurosaurs (e.g., Clark et al., 1994; Sues, 1997; Makovicky and Norell, 1998; Kobayashi and Barsbold, 2005; Norell et al., 2006). In IGM 100/1844, as in *Tyrannosaurus* (AMNH FARB 5117; Brochu, 2003), the dorsal margin of the supraoccipital is wider than the occipital condyle, not narrower as in *Guanlong* (IVPP V14531) and *Tarbosaurus* (ZPAL MgD-I/3; Hurum and Sabath, 2003).

The supraoccipital internally houses an expanded, tripartite, pneumatic sinus consisting of a dorsal midline chamber and two ventrolaterally positioned, parasagittal chambers (figs. 11–13; see Caudal Tympanic Recess and Sinus below). The midline chamber communicates with the external surface of the occipital plate through a number of small openings that most likely reflect an extreme thinning of the outer wall of the supraoccipital rather than true pneumatic foramina. The supraoccipital forms the dorsal cap of the ossified inner ear.

OTOCCIPITAL: The exoccipital and opisthotic are indistinguishably fused into an ''otoccipital,'' as in archosaurs and sauropsids generally (Bellairs and Kamal, 1981; Currie, 1997). This conjoined element is widely exposed on the occipital plate and lateral surfaces of the braincase, and forms the primary body of the paroccipital process, the lateral margins of the basal tubera, and the dorsolateral corners of the occipital condyle (figs. 3, 4). The condyle is eroded ventrally and on its right side, but it was approximately 30 mm wide and 25 mm deep. A ventrally projecting convexity along its dorsal margin renders the foramen magnum heart shaped (19 mm wide mediolaterally and 15 mm deep dorsoventrally). A similar condition is seen in large, presumably mature, specimens of *Tyrannosaurus* (AMNH FARB 5117). Sutural contacts with the prootic, basisphenoid, and parietal are unfused and clearly visible. The sutural contact with the basioccipital on the occipital condyle and along the basal tubera remains visible but only barely so. The otoccipital-supraoccipital suture above the foramen magnum is fully fused, although its entire length does remain visible externally as a raised ridge. This suture is open in a subadult specimen of *Teratophoneus* (BYU 8120/9396), and it is partially or fully closed in both *Gorgosaurus* (ROM 1247) and *Tyrannosaurus* (AMNH FARB 5117). Despite the considerable degree of observed variation, among tyrannosaurids, the otoccipital-supraoccipital contact is one of the few neurocranial sutures that fully fuses.

The right and left otoccipitals form the lateral and most of the dorsal margin of the foramen magnum. Lateral to the foramen, the otoccipital forms the caudal surface of the paroccipital process, which is smooth, shallowly concave, and lacks the deep fossa present in *Dilong*, *Guanlong*, and a variety of other coelurosaurs (e.g., Clark et al., 1994; Norell et al., 2004, 2006). The paroccipital processes are extensive and extend more caudally than laterally (fig. 2). This orientation, which is somewhat exaggerated by crushing in IGM 100/1844, is also present in subadult *Gorgosaurus* (ROM 1247), *Daspletosaurus*, and *Tarbosaurus* (ZPAL MgD-I/3). Processes that are oriented more laterally than caudally are seen in larger, and presumably more mature, specimens of *Gorgosaurus* (AMNH FARB 5434) and *Daspletosaurus* (TMP 1985.062.0001). This wide condition is also seen in juveniles and subadults of *Tarbosaurus* (MPC-D 107/7), *Teratophoneus* (BYU 8120/9396), and *Tyrannosaurus* (CMNH 7541), and may represent the paedomorphic acquisition of a wide temporal region and short basicranium in these taxa.

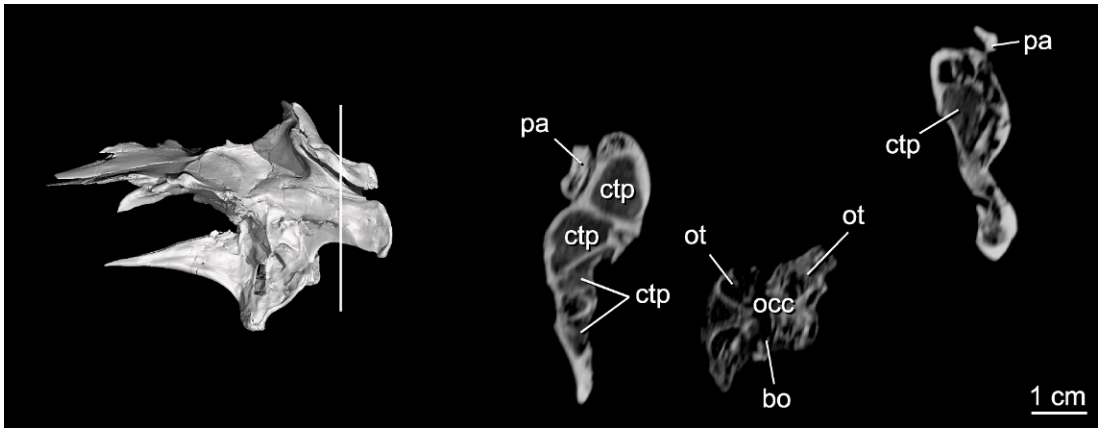

Fig. 14. Coronal slice through the occipital condyle and proximal ends of the paroccipital processes of *Alioramus altai* (IGM 100/1844). Note the highly complex pneumatic cavity within the paroccipital processes and how these processes taper to form a ventral flange.

The paroccipital processes of IGM 100/1844 are deep across their entire length and terminate in a slightly expanded, rounded, and thickened margin that is completely preserved on the left side (fig. 3A) but eroded away on the right side. The complete left process is 60 mm long, 50 mm deep at its base, and 40 mm deep at its distal end. The external surfaces of the paroccipital processes are highly inflated, reflecting the presence of an extensive and complex internal cavity of the caudal tympanic sinus (fig. 14; see below). This inflation is seen in all other large tyrannosauroids, including *Bistahieversor* (NMMNH P-25049), *Daspletosaurus*, *Gorgosaurus* (AMNH FARB 5336), *Tarbosaurus* (ZPAL MgD-I/3), and *Tyrannosaurus* (AMNH FARB 5117).

In IGM 100/1844, this expansion is largely restricted to the dorsal two-thirds of the process (the dorsodistal corner is unexpanded), resulting in a rostrocaudally thin ventral margin that may be best described as a ventral flange. This flange runs nearly the entire length of the process but is most distinct distally. A ventral flange characterizes the paroccipital processes of *Tarbosaurus* (Hurum and Sabath, 2003: fig. 17) and *Tyrannosaurus* (Brochu, 2003: fig. 5), but not *Daspletosaurus* (Currie, 2003: fig. 26) or apparently *Alioramus remotus*. A distinct ventral flange is occasionally present in maniraptorans (e.g., Currie, 1995; Norell et al., 2006), but it is generally rare among theropods. Additionally, the vertical ridge that sometimes delineates a lateral and medial partition of the process in caudal view (e.g., Makovicky et al., 2003; Norell et al., 2006) is absent in IGM 100/1844.

The ventral margin of the left paroccipital process, both near its base (defined here as the point where the ventral margin of the paroccipital process turns distinctly downward to form the lateral margin of the crista tuberalis) and at its distal end, is aligned approximately with the ventral margin of the occipital condyle (fig. 3). This may be an artifact of crushing because the base of the right paroccipital process is clearly level with the midpoint of the occipital condyle (distal end is broken). In *Daspletosaurus* (Currie, 2003: fig. 26) and *Guanlong*, both the base and distal end of the process are level with the midpoint of the condyle, but in *Tarbosaurus* (Hurum and Sabath 2003: fig. 17) and *Tyrannosaurus* (Brochu, 2003: fig. 5) the ventral lobe at the distal end of the process projects below the occipital condyle. The tyrannosauroid condition, in which the base and tip of the paroccipital process extend to midlevel of the occipital condyle or below, is also present in most coelurosaurs and is likely plesiomorphic for the group. However, some taxa (e.g., Currie, 1995; Makovicky and Norell, 1998; Makovicky et al., 2003) exhibit a morphologically intermediate condition

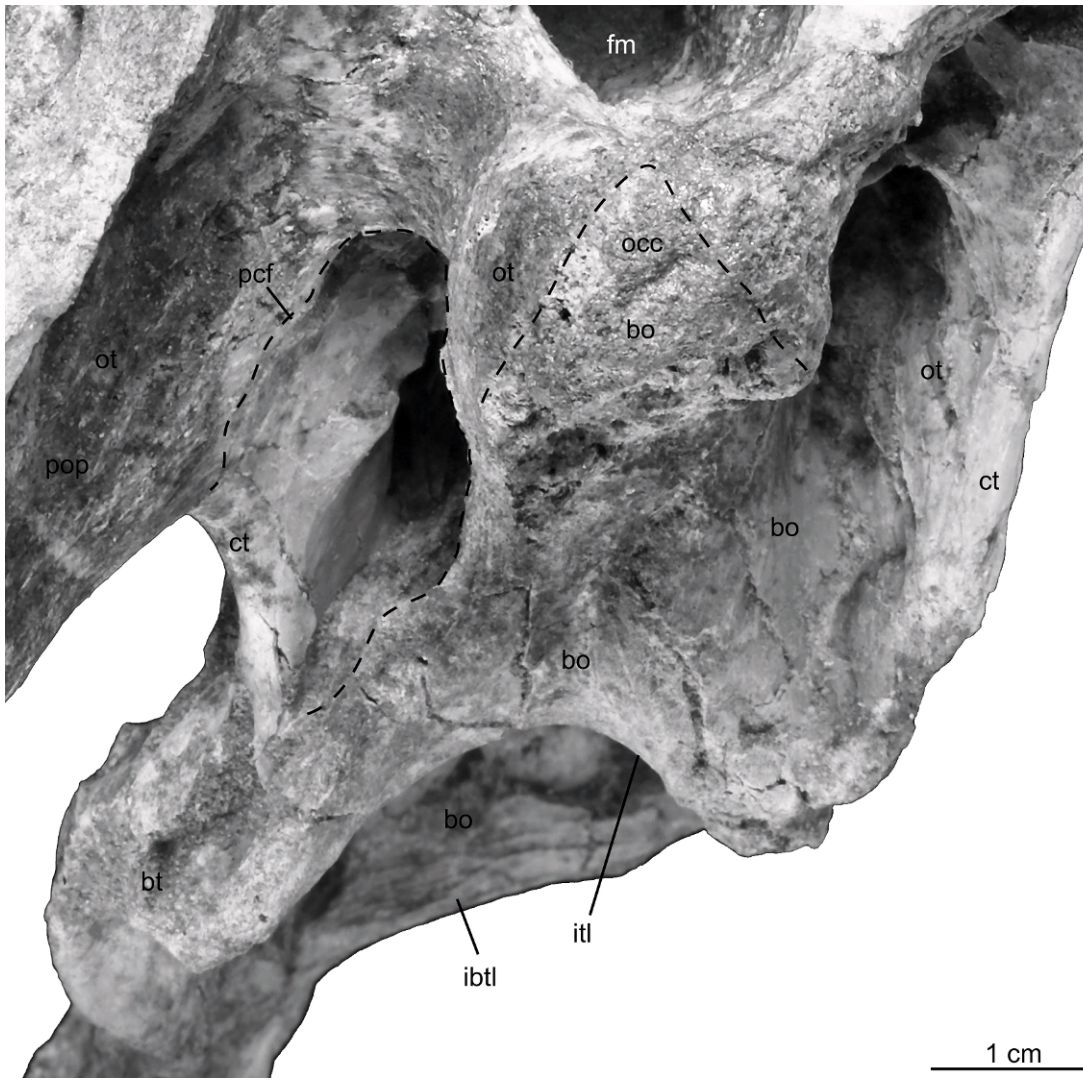

Fig. 15. Caudal view of the braincase of *Alioramus altai* (IGM 100/1844) ventral to the foramen magnum. The paracondylar fossae are deep and house the external openings of the subcondylar recess, hypoglossal canal, and vagal canal. See appendix 1 for anatomical abbreviations.

in which the ventral margin of the process is level with the bottom of the foramen magnum.

Ventral to the foramen magnum, pedicels of the otoccipitals form the caudodorsal corners of the occipital condyle. Their contacts with the basioccipital, which forms the remainder of the condyle, are visible and especially clear on the right side, where erosion reveals an unfused length of this suture lying deep to the condylar surface. Laterally, the otoccipital forms a stout condylar neck overlying a deep, somewhat triangular paracondylar pocket (fig. 15). The pocket is located nearly exclusively on the otoccipital, although the medial region excavates the basioccipital as described in *Tyrannosaurus* (Brochu, 2003). Multiple foramina are visible within each pocket although erosion on both sides makes it difficult to determine the exact number without the use of CT. The most common condition in

theropods is probably three foramina within the pocket—two separate exits for branches of the hypoglossal (XII) nerve and a multipurpose vagal foramen (e.g., Currie, 1997; Brusatte and Sereno, 2007; *Teratophoneus* (BYU 8120/9396). The vagal foramen represents the caudal division of the cavum metoticum and is formed by the exiting vagus (X) and accessory (XI) nerves and probably at least a small jugular vein (Rieppel, 1985; Gower and Weber, 1998; Sampson and Witmer, 2007). Variation within Theropoda centers largely on the number of hypoglossal foramina, although some basal theropods (e.g., *Tawa hallae*; Nesbitt et al., 2009) lack a divided cavum metoticum and thus a true vagal foramen.

CT shows that only two foramina penetrate the paracondylar pocket in IGM 100/1844. The first foramen, which is smaller and more medially positioned within the pocket, is the only foramen associated with the hypoglossal nerve and suggests XII may have ramified extracranially (i.e., after exiting the braincase through the single opening present) (fig. 16A). As is normal in reptiles, the hypoglossal nerve is communicated through a basically straight, ventrolaterally trending canal that enters the otoccipital from the caudolateral margin of the endocranial floor. A single hypoglossal foramen was reported for *Tyrannosaurus* (Brochu, 2000, 2003), suggesting a reduced number of hypoglossal canals may be a derived feature of or within Tyrannosauroidea. Another specimen of *Tyrannosaurus* (AMNH FARB 5117), however, has the expected number of three foramina on each side, indicating that polymorphism may complicate optimization of this variation as synapomorphy. In addition, some non-coelurosaurian theropods (e.g., *Baryonyx*: Charig and Milner, 1997; *Irritator*: Sues et al., 2002; *Majungasaurus*; Sampson and Witmer, 2007; possibly *Shaochilong*: Brusatte et al., 2010b; see Brusatte et al., 2010b, for discussion) also exhibit a single hypoglossal foramen, raising the possibility this condition may be plesiomorphic for tyrannosauroids, or at the very least is not unusual among theropods.

The vagal foramen lies dorsolateral to the hypoglossal foramen within the paracondylar pocket (figs. 16B, 17; see also Bever et al., 2011: fig. 5). It is the larger of the two foramina and opens into a relatively straight, caudolaterally trending canal that ultimately communicates with the endocranial cavity. There is no separate foramen for the accessory (XI) nerve. The proximal (rostromedial) portion of the crista tuberalis divides the cavum metoticum in the ossified skull producing the vagal foramen and fenestra pseudorotunda on the external surface of the ossified otic capsule. Thus, at least this portion of the crista tuberalis is homologous with the metotic strut or prevagal strut of Witmer (1990) and Baumel and Witmer (1993); see Gower and Weber (1998) and Sampson and Witmer (2007). The rostromedial end of the strut in IGM 100/1844 does not reach the lateral wall of the endocranial cavity. This leaves the medial aperture of the cavum metoticum undivided, as in most archosaurs (Gower and Weber, 1998; Bever and Norell, 2009).

The rostral division of the cavum metoticum (recessus scalae tympani) also lies in a rostromedial-caudolateral orientation, but on the rostral side of the crista tuberalis. An approximately 60° angle separates the two spaces (fig. 17). The medial aperture of the recessus scalae tympani opens into the undivided portion of the cavum metoticum, where it is confluent with the medial opening of the vagal canal. Rostral to this confluence and caudal to the position through which the cochlear branch of the vestibulocochlear (VIII) nerve enters the cochlear cavity, a short canal extends from the cranial cavity to the recessus scalae tympani. This penetration of what is presumably the opisthotic (the prootic-otoccipital suture is not clear) was interpreted by Bever et al. (2011) to be an independent path of the glossopharyngeal (IX) nerve into the recessus scalae tympani. The nerve likely traverses the recessus scalae tympani in all tyrannosauroids (Witmer and Ridgely, 2009; contra Brochu, 2000, who interpreted IX as entering the vagal canal), presumably entering this space through the common medial aperture of the cavum metoticum. The path of IX within the recessus scalae tympani of *Gorgosaurus*, *Tyrannosaurus*, and CMNH 7541 is marked by a groove on the rostral surface of the crista tuberalis (Witmer and Ridgely, 2009)

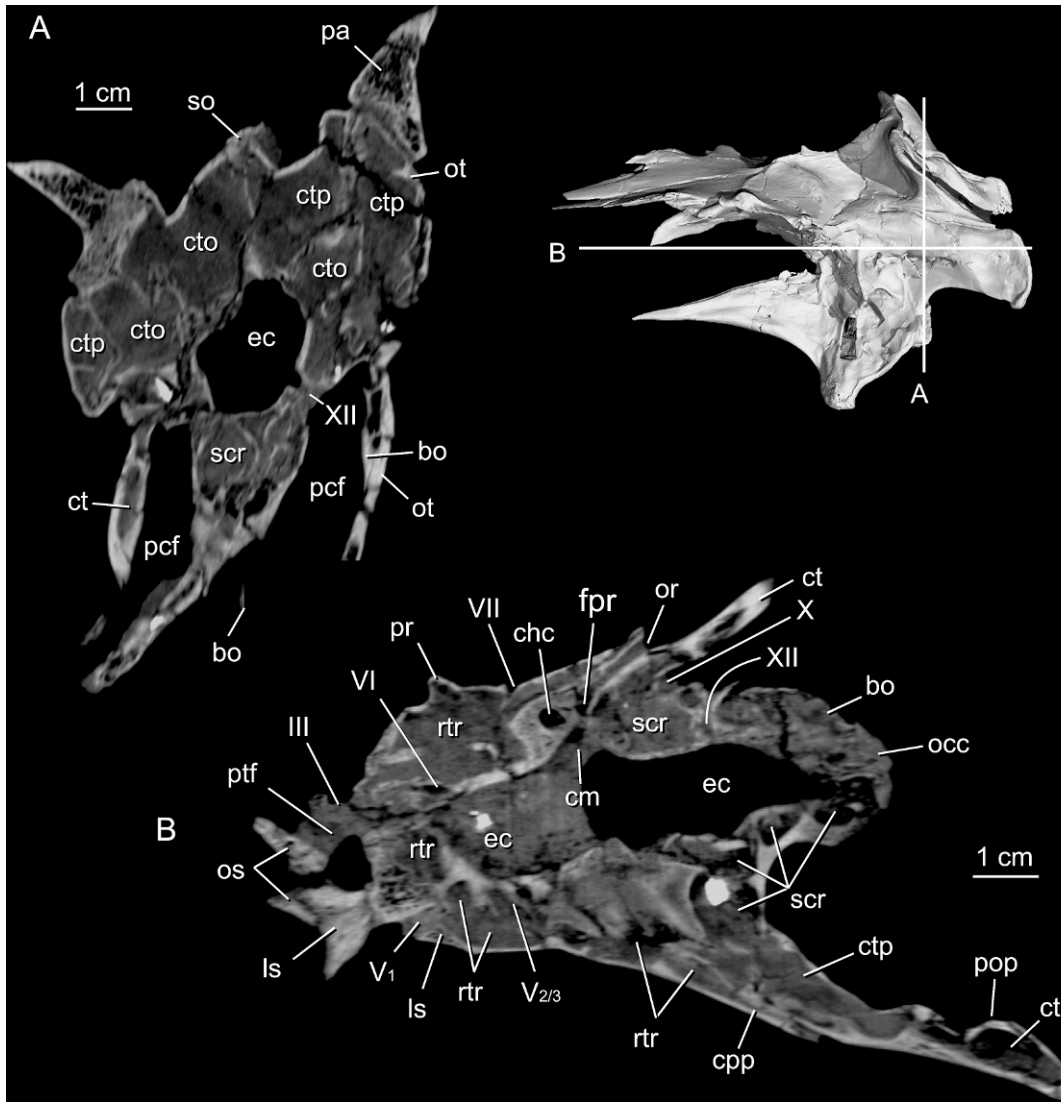

Fig. 16. Coronal (**A**) and horizontal (**B**) slices through the respective caudal and ventral margins of the endocranial cavity in *Alioramus altai* (IGM 100/1844). See appendix 1 for anatomical abbreviations.

that is absent in IGM 100/1844. The nerve does appear to have exited the braincase through the fenestra pseudorotunda, as there is no evidence of it passing through the pnuematized crista tuberalis (as in some coelurosaurs; e.g., Walker, 1985).

In addition to dividing the cavum metoticum, the crista tuberalis separates the lateral surface of the braincase from its caudal (occipital) surface (figs. 3, 15). The developmental origin of this structure in archosaurs is unclear (see Rieppel, 1985; Gower and Weber, 1998), but in IGM 100/1844, the crista lacks any sutural separation from the surrounding otoccipital. A ventral continuation of this structure forms the lateral wall of the basal tuber and approaches its ventral end. Erosion obscures whether it actually formed any of the tuber's ventral surface proper, but such a contribution is absent in other tyrannosaurids (e.g., *Tyrannosaurus*, Brochu, 2003; *Daspletosaurus*, Currie, 2003).

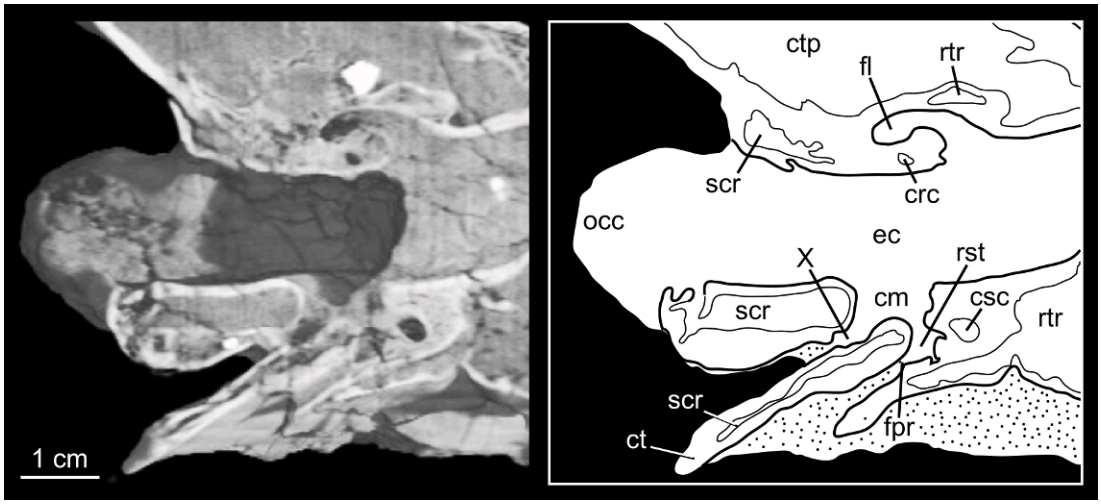

Fig. 17. Horizontal cutaway slice and line drawing of the caudoventral portion of the endocranial cavity in *Alioramus altai* (IGM 100/1844). Note the crista tuberalis (ct) fails to divide the medial extent of the cavum metoticum (cm). See appendix 1 for other anatomical abbreviations.

Laterally, the crista tuberalis of IGM 100/1844 overlaps the basisphenoid along an unfused, dorsoventrally long suture that approaches the caudal edge of the basal tuber, identical to the condition in *Tyrannosaurus* (Brochu, 2003). The basisphenoid of IGM 100/1844 marginally contributes to the tuber, forming a small region of its ventral tip where the m. longissimus capitis profundus and m. rectus capitis ventralis likely attached to the basicranium (Snively and Russell, 2007). This is in contrast to other tyrannosaurids where the ventral tip of the basal tuber is formed solely by the basioccipital. A basisphenoid contribution to this surface is present in *Guanlong*. This contribution differs from that of IGM 100/1844 in that it forms a pronounced ''corner'' that extends laterally and is widely visible in caudal view at the tip of the tuber (the basisphenoid contribution in IGM 100/1844 is only narrowly visible). To complicate matters further, a similar ''corner'' is present in *Dilong* but is formed entirely from the basioccipital and located further dorsally, above the ventral level of the basal tuber and not confluent with it. It is unclear whether the conditions are homologous, but as a consequence of these ''corners,'' both *Dilong* and *Guanlong* possess an extensive crista tuberalis that form a wide web in caudal view.

The otoccipitals form much of the caudal end of the cranial cavity. In addition to the internal hypoglossal foramen, the caudolateral walls of this space are penetrated by two foramina, one slightly dorsal and caudal to the other, within the endocranial cavity and approximately 15 mm rostral to the foramen magnum. Similar foramina are visible through the foramen magnum in a wide array of theropods (e.g., Currie, 1995; Makovicky and Norell, 1998; Brusatte and Sereno, 2007), including *Bistahieversor* (NMMNH P-25049) and *Teratophoneus* (BYU 8120/9396). Their identification historically has been problematic. Currie (1995) suggested that one or both of openings is for the endolymphatic duct or hypoglossal (XII) nerve. Makovicky and Norell (1998) suggested an association with the caudal cerebellar venous sinus. Kurzanov (1976) and Chure and Madsen (1998) indicated that the more medial foramen is for the jugular vein, and is located on the basioccipital, but also suggest the foramina may be pneumatic and associated with the subcondylar recess. In IGM 100/1844, the two openings are clearly located in the otoccipital as the suture with the basioccipital is traceable as a rugose, raised rim (confirmed in CT). CT also reveals that the rostroventral foramen is the undivided medial aperture of the cavum metoticum. The caudodorsal foramen opens

into a large pneumatic cavity associated with the subcondylar recess (described with the basioccipital). In *Bistahieversor* (NMMNH P-25049), *Tarbosaurus* (ZPAL MgD-I/4), and in *Teratophoneus* (BYU 8120/9396), the caudalmost opening is positioned ventrally, whereas the rostral foramen is positioned dorsally. Assuming the openings in these taxa are communicating with the same spaces as in IGM 100/1844, it is currently unclear whether the opening associated with the subcondylar recess is positioned ventral or rostral to that of the cavum metoticum.

BASIOCCIPITAL: The basioccipital forms dorsolateral contacts with the paired otoccipitals and a rostral contact with the midline parabasisphenoid. The basioccipital forms the majority of the basal tubera, the majority of the occipital condyle, and the caudal portion of the endocranial floor. These structural features are seen in other large tyrannosauroids, including *Albertosaurus* (CMN 5600), *Bistahieversor* (NMMNH P-25049), *Daspletosaurus* (CMN 8506), *Tarbosaurus* (ZPAL MgD-I/3), *Teratophoneus* (BYU 8120/9396), and *Tyrannosaurus* (AMNH FARB 5029). In caudal view, the basal tubera together are slightly wider than the occipital condyle and extend ventrally for at least 40 mm (figs. 4, 15). This condition is seen in all other large tyrannosauroids, including *Bistahieversor* (NMMNH P-27469), *Daspletosaurus*, *Gorgosaurus* (ROM 1247), *Tarbosaurus* (ZPAL MgD-I/3), *Teratophoneus* (BYU 8120/9396), and *Tyrannosaurus* (AMNH FARB 5117). The concave ventral margin that separates the right and left tubera, and which is present in other tyrannosaurids (Brochu, 2003; Currie, 2003; Hurum and Sabath, 2003) is part of a wall of bone (''basituberal web'' of Bakker et al., 1988) that contacts the parabasisphenoid rostrally and laterally and completes the basisphenoid recess caudally. The width of this concavity is slightly exaggerated due to crushing. The basisphenoid recess does not penetrate the basioccipital. The subcondylar recess excavates the caudal surface of the basal tubera as in all other large tyrannosauroids (fig. 15). This includes *Albertosaurus* (CMN 5600), *Bistahieversor* (NMMNH P-27469), *Daspletosaurus* (CMN 8506), *Gorgosaurus* (ROM 1247), *Tarbosaurus* (ZPAL MgD-I/3), *Teratophoneus* (BYU 8120/9396), and *Tyrannosaurus* (AMNH FARB 5117).

The concave dorsal surface of the occipital condyle is continuous with the basioccipital contribution to the floor of the endocranial cavity, which trends rostroventrally and lacks the sharp midline crest present in some theropods (e.g., Chure and Madsen, 1998; Brusatte and Sereno, 2007). This contribution is approximately 10 mm wide (mediolaterally) and extends for 35 mm before contacting the parabasisphenoid along a transverse, well-ossified suture. The basioccipital separates the otoccipitals to form the caudoventral surface of the endocranial floor on the midline in other large tyrannosauroids (e.g., *Albertosaurus*, *Bistahieversor*, *Teratophoneus*, *Tyrannosaurus*). However, in some specimens it appears that the otoccipitals contact each other, excluding the basioccipital from dorsal exposure, as is seen in one specimen (ROM 1247) of *Gorgosaurus*. Taken together, the occipital condyle of IGM 100/1844 is small and round (fig. 15), in contrast to the spheroid or reniform condition that is seen in larger and presumably more mature tyrannosaurid individuals. This small condition is seen in other subadult tyrannosauroids, including *Bistahieversor* (NMMNH P-25049), *Gorgosaurus* (TMP 1986.144.0001), *Daspletosaurus* (TMP 1996.143.0001), and *Tyrannosaurus* (CMNH 7541).

PARABASISPHENOID: The parabasisphenoid is 162 mm long rostrocaudally and 92 mm deep dorsoventrally at the basipterygoid process—its deepest point. The left side of this bone is complete and well preserved, whereas much of its right side is damaged by erosion (fig. 3). The parabasisphenoid abuts the basioccipital caudally and it is overlapped by the otoccipital caudodorsally. The prootic overlaps the parabasisphenoid along a suture that remains unfused and visible for all but its rostral extent near the caudodorsal corner of the cultriform process, where it is difficult to trace. All of these contacts are seen in other large tyrannosauroids (*Albertosaurus*, *Bistahieversor*, *Daspletosaurus*, *Gorgosaurus*, *Tarbosaurus*, *Teratophoneus*, *Tyrannosaurus*). The laterosphenoid and orbitosphenoid also are present in this region, but their exact spatial relationships to the parabasisphenoid are difficult to determine even with CT. A

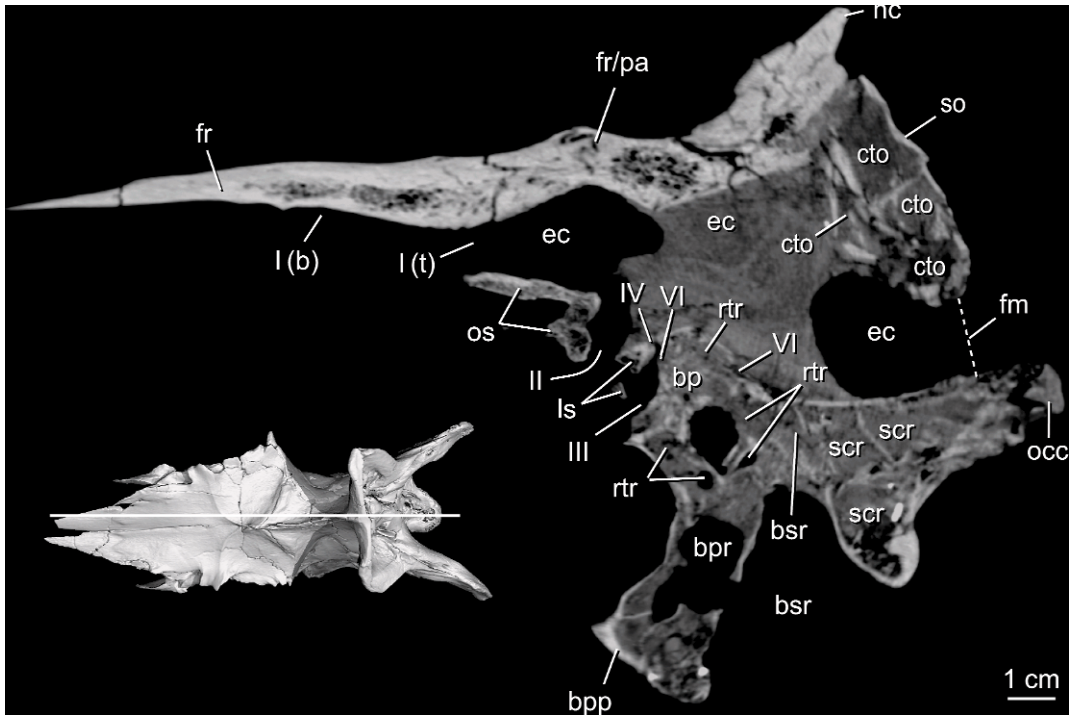

Fig. 18. CT slice along what is approximately the sagittal midline of the braincase of *Alioramus altai* (IGM 100/1844). The slice does not transect the cultriform process because distortion has shifted the process toward the left side of the specimen. See appendix 1 for anatomical abbreviations.

laterosphenoid-parabasisphenoid contact reflecting ossification of the pila antotica is the normal archosaurian condition (Bellairs and Kamal, 1981; Clark et al., 1993; Bhullar and Bever, 2009), which almost certainly was present in IGM 100/1844.

The parabasisphenoid contributes to the floor of the endocranial cavity, whose rostral limits are delineated by the dorsum sellae and sella turcica; the latter includes a deep pituitary (hypophyseal) fossa (fig. 10A). The paired abducens (VI) nerve and its associated vasculature emerge from the brainstem near the sagittal midline where they penetrate the caudal surface of the dorsum sellae (fig. 18). The abducens canal runs rostrolaterally and slightly dorsal through the dorsum sellae before emerging into a space in the lateral margin of the pituitary fossa that also housed the oculomotor (III) nerve and its associated veins, and probably the cerebral carotid arteries, although the latter do not leave a unique bony signature. This space, the sinus cavernosus (abducens-oculomotor fissure of Sampson and Witmer, 2007), is roughly delimited by the oribitosphenoid-laterosphenoid contact (dorsally) and the orbitosphenoid-parabasisphenoid contact (ventrally) (fig. 18B; see also Bever et al., 2011: fig. 7). Presence of a sinus cavernosus is the plesiomorphic condition for Archosauria, and the sinus is consistently present in non-coelurosaurian theropods. The derived loss of the sinus cavernosus is seen in all other known extinct and extant coelurosaurs, with the possible exception of the juvenile tyrannosaurid skull CMNH 7541 (Witmer and Ridgely, 2009: 1282) and now IGM 100/1844. As discussed by Bever et al. (2011), the retention of a sinus cavernosus in possibly two juvenile tyrannosaurid specimens suggests the initial loss of the sinus cavernosus in basal coelurosaurs was the result of a late-stage postnatal transformation. If correct, this transformation was subsequently pushed earlier in development (paedomorphosis),

resulting in the complete absence of a sinus cavernosus in the postnatal ontogeny of derived coelurosaurs, including crown birds.

The triangular cultriform process is 108 mm long and 52 mm deep at its proximal (caudal) base. It includes a horizontal dorsal margin and a concave ventral margin that ascends at a steep angle from its proximal base at the basipterygoid processes (fig. 3). Rather than quickly assuming a horizontal trajectory for the remainder of its length, as in *Gorgosaurus* (ROM 1247) and *Tyrannosaurus* (MOR 1125; Brochu, 2003: fig. 30), this margin continues along a slightly less steep rostrodorsal trajectory. The process becomes horizontal only at its distalmost end, where it meets the dorsal margin forming a sharp point. This shape is similar to that of *Guanlong*, in which the ventral margin is a smooth concave arch. It also resembles the long and deep process of juvenile *Tarbosaurus* (MPC-D 107/7) and *Tyrannosaurus* (CMNH 7541), whereas the process in subadult *Daspletosaurus* (TMP 1994.143.0001) is deep but short (although still with a curved ventral margin; Currie, 2003: fig. 26). This similarity suggests the shape of the process in IGM 100/1844 is at least partially a reflection of its immature stage of growth.

The lateral surfaces of the cultriform process are smooth and shallowly concave. This concavity is exaggerated by a thickened ventral margin—10 mm wide mediolaterally, compared to 5 mm for the dorsal margin—that reflects the excavation of the cultriform process by the the subsellar recess (fig. 2B). In contrast, the rostral 85 mm of the process is closed externally and smoothly rounded. A deep, thin trough, bordered on each side by a 1 mm thick wall, excavates the entire length of the rostum's dorsal surface. This trough likely housed a cartilage of the interorbital septum (Currie, 1997; Sampson and Witmer, 2007) that was confluent rostrally with the cartilage of the internasal septum. A low prominence at the caudal end of the dorsal margin of the cultriform process (fig. 3) may represent, at least functionally, the parasphenoid process of Currie (1985), which rises as a more vertical structure to demarcate the rostral margin of the hypophyseal fossa in some maniraptorans (e.g., Currie and Zhao, 1993; Bever and Norell, 2009; Norell et al., 2009).

The basipterygoid process, preserved only on the left side (fig. 3A), is located 38 mm ventral and 45 mm rostral to the basal tuber. Its ventral surface is convex, slightly rugose, and ovoid, with a long axis (26 mm) that extends caudolaterally-rostromedially and a minor axis of 15 mm. The roughened articular surface extends dorsally on the lateral and medial surfaces of the process. These extensions correspond to the fibrous capsule of the basisphenoid-pterygoid joint, whereas the smoother ventral articular surface was covered by hyaline cartilage (Holliday and Witmer, 2008). The extensions are seen in other tyrannosaurids, including *Gorgosaurus* (ROM 1247). In lateral view, the basipterygoid process is taller dorsoventrally than long rostrocaudally. The process in IGM 100/1844 is stout, a condition that is also seen in relatively immature tyrannosaurids, including *Daspletosaurus* (TMP 1994.143.0001), *Gorgosaurus* (ROM 1247), and *Tyrannosaurus* (CMNH 7541). In contrast, the process is a long, ventrally extending stalk in large, presumably more mature individuals, including *Daspletosaurus* (CMN 8506), *Gorgosaurus* (AMNH FARB 5458), and *Tyrannosaurus* (RSM 2523.8). The presence of a stout process in IGM 100/1844 is consistent with its subadult status, but it may also reflect the overall low form of the entire skull that is apomorphic in *Alioramus*. A relative lengthening of the process during the postnatal ontogeny of tyrannosaurs is in contrast to the more generally recognized trajectory in reptiles, in which is the process becomes stouter with age (e.g., Bever et al., 2005; Bhullar, 2012). The rostral corner of the process continues as a ridge that becomes confluent with the lateral bounding wall of the subsellar recess. Medially, a thick ridge connects the basipterygoid processes (''basipterygoid web'' of Bakker et al., 1988) and separates the subsellar and basipterygoid recesses (see below) from each other (figs. 2B, 19A). The parabasisphenoid is narrow in this region, as the ridge is only 21 mm wide.

A thickened crista ventrolateralis (''basicranial boxwork wall'' of Bakker et al., 1988) links the basipterygoid process with the basal tuber, forming the ventral margin of the

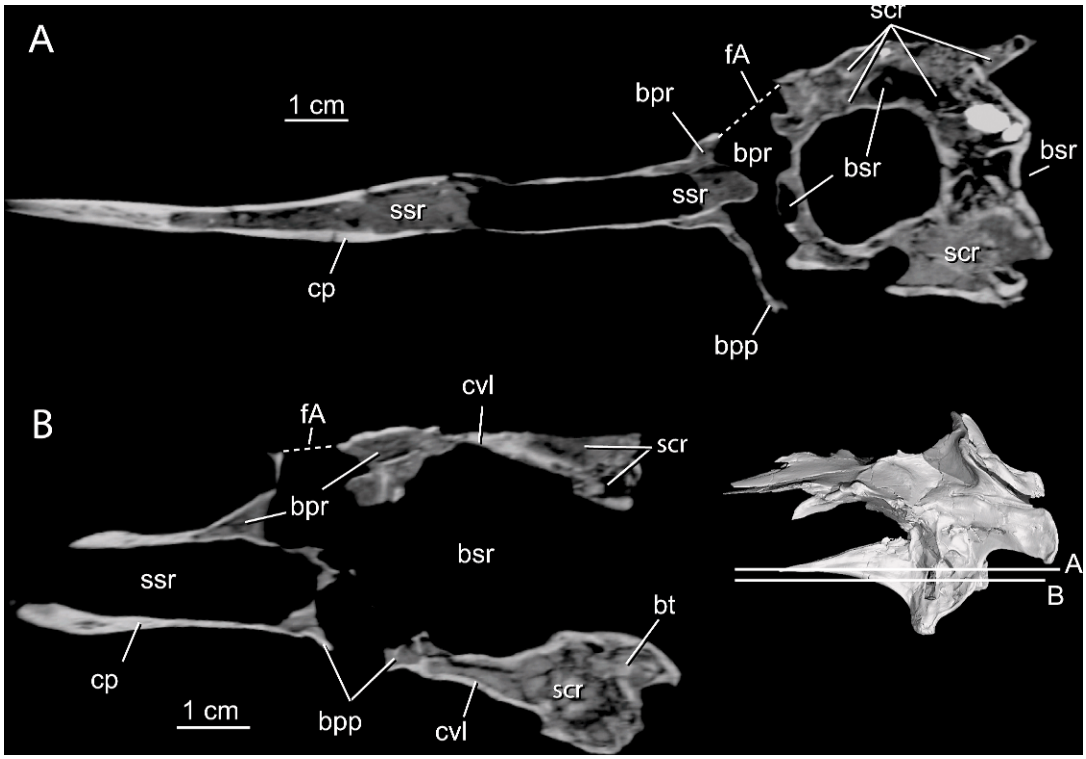

Fig. 19. Horizontal slices through the basicranium of *Alioramus altai* (IGM 100/1844) ventral to the endocranial cavity. Pneumatization of this region is complex and probably reflects diverticulae from multiple sources, although considerable communication between the resultant cavities does exist. See appendix 1 for anatomical abbreviations.

parabasisphenoid and bounding the ovoid basipterygoid recess laterally (figs. 2B, 19B). A lateral deflection of the crista demarcates a fossa (oval scar of Bakker et al., 1988) at the caudolateral corner of the ventral surface of the parabasisphenoid that is also present in all large tyrannosauroids (e.g., Currie, 2003: fig. 26), including *Alioramus remotus* (PIN 3141/1). The scar is present but not as clearly visible in *Tarbosaurus* and *Tyrannosaurus* because of their shortened and caudally oriented basisphenoid recesses. A similar fossa is present in nontyrannosaur theropods (e.g., *Ceratosaurus*: Madsen and Welles, 2000), absent in others (e.g., *Baryonyx*: Charig and Milner, 1997; *Majungasaurus*: Sampson and Witmer, 2007), but its presence is difficult to assess in most taxa due to poor preservation. The oval scar in IGM 100/1844 is smooth, similar to those seen in juvenile and subadult tyrannosauroids, including *Bistahieversor* (NMMNH P-25049), *Daspletosaurus* (TMP 1994.143.001), *Teratophoneus* (BYU 8120/1844), and *Tyrannosaurus* (CMNH 7541). In contrast, the texture of the oval scar is coarse in larger, presumably more mature individuals, as is seen in *Daspletosaurus* (CMN 8506), *Gorgosaurus* (ROM 1422), *Tarbosaurus* (ZPAL MgD-I/4), and *Tyrannosaurus* (AMNH FARB 5027). Three pneumatic recesses excavate the external surface of the parabasisphenoid—the basisphenoid recess, subsellar recess, and caudal tympanic recess (described below).

PROOTIC: The paired prootic contacts the laterosphenoid rostrally, parabasisphenoid rostroventrally, parietal dorsally, and otoccipital caudally. The sutural contacts with the parietal are difficult to see, but those with the laterosphenoid, parabasisphenoid, and otosphenoid are relatively clear in external view. A largely horizontal ridge, which extends

across the laterosphenoid rostrally and reaches the paroccipital process caudally, marks the dorsolateral surface of the prootic (fig. 20). The rostral length of this ridge can be referred to as the antotic crest, whereas the caudal portion, which runs above and caudal to the middle ear, is the otosphenoidal crest. If the ventrally extending preotic pendant is used to mark the positional boundary between these two structures, then the antotic crest is considerably shorter than the otosphenoidal crest. Together, these crests separate the lateral wall of the braincase from the supratemporal fossa dorsally. In large, presumably adult, *Daspletosaurus* (CMN 8506) and *Tyrannosaurus* (AMNH FARB 5117) the combined crest is prominent with a sharp lateral edge; the indistinct condition of the ridge in IGM 100/1844 likely is a reflection of its immaturity, as this condition is also seen in immature *Daspletosaurus* (TMP 1994.143.0001) and is known to characterize immature specimens of other reptile taxa (e.g., Bever et al., 2005; Bhullar, 2012).

The preotic pendant is a rugose, winglike flange that delineates the rostral margin of the rostral tympanic recess and anchors the pterygoideus muscles (Holliday and Witmer, 2008). The pendant is seen in all large tyrannosauroids, including *Bistahieversor* (NMMNH P-27469), *Daspletosaurus* (CMN 8506), *Gorgosaurus* (ROM 1247), *Tarbosaurus* (ZPAL MgD-I/4), *Teratophoneus* (BYU 8120/9396), and *Tyrannosaurus* (AMNH FARB 5117). The pendant is a common feature among theropods, although the bones comprising it are variable (Chure and Madsen, 1998; Sampson and Witmer, 2007) and often difficult to trace due to fusion (e.g., Currie, 1995; Norell et al., 2006). In IGM 100/1844, the pendant is formed solely by the prootic, as the prootic-parabasisphenoid suture is unfused and visible ventral and rostral to the pendant (fig. 20). In *Daspletosaurus*, the pendant is formed solely by the parabasisphenoid (Currie, 2003), whereas in *Tyrannosaurus* (AMNH FARB 5117), the pendant appears to receive contributions from both the parabasisphenoid and laterosphenoid. (Admittedly, the pendant in AMNH FARB 5117 is largely fused making its sutures difficult to trace.)

A tonguelike caudal process of the prootic extends above the middle ear and overlaps much of the rostral surface of the paroccipital process. The otosphenoidal crest runs along the dorsal margin of this caudal process. Lying between the caudal process and the preotic pendant is the superficial lamina of the prootic, which is characterized by two spikelike projections that cover the otic recess and the dorsocaudal portion of the rostral tympanic recess (fig. 20). A caudal process of the prootic is seen in nearly all other tyrannosauroids, including *Albertosaurus* (CMN 5600), *Bistahieversor* (NMMNH P-27469), *Daspletosaurus* (CMN 8506), *Gorgosaurus* (ROM 1247), *Tarbosaurus* (ZPAL MgD-I/4), *Teratophoneus* (BYU 8120/9396), and *Tyrannosaurus* (AMNH FARB 5117). A superficial lamina is absent in both *Guanlong* and *Dilong*.

The otic recess (external otic recess of Brochu, 2003) is present as a deep, funnellike fossa between the prootic and otoccipital. The rostral margin of the recess is marked by the confluence of the caudal process and superficial lamina of the prootic. Its caudal margin is formed by the paroccipital process. The dorsal portion of the recess is concealed from external view by the caudal process of the prootic, while its ventral portion is concealed by the more dorsal of the two secondary processes of the prootic's superficial lamina. The eroded right side of IGM 100/1844 reveals two openings in and around the recess (fig. 3B). These openings are also seen in *Bistahieversor* (NMMNH P-27469), *Daspletosaurus* (CMN 8506), *Gorgosaurus* (ROM 1247), *Tarbosaurus* (ZPAL MgD-I/3), *Teratophoneus* (BYU 8120/9396), and *Tyrannosaurus* juveniles (CMNH 7541; Witmer and Ridgley, 2009) and adults (AMNH FARB 5117). The larger, caudodorsal opening is the rostral foramen of the caudal tympanic recess, which penetrates the paroccipital process and is described with the otoccipital. The smaller, rostroventral opening is the otic recess proper (= stapedial recess or columellar canal). It is formed between the prootic and otoccipital, trends rostromedially into the braincase, and houses the fenestra vestibuli and fenestra pseudorotunda. The latter fenestra lies completely within the otoccipital. A space lying ventral to the superficial lamina communicates

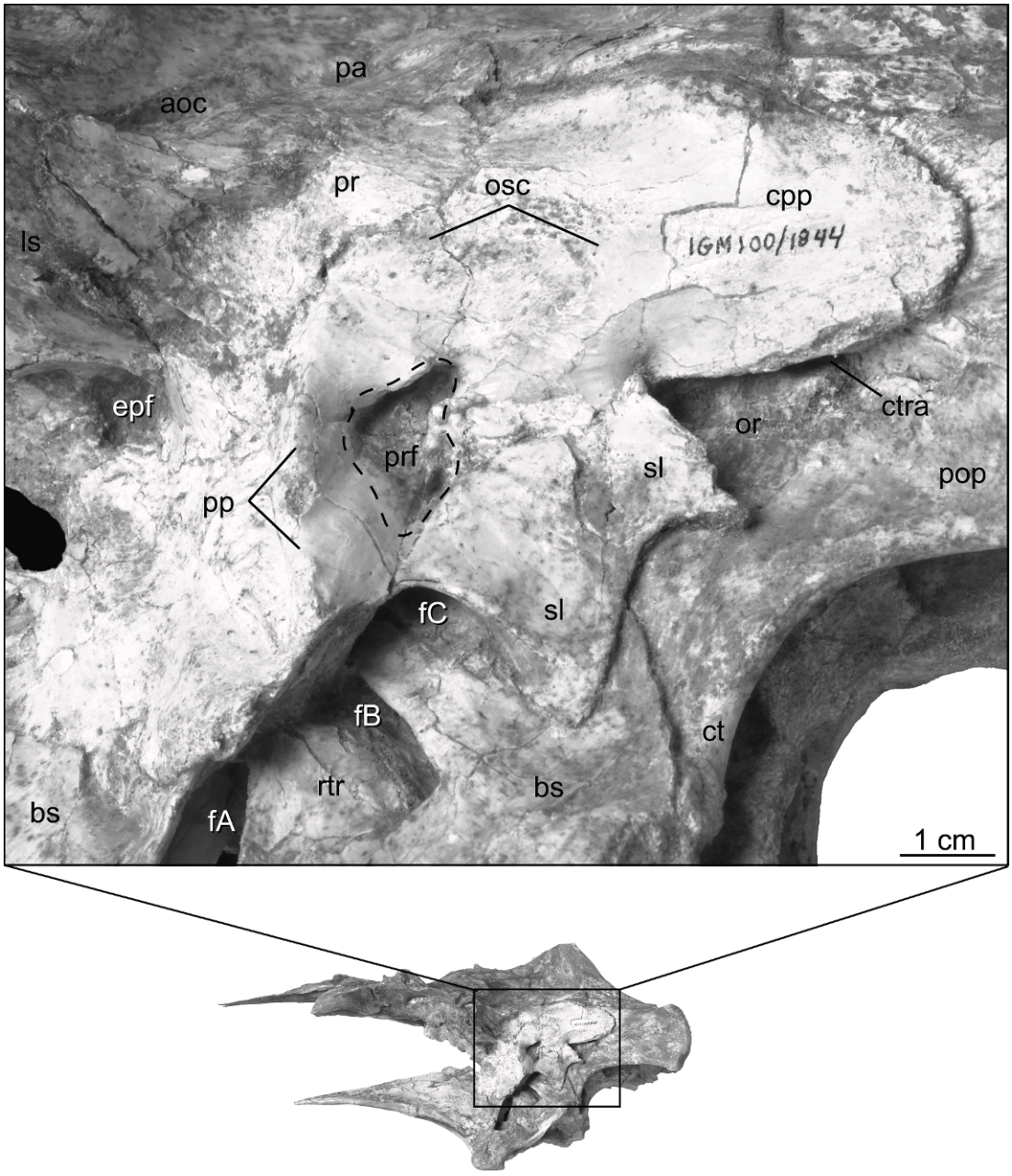

Fig. 20. Lateral surface of the left prootic (pr) and articulated surrounding structures of *Alioramus altai* (IGM 100/1844). See appendix 1 for other anatomical abbreviations.

with the otic recess, but it is unclear what, if any, neurovascular structures were communicated through this opening. The stapedial artery and glossopharyngeal (IX) nerve are two possibilities.

The otic recess in *Tyrannosaurus* (FMNH PR2081) is a slitlike aperture opening ventrally within the body of the prootic (Brochu, 2003). Extrapolating from this specimen, Brochu (2003) labeled a small incision within

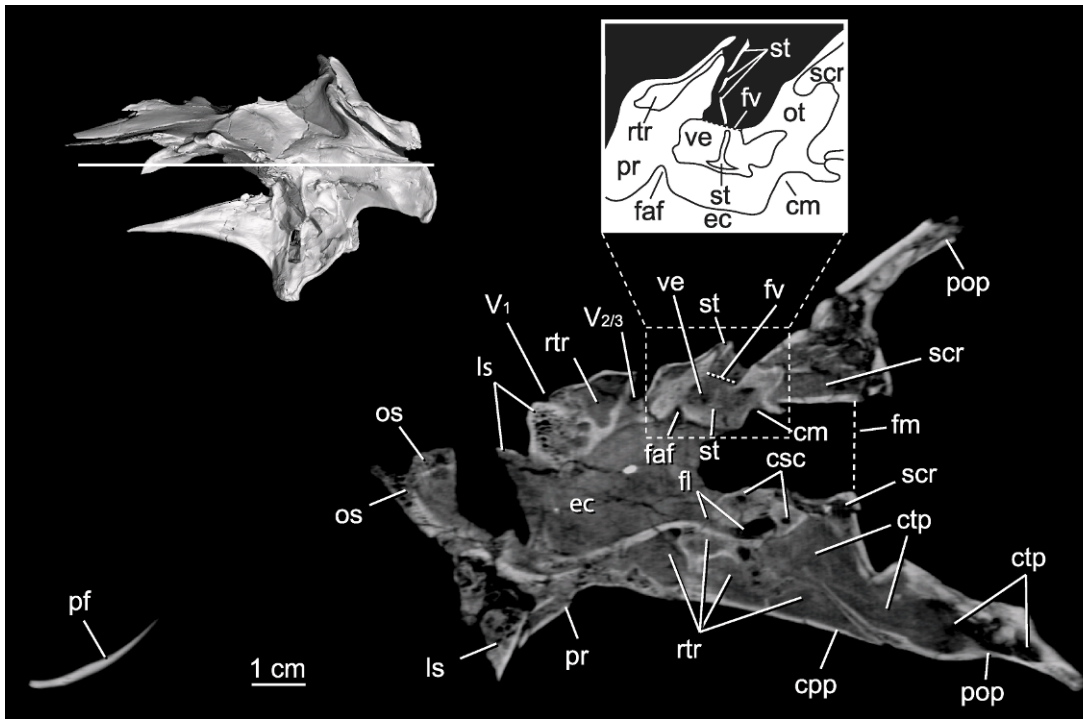

Fig. 21. Horizontal slice through the middle ear of *Alioramus altai* (IGM 100/1844). The associated line drawing highlights the broken stapes (st) whose proximal end (including the preserved footplate) has been pushed through the fenestra vestibule (fv) and is now lying within the vestibule of the inner ear (ve). See appendix 1 for other anatomical abbreviations.

the prootic of AMNH FARB 5117 as the stapedial recess. This structure, however, does not open into the otic capsule internally and appears to be a hairline crack. The otic recess in the AMNH specimen lies in the expected position between prootic and otoccipital. An alternative interpretation of the various foramina on the lateral wall of the tyrannosaur braincase was presented by Currie (2003: fig. 27). He considered the entire opening of the otic region between the prootic and otoccipital as the fenestra vestibuli, and the entire opening within the prootic (our ''prootic fossa'') as the facial foramen. This interpretation is correct in part, but it does not reflect the complexity of either structure, which is difficult to discern without exceptionally well-preserved braincases (e.g., AMNH FARB 5117 and IGM 100/1844) and/or CT data. The otic recess of *Dilong* is distinctly large, reflecting the plesiomorphic absence of the secondary process (superficial lamina) of the prootic.

The fenestra vestibuli, which would have housed the stapedial footplate, opens in a caudolateral direction in IGM 100/1844 (fig. 21), as opposed to the ventrolateral orientation described for *Tyrannosaurus* (Brochu, 2003). A broad, triangular, stapedial groove extends from this opening along the rostral surface of the paroccipital process. It becomes progressively less pronounced distally and eventually merges with the ventral edge of the paroccipital process. The right stapes is present but displaced medially, so that the stapedial footplate and a short length of the stapedial shaft now lie within the cavum labryinthicum, deep (medial) to the otic recess (fig. 21). The broken, distal length of the stapedial shaft remains within the otic recess in a position that probably reflects its natural orientation within the stapedial groove. The actual length of the stapedial shaft is not clear, but as in other tyrannosaurids (e.g., AMNH FARB 5117), it likely extended beyond the superficial lamina

of the prootic. The stapes is approximately 10 mm in total preserved length, with a footplate diameter of approximately 3.5 mm.

Rostral to otic recess and just caudal to the preotic pendant, the lateral surface of the prootic is excavated by a prominent fossa measuring 11 by 6 mm. This prootic fossa is subdivided into a large rostroventral pocket and a smaller caudodorsal subfossa (fig. 20; see also Bever et al., 2011: fig. 6). The rostral pocket houses a large foramen that transmitted the maxillomandibular branch of the trigeminal ($V_{2/3}$) nerve, whereas the caudal subfossa was penetrated by the palatine ramus of the facial (VII_1) nerve (see below; fig. 22). This observation agrees with that of Brochu (2002) and contra the interpretation of Saveliev and Alifanov (2007). The prootic fossa also contains a pair of small pneumatic foramina associated with the rostral tympanic sinus, which invests the bone surrounding the fossa. A small foramen that penetrates the caudal process of the prootic near the dorsal rim of the prootic fossa also communicates with the rostral tympanic recess and may have conveyed the rostral middle cerebral vein (see below; fig. 23). A prootic fossa housing the external foramina of the trigeminal and facial nerves is likely a synapomorphy of Tyrannosauroidea (Witmer and Ridgely, 2009, 2010; Tsuihiji et al., 2011) or a less inclusive tyrannosauroid subclade (Brusatte et al., 2010a). This ambiguity stems from the fact that its presence in the basalmost taxa, *Guanlong* and *Dilong*, is currently unclear (Bever et al., 2011). Regardless, the structure is present in *Albertosaurus* (CMN 5600), *Bistahieversor* (NMMNH P-27469), *Daspletosaurus* (CMN 8506), *Gorgosaurus* (ROM 1247), *Tarbosaurus* (ZPAL MgD-I/4), *Teratophoneus* (BYU 8120/9396), and *Tyrannosaurus* (AMNH FARB 5117).

There is no evidence of a dorsal tympanic recess, which, when present, is on the lateral surface of the prootic above the middle ear (Witmer, 1997; Rauhut, 2004). Absence of the dorsal tympanic recess is shared with other tyrannosaurids (*Alioramus remotus*: PIN 3141/1; *Daspletosaurus*: Currie, 2003; *Tarbosaurus*: ZPAL MgD-I/3, Hurum and Sabath, 2003; *Tyrannosaurus*: AMNH FARB 5117, Brochu, 2003). The recess is present in *Guanlong*, but the evolutionary history of this structure among nonavian coleurosaurians is complex and its homology with the avian dorsal tympanic recess is questionable (Elzanowski and Wellnhofer, 1996; Witmer, 1997; Rauhut, 2004; Sampson and Witmer, 2007). In any case, it is likely that the lack of a recess on the lateral surface of the prootic above the middle ear, whether or not it is homologous with the avian condition, characterizes a subclade of tyrannosauroids more derived than *Guanlong*.

LATEROSPHENOID: The right and left laterosphenoids are well preserved and their sutures are open and visible. The only exception is in the diencephalic region where compression has complicated the interpretation of bony contacts. The laterosphenoid overlaps the rostrodorsal margin of the prootic and the rostroventral margin of the parietal within the supratemporal fossa (the laterosphenoid contribution to the supratemporal fossa is large, and this bone is widely visible within the fossa in dorsal view). The capitate process of the laterosphenoid meets the articular peg of the frontal and a narrow process of the parietal to form an articular surface for the postorbital, as described above. A rostral contact with the orbitosphenoid and a rostroventral contact with the parabasisphenoid also are present. These contacts are seen in other large tyrannosauroids, including *Bistahieversor* (NMMNH P-25049), *Daspletosaurus* (CMN 8506), *Gorgosaurus* (ROM 1247), *Tarbosaurus* (ZPAL MgD-I/4), *Teratophoneus* (BYU 8120/9396), and *Tyrannosaurus* (AMNH FARB 5117).

The external surface of the laterosphenoid is marked by a robust antotic crest (fig. 18), to which presumably attached the circumorbital membrane that partitioned the adductor chamber from the orbital fossa (Sampson and Witmer, 2007). The rostrolateral surface of the laterosphenoid, with the prootic, forms the caudodorsal corner of the orbit. The antotic crest begins dorsally at the tip of the capitate process and extends caudoventrally for 30 mm before bifurcating. This bifurcation occurs within the laterosphenoid and is also seen in *Daspletosaurus* (TMP 1994.143.0001), *Gorgosaurus* (ROM 1247), *Tarbosaurus* (ZPAL MgD-I/3), and *Tyrannosaurus* (AMNH FARB 5117). The resultant dorsal ridge continues horizontally, eventually

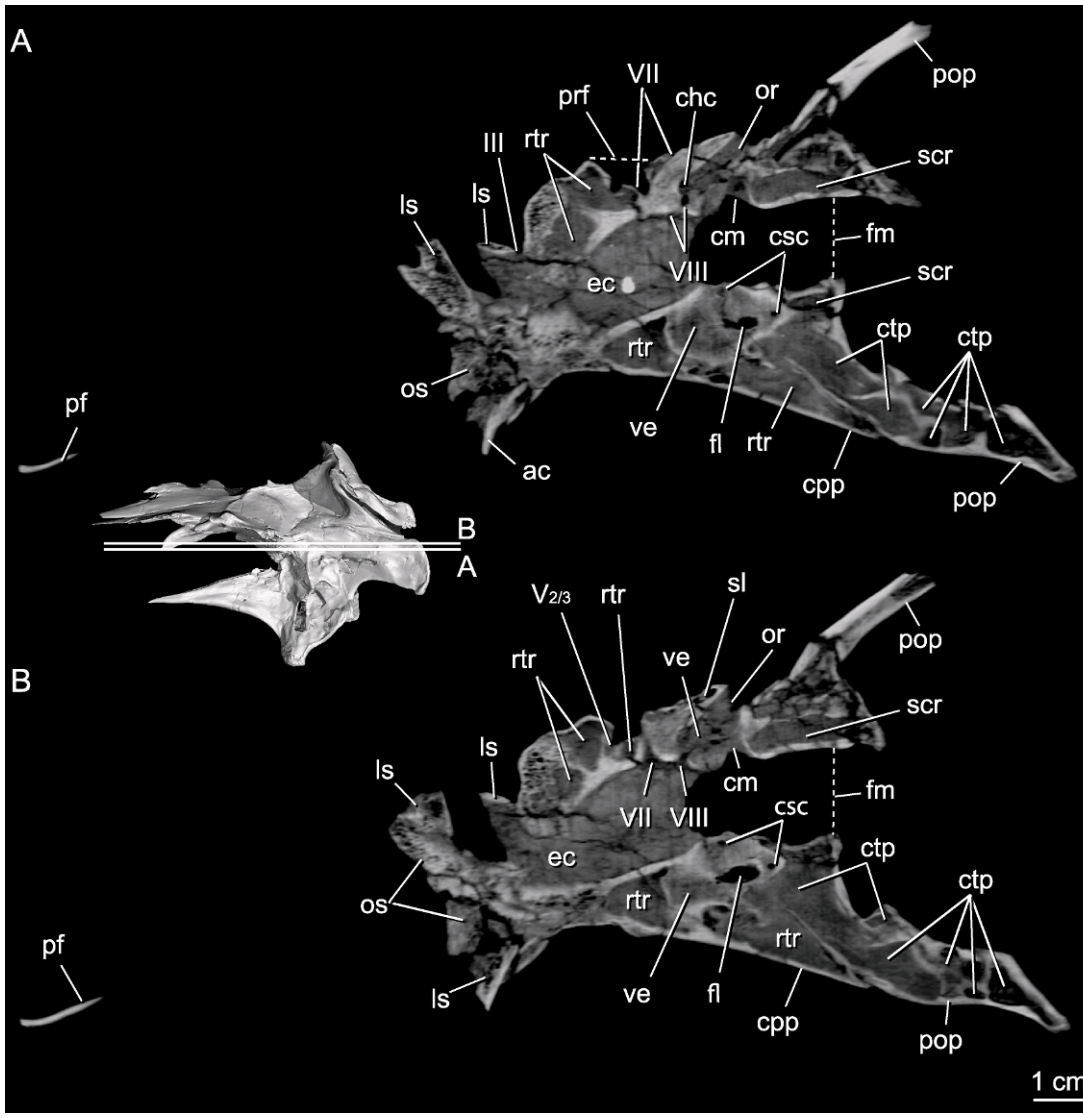

Fig. 22. Horizontal slices through the braincase of *Alioramus altai* (IGM 100/1844). The slices expose the ventral portion of the endocranial cavity (ec) and inner ear. See appendix 1 for other anatomical abbreviations.

merging with the otosphenoidal crest on the lateral surface of the prootic (see above).

The ventral ridge resulting from this bifurcation decreases in prominence as it descends and stops immediately rostrodorsal to the ovoid foramen for the ophthalmic branch (profundus nerve, V_1) of the trigeminal nerve. This foramen, which is present in other tyrannosauroids and is likely plesiomorphic for the group (Molnar, 1991; Brochu, 2003; Sampson and Witmer, 2007; Holliday and Witmer, 2008; Witmer and Ridgely, 2009, 2010), is located entirely within the laterosphenoid and is positioned 16 mm rostral to the prootic fossa (figs. 13B, 24). Between these two openings and within the bounds of the bifurcated rami of the antotic crest (thus rostral to the preotic pendant), the prootic and laterosphenoid are marked by a deep, triangular fossa that

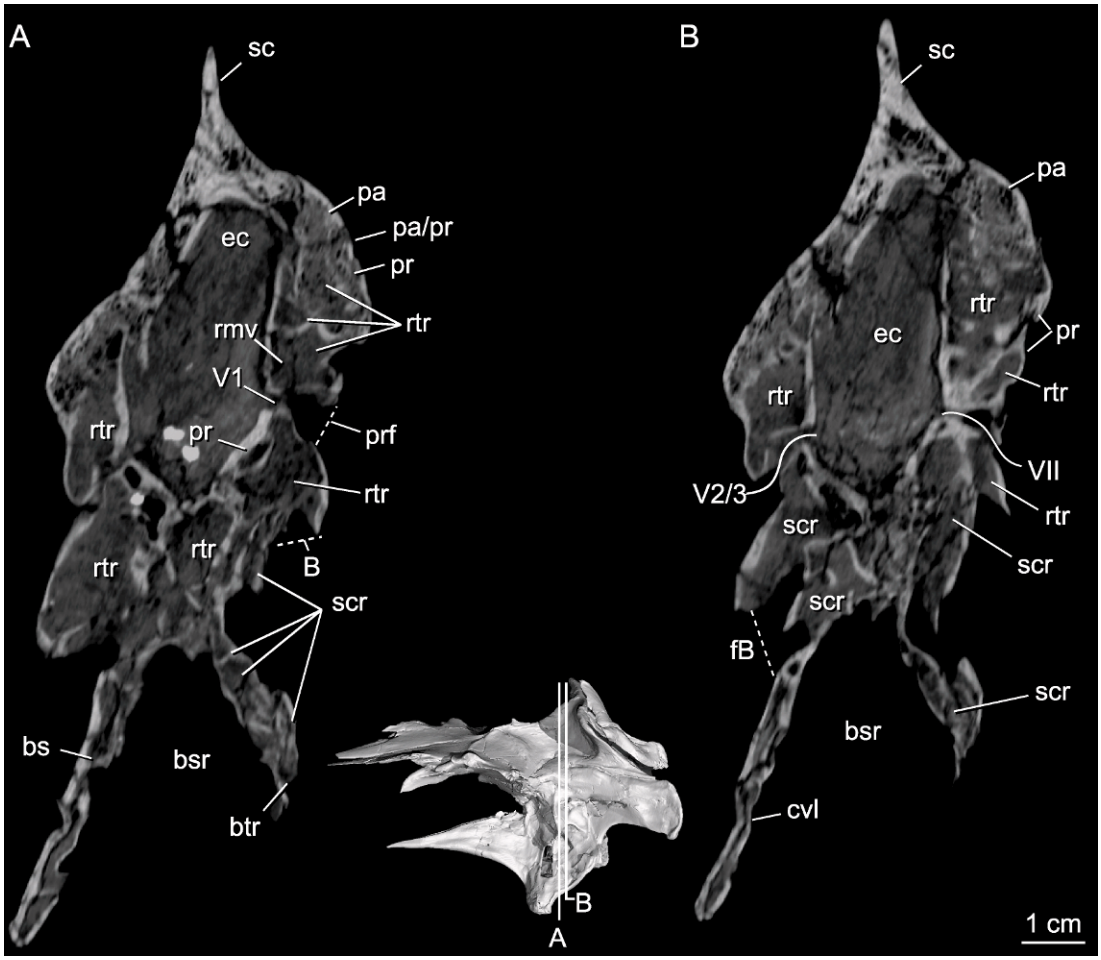

Fig. 23. Coronal slices through the braincase of *Alioramus altai* (IGM 100/1844). Both slices intersect the prootic fossa (prf). See appendix 1 for other anatomical abbreviations.

would have accepted the head of the epipterygoid and probably the origin of the m. levator pterygoideus (Holliday and Witmer, 2007, 2008). This fossa is seen in all large tyrannosauroids, including *Bistahieversor* (NMMNH P-25049), *Daspletosaurus* (CMN 8506), *Gorgosaurus* (ROM 1247), and *Tarbosaurus* (ZPAL MgD-I/4), *Teratophoneus* (BYU 8120/9396), and *Tyrannosaurus* (AMNH FARB 5117). The epipterygoid fossa in *Tyrannosaurus* (AMNH FARB 5117) is excavated by several subpockets and coarsened by numerous rugose lineations. The most common condition in Theropoda is to have the epipterygoid fossa restricted to the laterosphenoid, although a more rostral extension of this fossa onto the prootic was described for *Majungasaurus* and may represent the plesiomorphic condition for both Tyrannsauroidea and Theropoda (Sampson and Witmer, 2007).

There is no evidence that the rostral middle cerebral vein pierced the laterosphenoid of IGM 100/1844 through an independent canal as described for other tyrannosauroids (Witmer and Ridgely, 2009; identified as the trochlear nerve in Saveliev and Alifanov, 2007). The vein may have exited the braincase in a more caudal position (through the foramen positioned above the prootic fossa described above). It may also have exited through one of the two canals associated with the trigeminal

nerve—either with the maxillomandibular nerve through the prootic fossa or with the ophthalmic branch through the laterosphenoid. A maxillomandibular path for this vein was inferred for *Carcharodontosaurus saharicus* (Larsson, 2001). There is also no evidence in IGM 100/1844 for a foramen that conducts the oculomotor nerve through the rostroventral portion of the laterosphenoid, as described for juvenile *Tarbosaurus* (Tsuihiji et al., 2011), which supports our interpretation that this nerve exited through the slightly more rostrally positioned sinus cavernosus (see below).

ORBITOSPHENOID: The paired orbitosphenoids are eroded both rostrally and ventrally. Both bones are rotated somewhat counterclockwise relative to the remainder of the braincase. This is largely a product of their unfused and displaced contact with the overlying frontals. The original contact surface with the frontals is visible as a roughened and thick caudal region of the crista cranii. The right orbitosphenoid is pushed medially relative to the left orbitosphenoid resulting in an artifactual ventral keel. Displacement is along a midline crack that may represent an unfused suture or more likely a sagittal fracture. This midline suture appears to fully fuse in at least some mature tyrannosaurids (e.g., *Tyrannosaurus*; AMNH FARB 5117). Together, the paired orbitosphenoids form a cuplike structure that supports the overlying olfactory (I) tracts.

The orbitosphenoids contact the laterosphenoids caudolaterally along a broad, overlapping suture (fig. 13B). This suture ends ventrally at the dorsal margin of the sinus cavernosus, whose rostral and caudal margins are formed by the orbitosphenoid and laterosphenoid, respectively. The sinus cavernosus transmitted the oculomotor (III), trochlear (IV), and abducens (VI) nerves and their associated vasculature (Sedlmayer, 2002) to the orbital wall (fig. 18A). The relative contribution of the oculomotor nerve to this fissure is not delineated in bone. The trochlear nerve and its associated vein passed through a small foramen penetrating the orbitosphenoid-laterosphenoid suture near its ventral end. As in *Tyrannosaurus* (Brochu, 2003; Witmer and Ridgely, 2009), the diameter of the trochlear foramen is greater than that of the abducens canal.

The orbitosphenoid contacts the parabasisphenoid caudoventrally along a narrow, abutting suture that forms the rostroventral margin of the cavernous sinus (fig. 18). The cavernous sinus and the optic (II) canal are partially confluent in this region, communicating via a constricted gap that may reflect, at least in part, damage to the orbitosphenoid. The optic nerve exited the braincase rostromedial to the orbitosphenoid, as expected. The right and left optic foramina are confluent along the midline (i.e., not separated by a bony strut), perhaps reflecting an unossified interorbital septum.

ETHMOID COMPLEX: An ossified sphenethmoid/mesethmoid complex was either not ossified or not preserved in IGM 100/1844. As mentioned above, crescentic scars surrounding the olfactory bulb depressions laterally and rostrally, as well as a coarse midline scar extending rostral to the bulb depressions, mark the ventral surface of the frontal. Similar scars indicate the presence of a sphenethmoid and mesethmoid in other theropod taxa (e.g., Ali et al., 2008; Sereno and Brusatte, 2008). As the orbitosphenoid is clearly eroded rostrally, it is possible that an ossified sphenethomid and mesethmoid were simply eroded away. An ossified interorbital septum, linking the ethmoid complex and cultriform process, is clearly absent in IGM 100/1844, as the well-preserved dorsal margin of the cultriform process is marked by a deep trough that likely housed cartilage associated with the septum. Whether or not this trough supported such a cartilage, it is clear that its dorsal surface is original bone and did not support an ossified sheet. Ossified sphenethmoids and mesethmoids are common in large tyrannosaurid specimens (Ali et al., 2008), but ossified interorbital septa have yet to be described for tyrannosauroids (although they are common in some other large-bodied theropods: e.g., Sampson and Witmer, 2007; Brusatte and Sereno, 2008).

PNEUMATIC RECESSES AND CAVITIES

The braincase of IGM 100/1844, like that of all known tyrannosauroids, is highly pneuma-

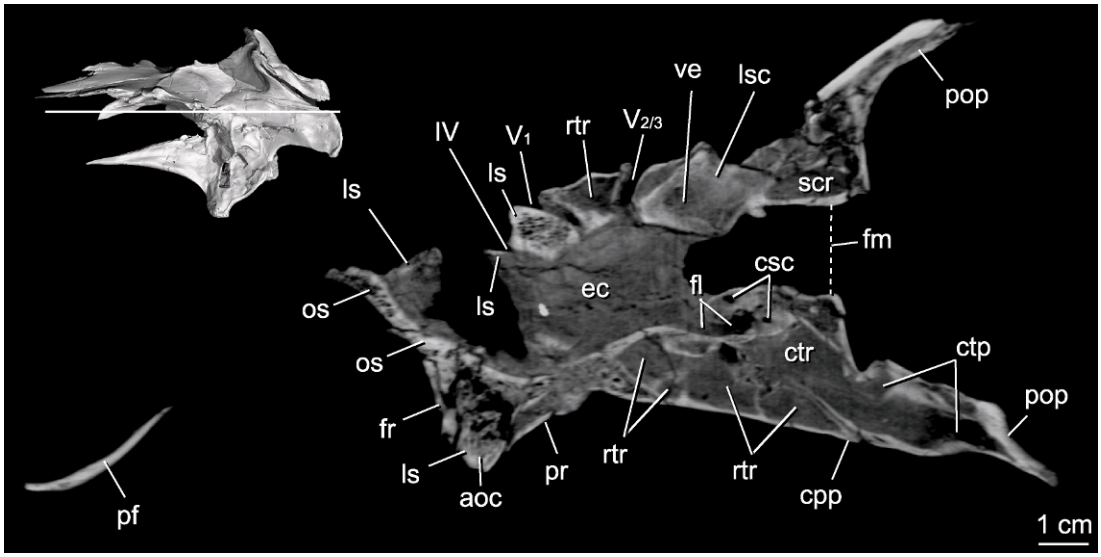

Fig. 24. Horizontal slice through the braincase of *Alioramus altai* (IGM 100/1844) showing the separate canals for the ophthalmic (V_1) and maxillomandibular ($V_{2/3}$) branches of the right trigeminal nerve projecting from a shared fossa within the endocranial cavity. See appendix 1 for other anatomical abbreviations.

tized. A series of five complex internal pneumatic cavities are associated with five external recesses and include: rostral tympanic, caudal tympanic, basisphenoid, subsellar, and subcondylar recess/cavity complexes (fig. 25). The origins of these spaces are divided between diverticula of the tympanic, median pharyngeal, and subcondylar sinuses (Russell, 1970; Bakker et al., 1988; Molnar, 1991; Witmer, 1997; Brochu, 2003; Rauhut, 2004; Witmer and Ridgely, 2009, 2010). All tyrannosauroids lack the subotic recess of ornithomimosaurs and some troodontids (Currie, 1985; Makovicky and Norell, 1998; Makovicky et al., 2003; Xu et al., 2002; Tahara and Larsson, 2011) with the possible exception of *Teratophoneus* (Carr et al., 2011). Additionally, the pneumatic recess that excavates the lateral surface of the cultriform process above the basipterygoid recess and ventral to the pituitary fossa region in some troodontids (Xu et al., 2002) and the basal dromaeosaurid *Sinornithosaurus* (Xu and Wu, 2000) is absent.

ROSTRAL TYMPANIC RECESS AND CAVITY: The rostral tympanic recess excavates the lateral surface of the parabasisphenoid and prootic and is delimited rostrodorsally by the preotic pendant (fig. 3). This recess is absent in some maniraptorans (e.g., Norell et al., 2004, 2006), but it is present in most basal theropods and other basal coelurosaurs (Rauhut, 2004), including all known tyrannosauroids (Witmer and Ridgely, 2009, 2010). The tyrannosauroid recess is often an overlooked, subtle feature. For example, Chure and Madsen (1996, 1998) considered this recess, which they termed the *lateral basisphenoid depression*, a feature uniquely shared by the puzzling theropod genus *Itemirus* and an isolated braincase from the Morrison Formation (UMNH 2455), and stated that no tyrannosaurids possess pneumaticity in this region of the braincase. In fact, this recess is present in tyrannosaurids, but it is often less pronounced than the other pneumatic recesses of the braincase. Among tyrannosaurids, *Alioramus altai* possesses a particularly prominent rostral tympanic recess, which is larger, deeper, and more discrete than that of *Albertosaurus* (CMN 5600), *Daspletosaurus* (Currie, 2003), *Gorgosaurus* (ROM 1247), *Tarbosaurus* (ZPAL MgD-I/4), *Teratophoneus* (BYU 8120/9396), or *Tyrannosaurus* (AMNH FARB 5117).

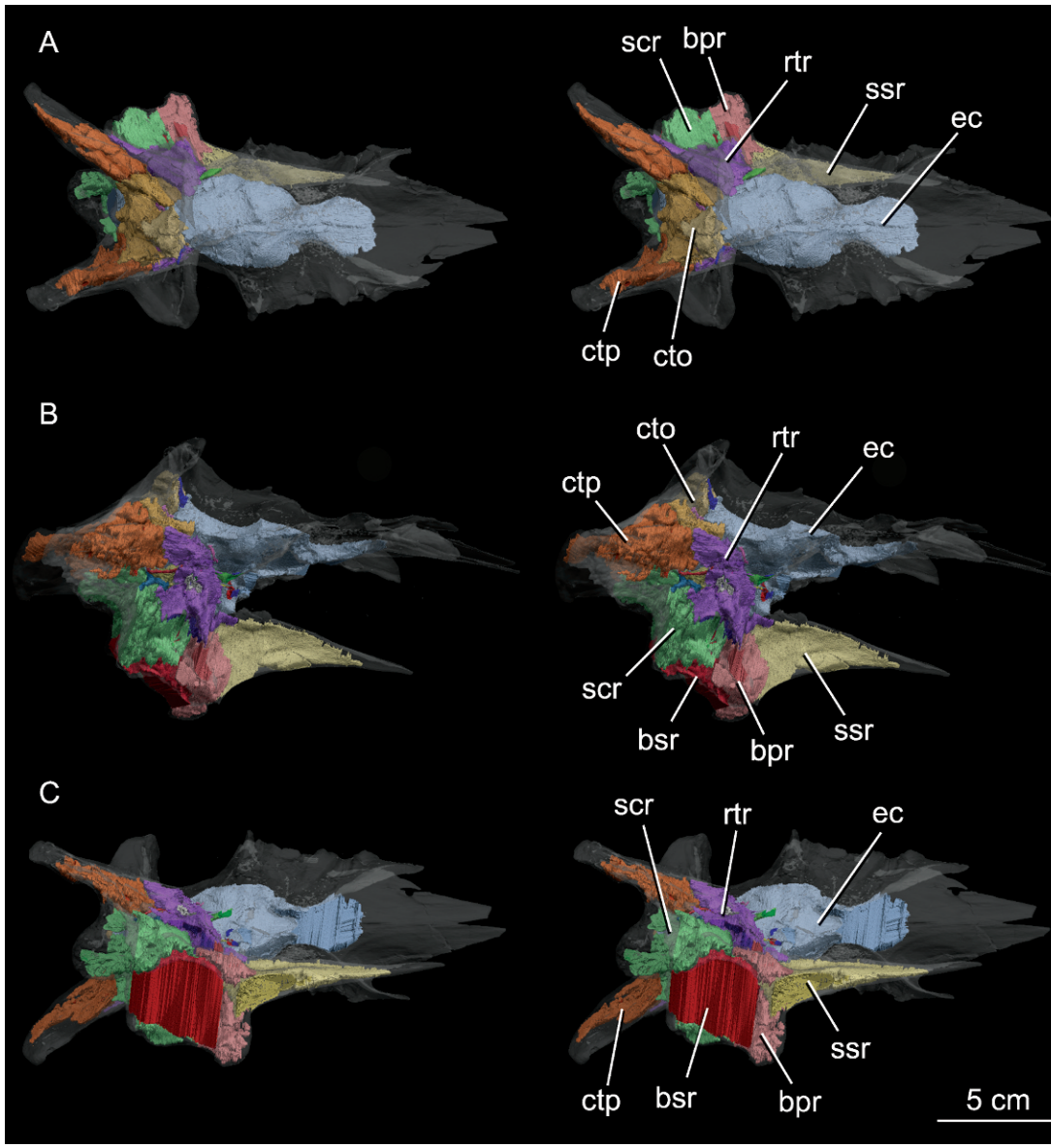

Fig. 25. Stereopairs of the articulated braincase of *Alioramus altai* (IGM 100/1) showing the pneumatic sinuses of the neurocranium in dorsal (**A**), right lateral (**B**), and ventral views (**C**). The braincase itself is rendered transparent to reveal the enclosed sinus cavities, as well as the endocranial (ec) and inner ear cavities, that were digitally segmented and reconstructed. See appendix 1 for other anatomical abbreviations. Modified from Bever et al. (2011: fig. 2).

Guanlong also possesses a corresponding recess that is proportionally deeper and larger than that in derived tyrannosaurids (except for *Alioramus*).

The rostral tympanic recess in IGM 100/1844 circumscribes three fenestra-sized openings (hereafter referred to as A, B, and C; fig. 26). The largest of these (A) penetrates the lateral surface of the basipterygoid process and, unlike B and C, which open directly into the expansive rostral tympanic cavity, fenestra A opens into a cavity filling

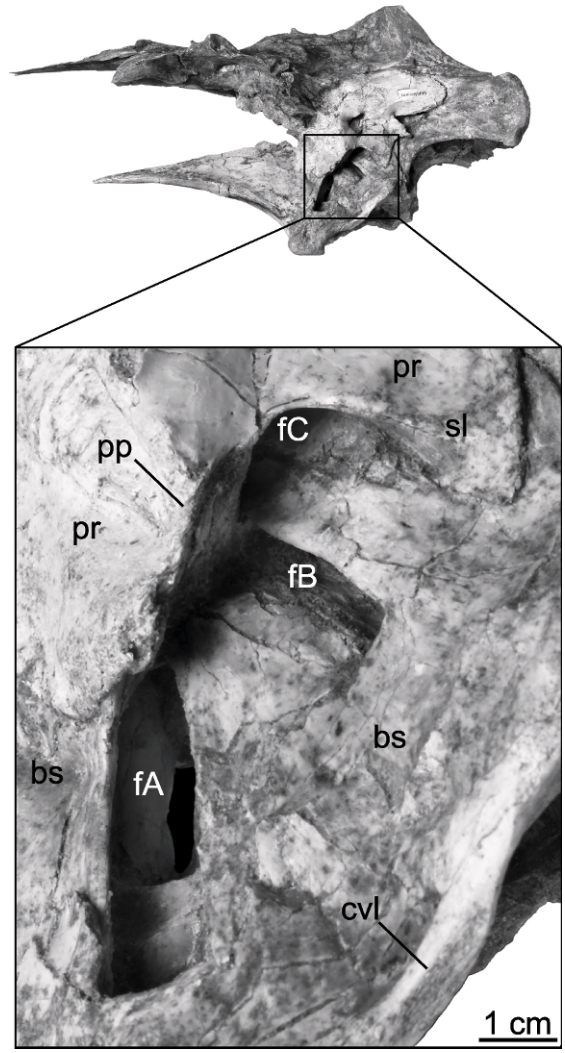

Fig. 26. The ventral portion of the left rostral tympanic recess in *Alioramus altai* (IGM 100/1844). This region is characterized by three large fenestrae: fenestra A (fA) opens into a pneumatic cavity that invests the basipterygoid process and is generally associated with the basisphenoid recess; fenestra B (fB) and fenestra C (fC) open directly into the rostral tympanic cavity. See appendix 1 for other anatomical abbreviations.

the basipterygoid process (figs. 10B, 13, 18A). Fenestra A and its associated cavity are sometimes referred to collectively as the basipterygoid recess and are broadly confluent internally with a pneumatic cavity enclosed by the parabasisphenoid (see Basisphenoid Recess below). This opening is also seen in juvenile *Bistahieversor* (NMMNH P-25049), juvenile *Daspletosaurus* (TMP 1994.143.0001), and in juvenile *Tarbosaurus* (MPC-D 107/7; Tsuihiji et al., 2011: fig. 4B). Fenestra A is absent from *Gorgosaurus* (ROM 1247), *Tarbosaurus* (ZPAL MgD-I/3), *Teratophoneus* (BYU 8120/9396), and *Tyrannosaurus* (AMNH FARB 5117).

The second opening circumscribed by the rostral tympanic recess (B) is rectangular with its long axis trending strongly rostro-

dorsal-caudoventral. Fenestra B is also present in juvenile *Daspletosaurus* (TMP 1994. 143.0001; Currie, 2003: fig. 26A) but is not seen in *Gorgosaurus* (ROM 1247), *Tarbosaurus* (ZPAL MgD-I/4), *Teratophoneus* (BYU 8120/9396), or in *Tyrannosaurus* (AMNH FARB 5117). The preotic pendant obscures its dorsal margin in lateral view. The fenestra may have communicated a diverticulum of the tympanic sinus, but it was also likely traversed by the cerebral carotid artery, whose bifurcation into the cerebral carotid and palatine arteries must have occurred external to the braincase. Pneumatization of the parabasisphenoid and a slight compression of the floor of the pituitary fossa obscure the path of the cerebral carotid artery through the basicranium (fig. 27).

The third and most caudal penetration of the rostral tympanic recess (C) is exposed in lateral view as a narrow slit between the parabasisphenoid and prootic. This slit opens dorsomedially and is positioned behind the dorsal margin of fenestra B and below the prootic fossa (fig. 27). The same opening is not seen in *Gorgosaurus* (ROM 1247), *Tarbosaurus* (ZPAL MgD-I/4), or *Tyrannosaurus* (AMNH FARB 5117), but a possible homolog penetrates the ventrolateral surface of the superficial lamina of the prootic in a juvenile specimen of *Daspletosaurus* (TMP 1994.143.0001; Currie, 2003: fig. 26A).

The rostral tympanic cavity is comprised of a series of smaller, confluent chambers that fill the dorsal portions of the parabasisphenoid, the caudoventral corner of the laterosphenoid, and most of the prootic (figs. 10B, 13, 15, 21–24, 27). A significant ascending diverticulum reaches, but does not extend through, the prooticoparietal suture. It clearly extended between the ophthalmic and maxillomandibular canals of the trigeminal nerve—a condition shared with *Gorgosaurus*, CMNH 7541, and a juvenile specimen of *Tarbosaurus*, but lacking in *Daspletosaurus* and adult *Tyrannosaurus* (Witmer and Ridgely, 2009, 2010; Tsuihiji et al., 2011). The sinus failed to invest the otoccipital, but it extends above the middle ear, reaching the distal tip of the caudal process of the prootic. The cavity is confluent caudoventrally with the subcondylar recess, which lies near and may be partially confluent with fenestra A. The right and left cavities form a contralateral communication behind the pituitary fossa. This retrohypophyseal space also is present in *Gorgosaurus*, *Tyrannosaurus* and CMNH 7541 (Witmer and Ridgely, 2009, 2010). The prohypophyseal cavity of *Gorgosaurus* and CMNH 7541, which is absent in adult *Tyrannosaurus*, also is not seen in IGM 100/1844. In contrast to *Tyrannosaurus*, the rostral tympanic cavity extends beneath the pituitary fossa and may have formed a contralateral communication rostral to the fossa, a region that is not enclosed in bone. The rostral tympanic cavity surrounds the trigeminal and facial canals within the prootic and communicates with the lateral surface of the braincase through the prootic fossa.

Caudal Tympanic Recess and Cavity: The caudal tympanic recess excavates the lateral surface of the otoccipital and rostral surface of the paroccipital process below the otosphenoidal crest. The recess, which is present in most coelurosaurs, but is absent outside of this group (Witmer, 1990, 1997; Brusatte and Sereno, 2007; Sampson and Witmer, 2007; Brusatte et al., 2010b; Tahara and Larsson, 2011), is pierced by a foramen set caudolateral to the stapedial recess (in the base of the paroccipital process) and opens into the caudal tympanic cavity (fig. 20). This opening is seen in *Bistahieversor* (NMMNH P-25049), *Daspletosaurus* (CMN 8506), *Gorgosaurus* (ROM 1247), *Tarbosaurus* (ZPAL MgD-I/3), *Teratophoneus* (BYU 8120/9396), and *Tyrannosaurus* (AMNH FARB 5117).

In IGM 100/1844, a second, larger foramen opens into the cavity through the caudodorsal margin of the paroccipital process (fig. 28). This foramen is also seen in *Daspletosaurus* (CMN 8506), *Gorgosaurus* (ROM 1247), *Tarbosaurus* (ZPAL MgD-I/3), *Teratophoneus* (BYU 8120/9396), and *Tyrannosaurus* (AMNH FARB 5117). A caudodorsal foramen is seen in other coelurosaurs (e.g., Kobayashi and Barsbold, 2005), but its presence is highly variable. For example, a caudal foramen, nearly identical to that of IGM 100/1844, penetrates the paroccipital process of *Tyrannosaurus* (FMNH PR2081), but only on the right side (Brochu, 2003).

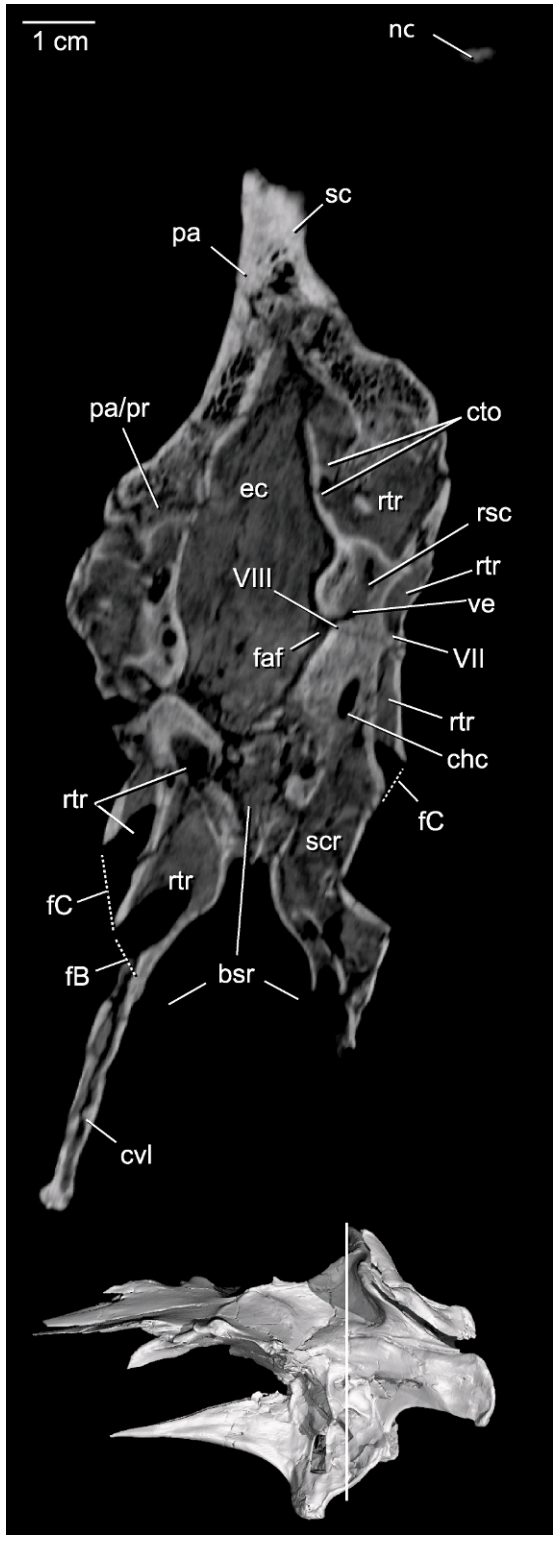
1 cm
nc
sc
pa
pa/pr
cto
ec
rtr
rsc
rtr
VIII
ve
faf
VII
rtr
chc
rtr
fC
scr
rtr
fC
fB
bsr
cvl

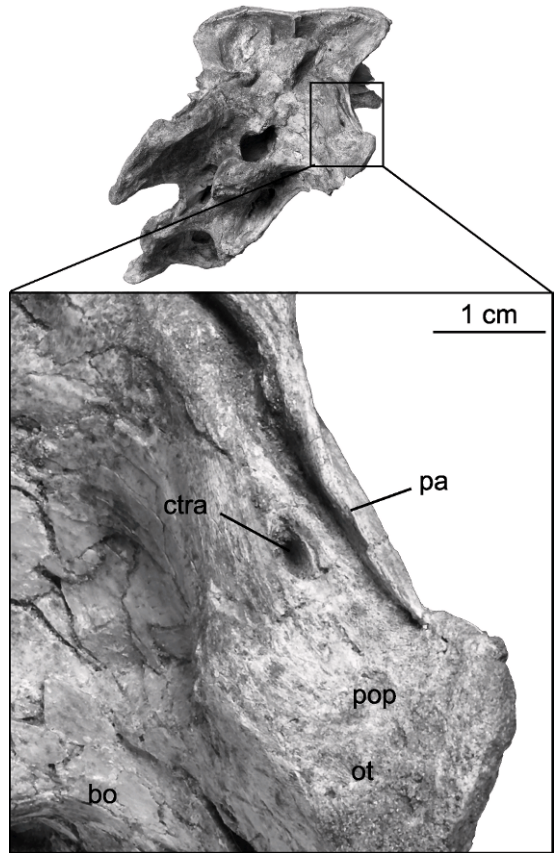

Fig. 28. The dorsocaudal surface of the paroccipital process (pop) of *Alioramus altai* (IGM 100/1844). Note the thin process of the parietal (pa) that participates in the process and the relatively large foramen (ctra), which communicates directly with an internal cavity of the caudal tympanic recess. See appendix 1 for other anatomical abbreviations.

The caudal tympanic cavity pneumatizes nearly the entire length of the paroccipital process, but it is largely restricted to the dorsal two-thirds of the structure (fig. 12). The cavity is partitioned distally into a complex array of smaller chambers and achieves its greatest volume proximally, where it forms a large chamber lateral to the hindbrain region of the endocranial cavity. A dorsally positioned and subdivided chamber is also seen in *Tyrannosaurus* (AMNH FARB 5117). In IGM 100/1844, the ventral extension of this proximal chamber is confluent with the subcondylar recess (figs. 16A, 22); this is a shared feature of IGM 100/1844 and CMNH 7541. In contrast, this connection is not seen in adult *Tyrannosaurus* or in *Gorgosaurus* (Witmer and Rid-

←

Fig. 27. Coronal slice through the braincase of *Alioramus altai* (IGM 100/1844). Fenestra A (fA) and fenestra B open directly into an expanded rostral tympanic cavity (rtr) that includes a chamber lying directly over the inner ear. The basisphenoid recess (bsr) nearly penetrates the floor of the endocranial cavity (ec). See appendix 1 for other anatomical abbreviations.

gely, 2009, 2010) and may disappear late in tyrannosaurid postnatal ontogeny.

The proximal chamber is confluent dorsally with an expanded, tripartite extension of the caudal tympanic cavity that is housed within the supraoccipital (figs. 11–13). This supraoccipital cavity consists of a dorsal midline chamber and two ventrolateral chambers that extend parasagittally to flank the medullary portion of the hindbrain. Together these chambers fill nearly the entire volume of the supraoccipital. A caudal tympanic cavity comprised of confluent paroccipital and supraoccipital chambers is also present in *Gorgosaurus*, *Daspletosaurus*, *Tyrannosaurus*, and CMNH 7541 (Russell, 1970; Brochu, 2003; Witmer and Ridgely, 2009), but its presence in *Tarbosaurus* has been questioned (Brochu, 2003). Regardless, the presence of this cavity is likely plesiomorphic for Tyrannosauridae, if not Tyrannosauroidea. The parasagittal and dorsal midline cavities are separated by internal bony partitions for most of their length, and a clear connection is present rostrally. The parasagittal chambers are separated from each other caudally by a thin wall that extends vertically from the dorsal apex of the endocranial cavity along the sagittal midline. As the endocranial cavity expands rostrally, the parasagittal chambers lose their midline contact, as in *Gorgosaurus*, CMNH 7541, and adult *Tyrannosaurus* (Witmer and Ridgely, 2009). These chambers lie directly over the vestibular cavity of the inner ear (fig. 27), extending rostrally distinctly further than their dorsal, midline counterpart. With regard to the relative size and postion of the midline and parasagittal chambers, the condition of IGM 100/1844 more closely resembles the morphology of *Gorgosaurus* than that of CMNH 7541 or *Tyrannosaurus* (Witmer and Ridgely, 2009). The parasagittal chambers exhibit small, but distinct, internal connections with the rostral tympanic cavity. It is unclear whether similar internal connections are present in other tyrannosaurids.

Basisphenoid Recess and Cavity: The basisphenoid pneumatic complex includes a caudal and rostral component. The caudal component is expressed as a deep, funnel-shaped basisphenoid fossa, filling the space in the parabasisphenoid between the basipterygoid processes and basal tubera (figs. 10, 12, 13, 16A, 18, 19, 23, 27). The rostral component invests the basipterygoid processes and is thus referred to as the *basipterygoid cavity*.

This basisphenoid fossa measures 50 mm rostrocaudally by 35 mm mediolaterally (fig. 2B). Its presence is plesiomorphic for tyrannosauroids and is retained in all known tyrannosauroid taxa including *Guanlong*, although in this taxon, as in many other theropods (e.g., ornithomimosaurs; Makovicky and Norell, 1998; Tahara and Larsson, 2011), the fossa widens caudally rather than exhibiting the ovoid or circular shape present in IGM 100/1844. The fossa of *Guanlong* and many other coelurosaurs (e.g., Kurzanov, 1976; Currie, 1995; Makovicky and Norell, 1998; Kirkland et al., 2005; Norell et al., 2006) also differs from the seemingly derived tyrannosaurid condition (e.g., IGM 100/1844, *Albertosaurus*, *Alioramus remotus*, *Bisahieversor*, *Daspletosaurus*, *Gorgosaurus*) in opening ventrally and being obscured in caudal view rather than opening caudoventrally and being visible in caudal view. This "derived" condition also is present in ornithomimids (Tahara and Larsson, 2011), complicating its phylogenetic polarity.

Tarbosaurus (ZPAL MgD-I/3; Hurum and Sabath, 2003) and *Tyrannosaurus* (AMNH FARB 5117, CMNH 7541; Brochu, 2003) share a unique and highly derived morphology in which the basicranium is rostrocaudally shortened so that the basipterygoid processes lie nearly underneath the basal tubera (Carr, 1999; Brochu, 2003: fig. 30). The result is an extreme reduction of the basisphenoid fossa (Carr, 1999; Witmer and Ridgely, 2009). A similar morphology is seen in the oviraptorosaur *Chirostenotes* (Sues, 1997) and the spinosaurids *Baryonyx* (Charig and Milner, 1997) and *Irritator* (Sues et al., 2002). The basisphenoid fossa in IGM 100/1844 terminates dorsally deep in the floor of the parabasisphenoid as blind parasagittal pockets communicating only with each other above a thin bony septum (figs. 18, 27). Similar pockets are present at least in *Albertosaurus* among tyrannosaurs (Currie, 2003: 213), as well as a variety of other theropods (e.g., Chure and Madsen, 1998; Norell et al., 2004, 2006; Sampson and Witmer, 2007). The *Albertosaurus* condition

includes a medial depression rostral to the pockets that is absent in IGM 100/1844.

The rostral wall of the basisphenoid fossa contains a pair of bilateral openings confluent with a paired internal cavity (figs. 2B, 29). These openings are also seen in *Albertosaurus* (CMN 5600), *Bistahieversor* (NMMNH P-25049), *Daspletosaurus* (TMP 1994.143.0001), *Gorgosaurus* (ROM 1247), and *Tyrannosaurus*. Instead of openings, depressions are seen in this position in *Teratophoneus* (Carr et al., 2011). This cavity extends the entire internal length of the basipterygoid processes and represents the rostral component of the basisphenoid recess (Witmer and Ridgely, 2009). The right and left cavities are broadly confluent along the median plane. The sinus also invests the crista ventrolateralis, which connects the basipterygoid processes with the more caudal basal tubera, resulting in a confluence with the rostral extension of the subcondylar cavity. The basipterygoid cavity opens onto the lateral surface of the basipterygoid process through the large fenestra A, positioned inside the rostral tympanic recess and measuring 28 × 10 mm (see above). A lateral recess of the basipterygoid process is common among theropods (Rauhut, 2004), but a recess containing a distinct foramen, however, is rare (e.g., Norell et al., 2006). The origin of the foramen is unclear, but a pneumatic contribution from the tympanic air sac cannot be ruled out (Rauhut, 2004). A diverticulum of this sinus is likely not solely responsible for pneumatizing the basipterygoid processes, considering that some taxa lack the lateral foramen but still possess pneumatized processes (e.g., *Tyrannosaurus* and *Tarbosaurus*). Many theropods possess a large external pocket of the basipterygoid process that does not penetrate the bone (e.g., Kurzanov, 1976; Chure and Madsen, 1998; Xu et al., 2002; Rauhut, 2004), and several taxa completely lack even a shallow fossa (e.g., Currie, 1995; Sues, 1997). It is possible that these lateral structures have a nonpneumatic origin (Witmer, 1997), perhaps as a muscle attachment site (Kurzanov, 1976). Although based on its position, it seems unlikely that fenestra A of IGM 100/1844 did not house a diverticulum of the rostral tympanic sinus.

Subsellar Recess and Cavity: The subsellar recess is a deep, triangular excavation in the ventral surface of the cultriform process (fig. 2B). The fossa is 42 mm long, 20 mm wide caudally, and 10 mm wide at its rostral end. Its transverse caudal margin is straight, whereas its rostral margin is distinctly rounded. The fossa is confluent with an internal cavity extending nearly to the distal tip of the cultriform process (figs. 8, 10, 19, 29). This progressively narrow space is fully enclosed within the cultriform process except at its distalmost length, where it is expressed as a ventral groove. Caudally, the subsellar cavity terminates as a fingerlike extension that extends medial to the right and left basipterygoid sinuses, above the transverse wall connecting the left and right basipterygoid processes (*basipterygoid web* of Bakker et al., 1988), and below the pituitary fossa. This caudal extension stops above the basisphenoid fossa and below the rostral tympanic cavity. The subsellar recess is also seen in *Gorgosaurus* (ROM 1247), *Daspletosaurus* (TMP 1994.143.0001; Currie, 2003: fig. 26C), and *Tyrannosaurus* (AMNH FARB 5117).

The extent to which the subsellar recess fills the cultriform process is unique among the small number of tyrannosauroids studied using CT (Witmer and Ridgely, 2009). The subsellar cavity in adult *Tyrannosaurus* is largely restricted to the base of the cultriform process, whereas that of CMNH 7541, and especially *Gorgosaurus*, extends significantly into the distal length of the process (Witmer and Ridgely, 2009: fig. 10). However, even in these latter taxa, the expansion of subsellar cavity falls well short of that in IGM 100/1844, in which the cavity extends the full length of the cultriform process.

Subcondylar Recess and Cavity: The subcondylar cavity opens into the basicranium through the deep, dorsoventrally ovoid subcondylar recess (fig. 15). The recess excavates the surface of the basiocciptial and otoccipital contributions to the basal tubera. This is in contrast to the condition in *Tyrannosaurus* where the recess is restricted to the basioccipital contribution (Brochu, 2003). Indeed, the unfused suture between these elements in IGM 100/1844 can be traced within the recess as an elongate, raised

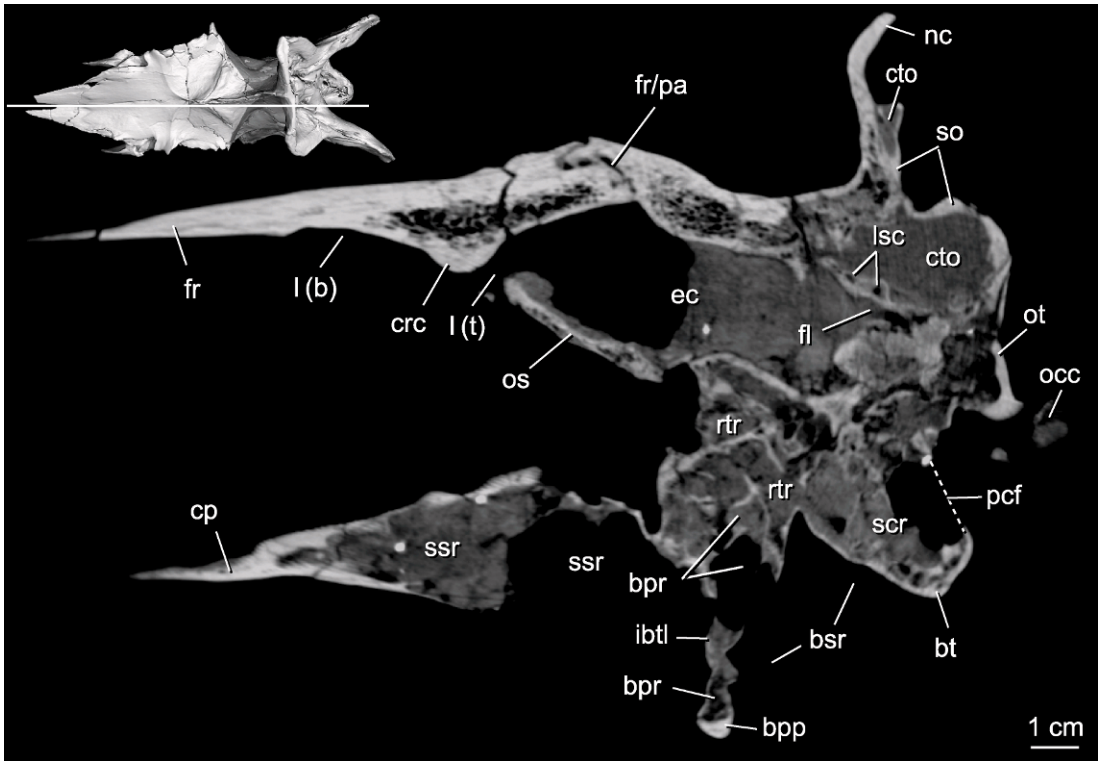

Fig. 29. Sagittal slice through the braincase of *Alioramus altai* (IGM 100/1844). Note the confluence of the basisphenoid (bsr), subsellar (ssr), and basipterygoid recesses (bpr) through the interbasipterygoidal lamina (ibtl). See appendix 1 for other anatomical abbreviations.

ridge separating two subpockets. This is also seen in *Gorgosaurus* (ROM 1247), *Tarbosaurus* (ZPAL MgD-I/3), *Teratophoneus* (BYU 8120/9396), and *Tyrannosaurus* (AMNH FARB 5117). The larger, relatively shallow subpocket in the otoccipital is the only portion of the recess visible in caudal view. This condition is also seen in *Gorgosaurus* (ROM 1247) and *Tarbosaurus* (ZPAL MgD-I/4), whereas both openings are clearly seen in *Tyrannosaurus* (AMNH FARB 5117). In IGM 100/1844, the basioccipital subpocket is smaller, deeper, and more circular. Many theropods have an external depression in this region, but it is often unclear whether it is pneumatic in origin (Rauhut, 2004) or simply serves as an attachment site for cervical musculature (e.g., Kurzanov, 1976). In IGM 100/1844, the medial (basioccipital) and lateral (otoccipital) pockets are clearly pneumatic, both being pierced by large foramina opening into an extensive internal cavity (figs. 12–14, 16, 18, 19, 21–24, 27). A paired subcondylar recess is present in a variety of theropods (see review in Rauhut, 2004) and most other tyrannosauroids, including *Dilong* and *Guanlong* (Russell, 1970; Currie, 2003; Hurum and Sabath, 2003; Xu et al., 2004, 2006; Witmer and Ridgely, 2009, 2010), but apparently not *Xiongguanlong* (Li et al., 2010). The depth of the recess and width between the pneumatic apertures compares closely with most other tyrannosauroids, but differs from the uniquely shallow recess and closely positioned apertures that are seen in *Tyrannosaurus* (Witmer and Ridgely, 2009).

The subcondylar cavity is a complex series of confluent chambers that extends through portions of the otoccipital and parabasisphenoid and nearly the entire basioccipital. Although the morphology of the individual chambers is far from bilaterally symmetrical, their internal extent on the right and left sides

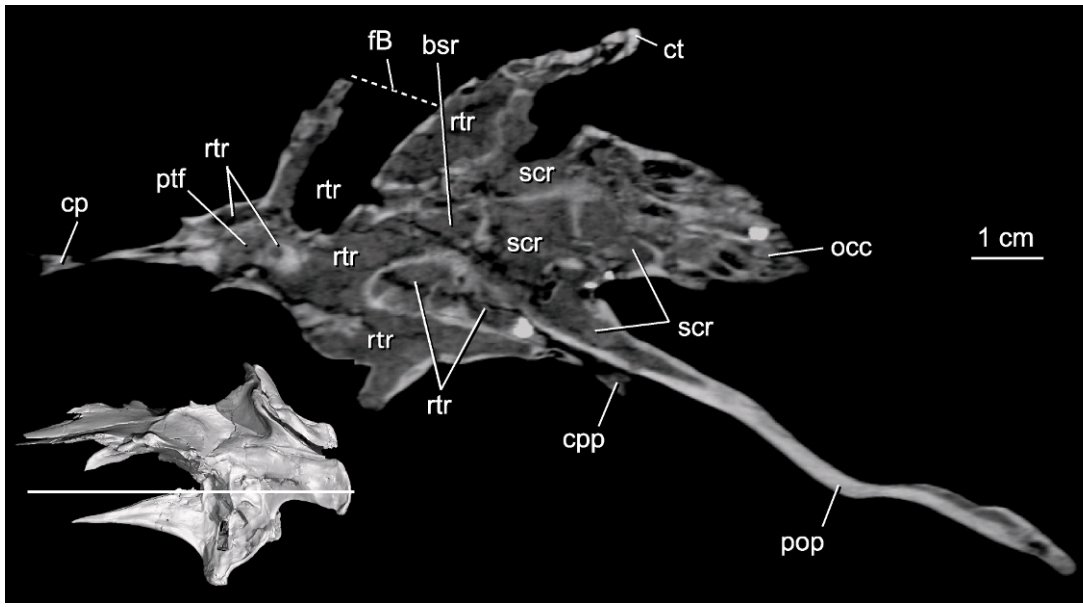

Fig. 30. Horizontal slice through the basicranium of *Alioramus altai* (IGM 100/1844). Note the medial confluence of the subcondylar recess (scr) and its invasion of the occipital condyle (occ). See appendix 1 for other anatomical abbreviations.

of the skull is highly comparable. The chamber associated with the medial aperture of the subcondylar recess is broadly confluent with the same space on the opposing side and together they occupy the midline portion of the basioccipital, including the neck of the occipital condyle (fig. 30) (as in adult *Tyrannosaurus* and CMNH 7951: Osborn, 1912, Witmer and Ridgely, 2009, 2010). This cavity underlies the endocranial cavity and overlies the basisphenoid recess, without connecting to either space. The chamber associated with the lateral aperture is broadly confluent with that of the medial aperture, but it also extends rostrolaterally and dorsally to pneumatize a portion of the parabasisphenoid and otoccipital, respectively. Within the parabasisphenoid, the subcondylar and rostral tympanic cavities are broadly confluent, as in CMNH 7541, but in contrast to *Gorgosaurus* and adult *Tyrannosaurus* where these cavities are distinctly separated (Witmer and Ridgely, 2009). The extent of these cavities along their shared margin in IGM 100/1844 is difficult to delineate with precision, but they appear not to enter the prootic. A narrow confluence with the pneumatic basipterygoid cavity occurs lateral to the basisphenoid recess within the thin crista ventrolateralis (figs. 19, 23). The subcondylar cavity invests the bone surrounding the hypoglossal and vagal canals, but does not communicate directly with either. A small foramen in the caudolateral wall of the endocranial cavity likely transmitted a vein associated with the dural venous sinuses surrounding the hindbrain (Sedlmayer, 2002). This foramen opens directly into a dorsal extension of the subcondylar cavity. The lateral cavity also invests the crista tuberalis (the bony rod extending ventrally from the base of the paroccipital process) and it is confluent with the caudal tympanic cavity within this structure. This feature is shared with *Gorgosaurus* and CMNH 7541 but is absent in adult *Tyrannosaurus* (Witmer and Ridgely, 2009).

Cranial Endocast and Osseous Labyrinth

Endocranial Orientation and Shape: The cranial endocast is a reconstruction of the space that housed the brain, cerebral arteries and veins, cranial nerve roots, dural

venous sinuses, and meninges. For descriptive purposes, the endocast of IGM 100/1844 was oriented so that the lateral semicircular canal is horizontal, which is the typical ''alert'' position in vertebrates (Witmer et al., 2003). This orientation results in the head being held in a slightly downturned position, in agreement with that of *Gorgosaurus* and adult *Tyrannosaurus* but in marked contrast to the strongly downturned orientation of CMNH 7541 (but see below) and tyrannosauroid outgroups (Witmer and Ridgely, 2009). This angle of head orientation in IGM 100/1844 is greater than the nearly horizontal orientation of some non-coelurosaurian theropods (e.g., *Allosaurus fragilis* and *Majungasaurus crenatissimus*; Sampson and Witmer, 2007) and less than the strongly downturned angle of maniraptorans (including birds). Thus, the orientation of IGM 100/1844 and other tyrannosaurids is apomorphically intermediate between the non-coelurosaurian and maniraptoran conditions and, if biologically meaningful, probably represents the ancestral coelurosaurian orientation (with a convergently derived angle in maniraptorans).

Extensive observation of the CMNH 7541 skull by one of us (T.D.C.) suggests that many of the bizarre features noted by Witmer and Ridgely (2009) may alternatively be artifacts of crushing. This includes the strongly downturned orientation of the head. A lateral view of the skull (Witmer and Ridgely, 2009: fig. 1) shows that the temporal region is crushed forward, which reduced the laterotemporal fenestra to a slot. This forward displacement also shifted the quadrate, quadratojugal, and squamosal rostrally, breaking their original articulations with other bones.

The basicranium also appears to have been affected. The basioccipital is shifted rostrally relative to the otoccipital on both sides of the occipital condyle. The left basipterygoid process is also shifted rostral to its normal position on the pterygoid, and the entire basicranium is oriented almost horizontally. The endocast (Witmer and Ridgely, 2009: figs. 3M, N, O) is foreshortened and wide relative to the other tyrannosaurids, where ventral landmarks such as the pituitary fossa, facial and maxillomandibular canals, floccu-lus, osseous labyrinth, and vagal canal are shifted rostrally relative to dorsal landmarks (e.g., dorsal peak). This arrangement is consistent with the distortion that can be seen externally and would have affected the shape of the endocranial cavity. The unnatural displacement of the entire basicranium forward and up may account for the downturned orientation of the head, as reconstructed by Witmer and Ridgely (2009). However, their reconstruction is based on the lateral semicircular canal being held horizontally, so if the orientiation reflects distortion rather than an apomorphic head orientation, then the basicranium and otic capsule must have been differentially distorted. A uniformly downturned distortion would also be uniformly ''corrected'' when the lateral semicircular canal was brought back to a horizontal orientation.

In IGM 100/1844, the endocast, like the neurocranium, exhibits considerable distortion along the long axis of the skull, such that features on the left side of the endocast are less clearly discerned and lie distinctly ventral to their right-side counterparts. The distortion does not significantly affect the morphology and orientation of endocranial features on the right side of the skull, nor does it significantly affect the spatial relationships between these features and the lateral semicircular canal (based on comparisons with other theropod endocasts, including tyrannosaurids; Brochu, 2000; Witmer and Ridgely, 2009). Thus, the following descriptions are based largely on the right side of the skull, with supplementary observations from the left side.

The cranial endocast is complete (fig. 31). Its long, narrow, and overall tubular shape conforms closely to that of other tyrannosaurids (Brochu, 2000, Witmer and Ridgely, 2009). This general shape is distinctive in its reduction of the prominent midbrain flexure characterizing the cranial endocasts of other coelurosaurian and non-coelurosaurian theropods (e.g., Larsson, 2001; Alonso et al., 2004; Franzosa and Rowe, 2005; Brusatte and Sereno, 2007; Sampson and Witmer, 2007; Balanoff et al., 2009; Witmer and Ridgely, 2009). The seemingly strong angles in non-coelurosaurian and coelurosaurian outgroups (becoming more pronounced to-

ward birds; Bhullar et al., 2012) suggest the low angle of IGM 100/1844 is a synapomorphy of tyrannosauroids (or a constituent subclade) and likely does not reflect the ancestral morphology of Coelurosauria. This hypothesis awaits a rigorous comparative analysis of shape based on homologous landmarks.

The length of the cranial endocast of IGM 100/1844 from the foramen magnum to the rostral tip of the olfactory bulbs is 143 mm. Measurements of width and depth are somewhat less reliable due to the aforementioned distortion, but the greatest measured width and depth of the hindbrain is 29.4 mm and 18.8 mm, respectively; midbrain (including dural peak) 53.4 mm and 22.9 mm, respectively; and forebrain (width across cerebral hemispheres and height includes the pituitary fossa) 68.5 mm and 23.2 mm, respectively. The volume of the endocranial cavity is approximately 81 cm^3, which is larger than that of adult *Tyrannosaurus* (343 cm^3; Brochu, 2000) when considered as an encephalization quotient (2.4 versus 2.0, respectively; Brusatte et al., 2009).

The degree to which details of endocranial shape reflects the morphology of the brain rather than the surrounding dura is unclear. As in most other theropods, the rostral half of the endocast likely reflects the contours of the forebrain with general accuracy, with this accuracy decreasing in the mid- and hindbrain regions where the dorsal surfaces appear to be enveloped in extensive venous sinuses (Sedlmayer, 2002). It is possible that the thickness of the dural envelope increased during postnatal development, so that the endocasts of ontogenetically young tyrannosauroids more accurately reflect the contours of the brain than their mature conspecifics (Witmer and Ridgely, 2009). What this means for a nine-year-old specimen of *Alioramus altai* is unclear.

The most obvious dural structure is the tall pyramidal peak that rises dorsally above the midbrain region. Its apex excavates the ventral surface of the parietal-supraoccipital suture, in agreement with that of *Gorgosaurus*, adult *Tyrannosaurus*, and CMNH 7541 (Witmer and Ridgely, 2009). The peak of IGM 100/1844 is more prominent than that of the other known tyrannosaurid specimens with the exception of a single specimen of adult *Tyrannosaurus* (AMNH FARB 5029; Osborn, 1912; Witmer and Ridgely, 2009: fig. 3). The peak in this specimen and IGM 100/1844 likely reflects a hypertrophied confluence of the dorsal longitudinal and transverse sinuses and not the cerebellum as suggested by Saveliev and Alifanov (2007) or the pineal body as concluded for some non-coelurosaurian theropods (Sampson and Witmer, 2007; see Witmer and Ridgely, 2009).

The transverse dural sinus, as in other tyrannosaurs, is reflected on the endocast as a raised ridge extending in an arclike trajectory between the caudal and rostral middle cerebral veins. As noted above, the exact position of the rostral vein is somewhat unclear, but it did not pass through its own canal in the laterosphenoid as described for *Gorgosaurus*, adult *Tyrannosaurus*, and CMNH 7541. It may have exited through the laterosphenoid with the ophthalmic branch of the trigeminal nerve, through the prootic fossa with the maxillomandibular branch of the trigeminal nerve, or through the prootic dorsal to the fossa within a separate canal that is not well delineated in bone (discontinuous) because of the dorsal extension of the rostral tympanic sinus (our interpretation). A shared path with the trigeminal nerve would be a reversal to nonsaurischian condition (Rauhut, 2003). Either way, based on the phylogenetic position of *Alioramus altai* within Tyrannosauridae, the path of the rostral vein in IGM 100/1844 is autapomorphically derived.

A third venous channel associated with the transverse sinus exits laterally through a foramen in the supratemporal fossa near the laterosphenoid, parietal, prootic suture. It is positioned well rostral to the dorsal head vein in *Tyrannosaurus* (AMNH FARB 5117), which is closely associated with the caudal middle cerebral vein (Witmer and Ridgely, 2009). The structure in IGM 100/1844 may represent the rostral middle cerebral vein or an unnamed orbitocerebral vein.

FOREBRAIN: Visible features of the forebrain in IGM 100/1844 include the cerebrum (cerebral hemispheres), olfactory tracts, and pituitary body. The cerebral hemispheres lie beneath the frontals and parietals, their

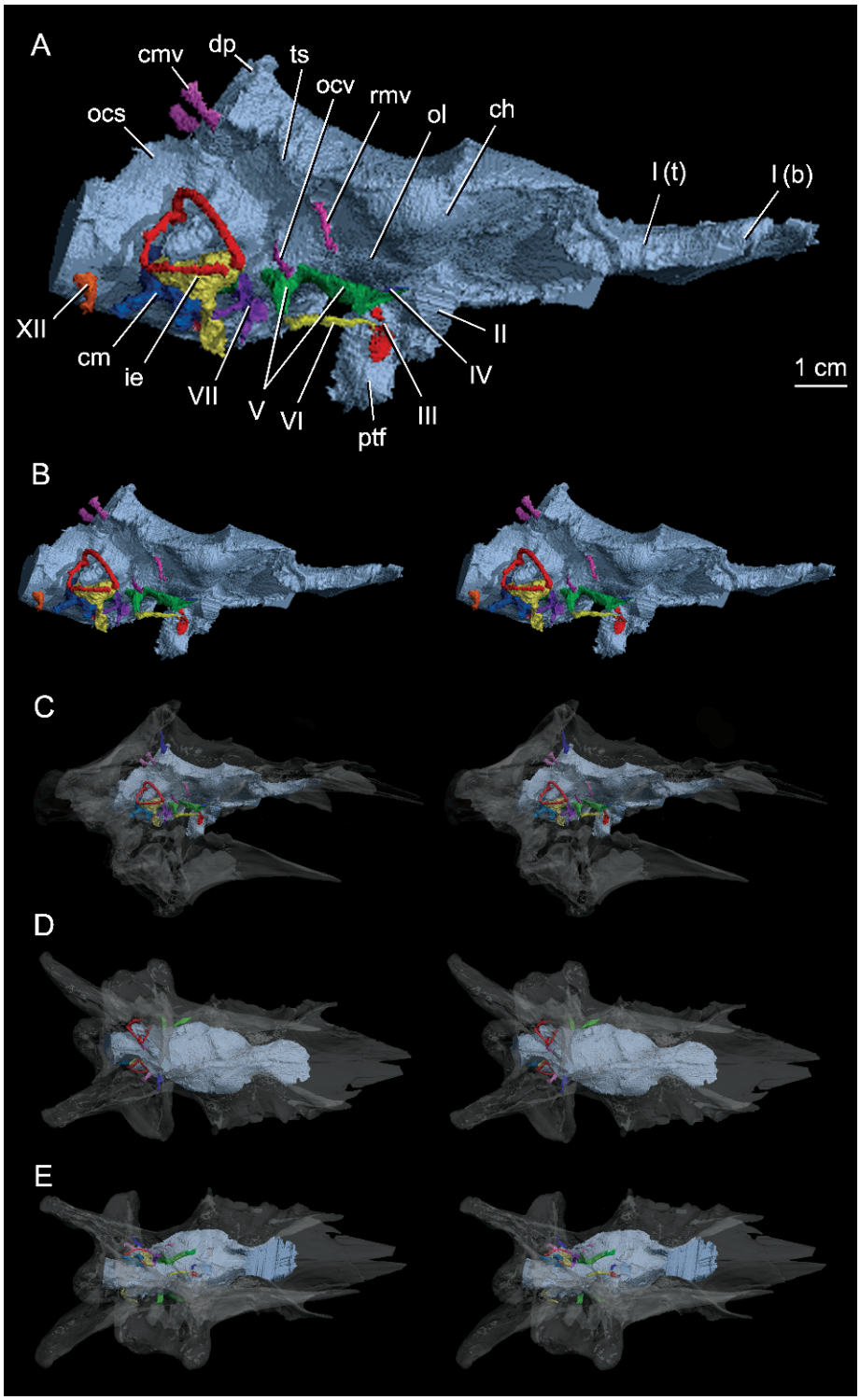
A
cmv
dp
ts
ocv
rmv
ol
ch
ocs
I (t)
I (b)
XII
cm
ie
VII
V
VI
ptf
III
IV
II
1 cm
B
C
D
E

suture being clearly reflected on the dorsal surface of the cerebrum. This surface is obscured in most other theropods by a pineal peak absent in tyrannosaurids (Witmer and Ridgely, 2009). The hemispheres are distinct and expanded relative to those of non-coleurosaurian theropods, but not to the degree found in maniraptorans (in agreement with other tyrannosaurids; Brochu, 2000; Larsson et al., 2000; Witmer and Ridgely, 2009).

The olfactory tracts are extremely short and broad, even among tyrannosaurids whose tracts are apomorphically broad compared to the plesiomorphic elongate tracts of non-coelurosaurian theropods (e.g., *Carcharodontosaurus*; Larsson, 2001, Brusatte and Sereno, 2007). The relative width of the tracts in the ontogenetically young IGM 100/1844 compares most closely to those of the juvenile CMNH 7541, which are slightly broader than those of adult *Tyrannosaurus*, whose tracts in turn are broader than those of *Gorgosaurus* (Witmer and Ridgely, 2009). The tracts and bulbs are roofed by the frontal, and the tracts are underlain by the orbitosphenoids. The ethmoid scar on the underside of the frontals demarcates the length and width of the olfactory bulbs, whereas the ventral margin of the bulbs is not delineated in bone because of the lack of a preserved ethmoid complex. This makes the dorsoventral extent of the olfactory bulbs unclear and discourages meaningful comparative statements regarding the volume of the olfactory bulbs. The bulbs, however, compare closely in relative length and width to those presented and discussed by Witmer and Ridgely (2009), and certainly did not fill the entire olfactory recess of the nasal cavity (Witmer, 1995; Ali et al., 2008; Witmer and Ridgely, 2009). The bulbs of IGM 100/1844 are consistent with the hypothesis that the olfactory bulbs of tyrannosauroids are larger than those of other theropod groups (Ali et al., 2008; Zelenitsky et al., 2009).

The pituitary body (hypophysis cerebri) is clearly defined and appears to generally reflect the true dimensions of the pituitary fossa despite some degree of mediolateral compression in this region of the skull. The body is approximately 30 mm in proximodistal length with a maximum mediolateral width of 10 mm and rostrocaudal thickness of 12 mm. This thickness appears greater than that of other known tyrannosaurs, with the possible exception of AMNH FARB 5029 (Witmer and Ridgely, 2009: fig. 3). The shape of the pituitary fossa, however, exhibits variation even among specimens of *Tyrannosaurus*. The body angles slightly caudally—a highly conservative feature among theropods despite differences in the degree of midbrain flexure. This suggests at least some degree of evolutionary independence between these angles. As described above, the path of the internal carotid artery through the lateral or ventral surface of the braincase is not clearly delineated in bone and its entry into the pituitary fossa cannot be definitely determined. A ventral point of entry into the sella turcica is conservative across Coelurosauria, including other known tyrannosauroids, and likely was present in IGM 100/1844.

MIDBRAIN: A subtle expansion of the endocast ventral and slightly caudal to the cerebral hemisphere gives rise to the optic (CN II) nerve. This expansion is bounded rostrally by the trochlear (CN IV) nerve canal and caudally by the rostral length of the transverse sinus. These landmarks delimit the optic tectum in extant sauropsids (Sampson and Witmer, 2007) and indicate that the tectum of IGM 100/1844 is caudoventrally displaced from the plesiomorphic position

←

Fig. 31. Digital reconstructions of the endocranial cavity (ec), inner ear, and cranial neurovasculature of *Alioramus altai* (IGM 100/1844). The labeled endocasts (**A**) and their steropairs (**B**) are in right lateral view. The stereopairs represented by **C** (right lateral), **D** (dorsal), and **E** (ventral), show the same structures within the context of the bony braincase that has been rendered transparent. See appendix 1 for other anatomical abbreviations. Modified from Bever et al. (2011: figs. 3, 4).

expressed in crocodiles and non-coelurosaurian theropods (Larsson et al., 2000). The extent of this displacement is moderate compared to that of birds and their close relatives among maniraptorans (Alonso et al., 2004, Norell et al., 2009; Bhullar et al., 2012), which is congruent with the moderate degree of cerebral expansion in IGM 100/1844 revealed by the same comparisons. The spatial and size relationships between the optic tecta and cerebral hemispheres of IGM 100/1844 compare closely to those of other skeletally immature tyrannosaurids. A late-stage thickening of the dural envelope likely obscures these relationships in more mature specimens (Brochu, 2000; Witmer and Ridgely, 2009; Bever et al., 2011).

HINDBRAIN: Extensive dural sinuses cover much of the hindbrain region, but the cerebellum can be inferred to lie caudal to the transverse sinus and between the right and left inner ears. Prominent floccular lobes (cerebellar flocculi; ≈15 mm long and ≈13 mm wide) extend caudolaterally and ventrally from the cerebellum to lie between the semicircular canals of the inner ear. The floccular cavity is distinctly larger than that of adult *Tyrannosaurus* and slightly larger than the same cavities of CMNH 7541 and ROM 1247 (*Gorgosaurus*). It compares most closely in size with the floccular cavity of PIN 553-3/1 (*Tarbosaurus*) (identified as the root of cranial nerve VIII by Saveliev and Alifanov, 2007; see also Witmer and Ridgely, 2009). In agreement with other tyrannosaurids and non-coelurosaurian theropods, the floccular cavity of IGM 100/1844 is tabular in shape, contrasting with the tubular flocculus of other coelurosaurs (Witmer and Ridgely, 2009). The distal extent, large size, and tabular shape of the floccular lobe in IGM 100/1844 each reflect the plesiomorphic condition for theropods.

The canals for cranial nerves VI–XII (and their associated vasculature; Sedlmayer, 2002) are visible projecting from the hindbrain region of the cranial endocast. The abducens (VI) nerve passes from the brainstem horizontally through the dorsum sellae and enters the sinus cavernosus in the lateral margin of the pituitary fossa that also houses the oculomotor (III) nerve and cerebral carotid arteries. The trochlear (IV) exits the endocranial space dorsally through an independent canal in the prootic. The sinus cavernosus is plesiomorphic for Theropoda, but to our knowledge it is absent from all other documented coelurosaurs, with the possible exception of CMNH 7541 (Witmer and Ridgely, 2009), where cranial nerves III, IV, and VI all exit the braincase through independent canals (see Bever et al., 2011).

The position at which the abducens nerve pierces the caudal wall of the dorsum sellae is directly ventromedial to a broad concavity in the prootic contribution to the lateral wall of the endocranial cavity. This concavity housed the gasserian ganglion of the trigeminal (V) nerve and is pierced by two large foramina. The smaller, rostral foramen conveyed the ophthalmic (profundus) branch of the trigeminal nerve (V_1) rostrodorsally where it exited the braincase through the laterosphenoid. The larger, caudal foramen conveyed the maxillomandibular branch of the trigeminal nerve ($V_{2/3}$). Its associated canal extends caudolaterally and opens in the rostral margin of the prootic fossa. An intracranial position of the gasserian ganglion is the derived condition within Theropoda (Bakker et al., 1988; Brochu, 2000; Witmer and Ridgely, 2009), but only in tyrannosaurids and avialans does the ganglion lie fully within the endocranial cavity rather than within the prootic (Witmer and Ridgely, 2009; Tsuihji et al., 2011).

Caudal and slightly ventral to the gasserian fossa, the facioacoustic fossa excavates the lateral wall of the endocranial cavity. A short canal pierces the caudal margin of this fossa and then dilates and bifurcates fully within the prootic. The longer of the two canals runs caudolaterally before exiting the braincase through an inconspicuous external foramen in the prootic positioned near the otic recess. The second canal, which has a greater diameter than the first, continues laterally before opening into the caudal margin of the prootic fossa. A small, secondary canal diverges from this lateral branch near the internal dilation of the facial canal and exits the braincase along the ventral margin of the prootic fossa. We interpret the dilation of the facial canal to mark the position of the geniculate ganglion (VII), with the caudolateral division of the

canal transmitting the hypoglossal ramus (VII_2) and the lateral division transmitting the palatine ramus (VII_1). The identity of the secondary branch of the palatine ramus is unclear, but it may represent a further ramification of the palatine nerve within the prootic. An intracranial position of the geniculate ganglion is an autapomorphy of *Alioramus altai* that may be unique among archosaurs (Bever et al., 2011). The presence of a lateral fossa in the prootic that houses the lateral foramen of the maxillomandibular canal of the trigeminal nerve and the external foramen of the facial nerve is a derived character shared between IGM 100/1844 and other known tyrannosaurids (Witmer and Ridgely, 2009).

The vestibulocochlear (VIII) nerve penetrates the facioacoustic fossa through two foramina, both of which are caudal to the internal facial foramen. The dorsal foramen and canal communicate with the vestibular cavity of the inner ear and thus reflect the path of the vestibular nerve. The more ventral foramen and canal communicate with the cochlear cavity and thus reflect the path of the cochlear nerve. The cochlear branch generally is small in theropods (Osborn, 1912; Currie and Zhao, 1993, Makovicky and Norell, 1998; Brochu, 2000), but its canal is slightly larger than that of the vestibular branch in IGM 100/1844 (both branches are smaller than the primary facial canal.)

The glossopharyngeal (IX) nerve, as described above, enters the recessus scalae tympani through an independent foramen in the opisthotic—a feature previously unknown in theropods. The nerve fails to penetrate the crista interfenestralis and therefore must have exited the braincase through the fenestra pseudorotunda, possibly passing ventral to a superficial lamina of the prootic that covers much of the otic recess laterally. The caudal division of the cavum metoticum (vagal canal) angles caudolaterally and transmits the vagus (X) and accessory (XI) nerves and presumably at least a small jugular vein to the occipital surface of the braincase. This external foramen lies within the paracondylar fossa adjacent to the openings of the subcondylar recess and a single canal of the hypoglossal (XII) nerve, which exits the medullary portion of the hindbrain caudoventral to the vagal foramen.

Osseous Labyrinth: The complete osseous labyrinth of the right inner ear, including the rostral, caudal, and lateral semicircular canals, vestibular cavity, and cochlear cavity, was digitally extracted and reconstructed from the CT images (fig. 32). The same structures of the left inner ear are less clear, but they are visible and were used to confirm anatomical observations. The overall shape of the osseous labyrinth is triangular in lateral view, with a caudodorsally expanded rostral semicircular canal that is longer than either the caudal or lateral canal. Both conditions are common among theropods (e.g., Fransoza and Rowe, 2005; Balanoff et al., 2009; Sampson and Witmer, 2007). The caudodorsal expansion and resultant twisting of the common crus present in IGM 100/1844 and other tyrannosaurids is intermediate between non-coelurosaurian and maniraptoran conditions (Witmer and Ridgely, 2009).

The rostral canal also exhibits a degree of rostral expansion comparable to that of *Gorgosaurus* but considerably less than that of adult *Tyrannosaurus*, CMNH 7541, and maniraptorans (Witmer and Ridgely, 2009: fig. 8; Balanoff et al., 2009). The common crus of IGM 100/1844 and *Gorgosaurus* retains the basically vertical orientation present in non-coelurosaurian theropods, whereas in adult *Tyrannosaurus*, CMNH 7541, and maniraptorans, the derived expansion of the rostral canal causes the common crus to lie at a more oblique angle. The lateral canal in dorsal view is not strongly bowed as in other tyrannosaurs and maniraptorans and more closely resembles the plesiomorphic canal of non-coelurosaurian theropods, which is basically straight, producing a strong medial hook where it meets the caudal canal. The caudal canal is not strongly bowed caudodorsally (in lateral view), in contrast to maniraptorans and most other tyrannosaurs and in general agreement with non-coelurosaurian theropods and CMNH 7541. The functional implications of these differences are unclear. For example, the relative lengths of the lateral semicircular canal suggests that mediolateral movements of the head were behaviorally less important in IGM 100/1844 than in *Tyrannosaurus*, but this interpretation stands in contrast to an interpretation that such movements were indeed important based

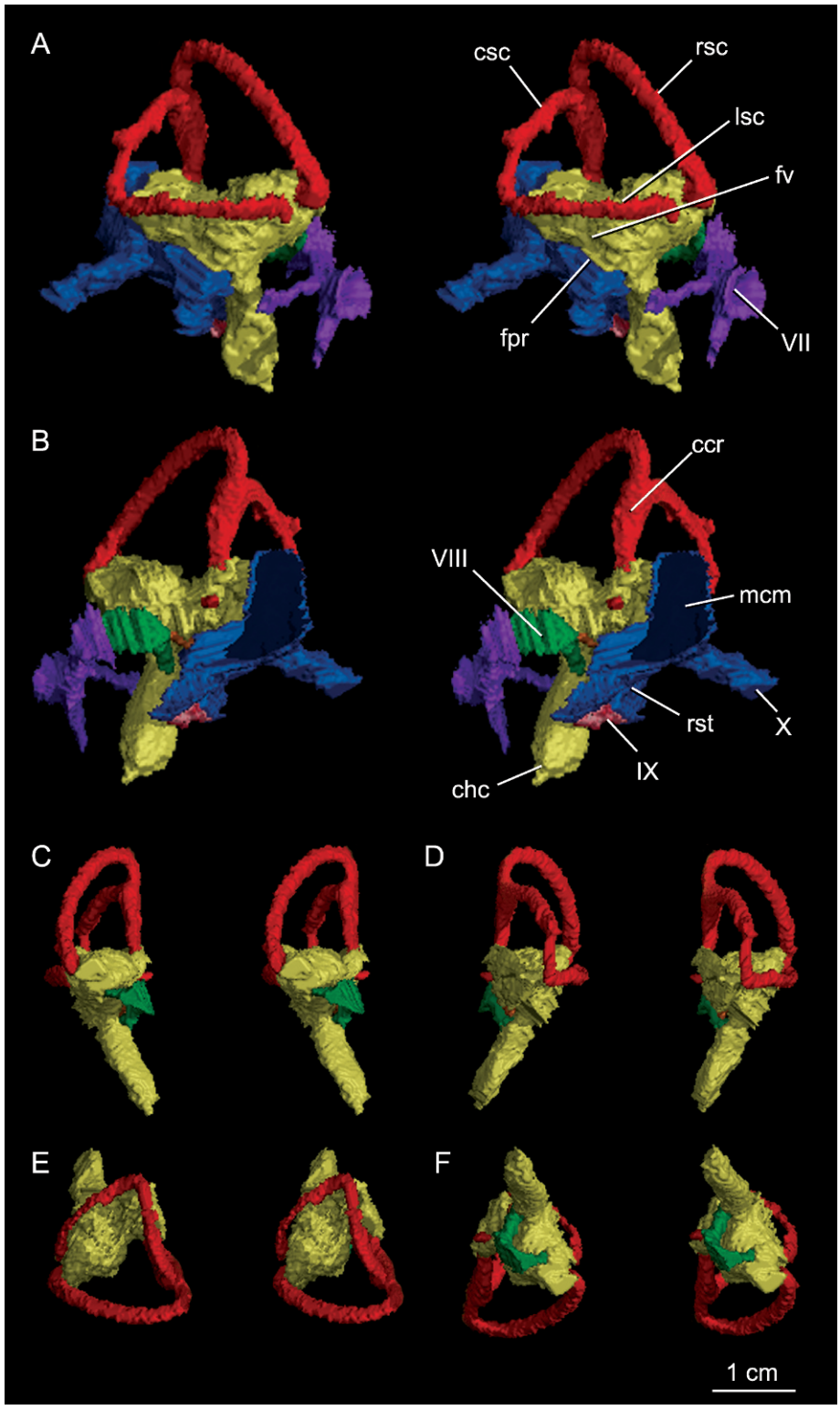
A
csc
rsc
lsc
fv
fpr
VII
B
ccr
VIII
mcm
rst
X
IX
chc
C
D
E
F
1 cm

on the relatively long floccular cavity of IGM 100/1844. Similar behavioral abilities can, of course, be achieved using different combinations of anatomical features (Witmer and Ridgely, 2009).

The vestibular cavity overall is expanded, with its dorsal margin extending beyond the horizontal plane occupied by the lateral semicircular canal. This is similar to the condition in crown birds but in contrast to the general archosaur condition, which is conserved in most theropods including other tyrannosaurids (Witmer and Ridgely, 2009). If biologically real, the expanded cavity of IGM 100/1844 might suggest a heightened sense of balance; however, this should be considered with caution, as similar expansions are present in other nontheropod dinosaurs (e.g., Knoll and Schwarz-Wings, 2009: fig. 3). The fenestra vestibuli is small and circular and compares closely to that of other tyrannosaurids, whose markedly small foramina have been considered autapomorphic among theropods (Brochu, 2000, 2003). This apomorphic status has yet to be established through broad comparisons, but the tyrannosaurid fenestra appears to be roughly the same relative size as found in other coelurosaurs and *Majungasaurus* (Sampson and Witmer, 2007). They are, however, smaller than in *Ceratosaurus* and *Allosaurus* (Sampson and Witmer, 2007; Witmer and Ridgely, 2009), suggesting that a size reduction is phylogenetically informative at some level. The medial wall of the cavum labyrinthicum is well ossified and lacks the broad communication between endocranial and vestibular cavities described in some theropods as the vestibular pyramid (Currie, 1997).

The well-formed cochlear cavity is long (13.5 mm) and straight, with a distinct neck near its confluence with the vestibule. IGM 100/1844 is thus congruent with the hypothesis that a long, slender, and straight cochlear cavity is a tyrannosaurid synapomorphy (Witmer and Ridgely, 2009). Length of the cochlear cavity correlates strongly with length of the basilar papilla and therefore corresponds at least roughly with auditory capability and sensitivity to low-frequency sounds (Manley and Köppl, 1998; Gleich et al., 2005; Walsh et al., 2009). As in other tyrannosaurids, the cochlea angles rostroventrally away from the vestibular cavity (approximately 20° from the vertical in lateral view). The greatest diameter of the cochlear cavity is nearly 10 mm wide and lies roughly along a rostrocaudal orientation (the cavity is not perfectly cylindrical). It narrows toward its distal terminus where the cochlea penetrates the ventral margin of the prootic and passes into the dorsal surface of the parabasisphenoid (just above the dorsalmost extent of the basisphenoid recess). The penetration of the ossified basal plate by the cochlear duct is a plesiomorphic character shared with noncoelurosaurian theropods, nontheropod dinosaurs, crocodilians, stem archosaurs, and turtles (Baird, 1970; Wever, 1978; Walker, 1990; Gower and Weber, 1998; Bever, 2009), although in turtles, the cochlear duct passes caudoventrally rather than rostroventrally and enters the basioccipital rather than the parabasisphenoid. The perilymphatic canal originates near the position where the cochlear nerve enters the cochlear cavity. The perilymphatic canal exits the cochlear cavity and enters the recessus scala tympani through a small, medial foramen in the opisthotic that lies just dorsal to lateral foramen of the glossopharyngeal (IX) canal described above.

DISCUSSION

The braincase of IGM 100/1844 expresses an abundance of anatomical information

←

Fig. 32. Stereopairs of the right osseous labyrinth of *Alioramus altai* (IGM 100/1844) in lateral (**A**), medial (**B**), rostral (**C**), caudal (**D**), dorsal (**E**), and ventral (**F**) views. The closely associated facial (VII) and vestibulocochlear (VIII) canals and the divisions of the cavum metoticum (mcm, rst, X) are not rendered in C, D, E, and F. See appendix 1 for other anatomical abbreviations. Modified from Bever et al. (2011: fig. 8).

that reveals and clarifies phylogenetically informative transformations within and around the tyrannosauroid neurocranium. The current comparative framework for many of these features, especially those revealed by CT, is largely restricted to Tyrannosauridae. Thus, a more comprehensive assessment of their transformational history and seemingly high potential for informing phylogenetic relationships awaits denser sampling within nontyrannosaurid tyrannosauroids. Examples include the presence/absence of a retro- and prohypophyseal space associated with the rostral tympanic cavity, the presence of a homolog of "fenestra C" of the rostral tympanic recess, the spatial extent of the caudal tympanic cavity within the supraoccipital, pneumatization of the crista lateroventralis by the basisphenoid cavity, the shape and extent of the subsellar recess, the presence of a confluence between the subcondylar and rostral tympanic cavities, the degree of midbrain flexion, the size and shape of the floccular lobes, the shape of the rostral, caudal, and lateral semicircular canals, the degree to which the vestibular cavity is expanded, the length and shape of the cochlear cavity, and the presence of an independent path of the glossopharyngeal nerve from the endocranial cavity to the recessus scalae tympani.

Other features, whose taxonomic distributions are better understood (at least somewhat) but have yet to be incorporated into a phylogenetic analysis, also await further study. Notable examples include: (1) a fossa in the lateral surface of the prootic that houses the external openings of the maxillomandibular branch of the trigeminal (V) nerve and the facial (VII) nerve; (2) the presence of a superficial lamina of the prootic, positioned between the preotic pendant and the otosphenoidal crest and covering much of the acoustic recess; and (3) the depth of the rostral tympanic recess. The prootic fossa almost certainly is a derived character within tyrannosauroids that is plesiomorphic for Tyrannosauridae, but where exactly on the tree it transforms is unclear. A superficial lamina of the prootic appears to diagnose a clade within Tyrannosauroidea that excludes *Dilong* and *Guanlong*, although exactly which taxa define this clade also remains unclear. The deeply excavated rostral tympanic recess found in *Guanlong* and *Alioramus altai* suggests this feature has a complicated evolutionary history within Tyrannosauroidea.

The recent phylogenetic analysis of Brusatte et al. (2010a) utilized a wealth of new anatomical information gleaned from the current study as well as a monographic description of the remainder of the *Alioramus altai* type specimen (Brusatte et al., 2012). This phylogenetic analysis included 21 braincase characters among the 307 total characters in the dataset. All characters in the analysis were simply listed, sometimes with a short description, in an online appendix. Here we discuss each of those 21 braincase characters in more detail, clarify the shorthand language used in the original character list, and note which tyrannosauroid taxa can be scored for the primitive and derived states of each character. In the following descriptions, if a tyrannosauroid taxon is not mentioned as possessing a certain state, then the character cannot be assessed in that taxon and is scored as questionable in the phylogenetic analysis.

Character 147. Braincase, orientation of occipital surface: faces caudally (0) or caudoventrally (1).

In most theropods the occipital surface of the braincase, formed primarily by the parietals, supraoccipital, otoccipital, and basioccipital, faces nearly straight caudally when the braincase is articulated in life position (with the dorsal surface of the frontals oriented in a horizontal plane). In some derived tyrannosauroids, however, this surface is orientated obliquely and faces both caudally and ventrally. This distinction was codified in a phylogenetic data matrix by Holtz (2001: char. 65), who noted the presence of the derived caudoventral state in *Albertosaurus*, *Alioramus*, *Tarbosaurus*, and *Tyrannosaurus*. On the contrary, Holtz (2001) scored *Daspletosaurus* and *Gorgosaurus* for the primitive caudally oriented condition. These scorings were followed by Holtz et al. (2004: char. 202). Later authors also utilized this character, but with some scoring differences. Currie et al. (2003: char. 63) scored *Albertosaurus* for the primitive state and *Daspletosaurus* for the derived state.

Brusatte et al. (2009: char. 3), Sereno et al. (2009: char. 46), and Carr and Williamson (2010: char. 3) agreed that *Daspletosaurus* possesses the derived state, but they retained Holtz's (2001) original scoring of *Albertosaurus* for the derived state.

The expanded dataset of Brusatte et al. (2010) accepted these general scoring decisions, but with some modifications: *Dilong*, *Guanlong*, *Proceratosaurus*, *Xiongguanlong*, and *Albertosaurus* were scored for the primitive state, whereas *Gorgosaurus*, *Alioramus*, *Daspletosaurus*, *Tarbosaurus*, and *Tyrannosaurus* were scored for the derived state. Therefore, in contrast to most previous studies, Brusatte et al. (2010) considered *Albertosaurus* to have a caudally facing occiput and *Gorgosaurus* a caudoventrally facing occiput. These scores were based mostly on the figures and descriptions of Currie (2003), and we acknowledge that size-related, ontogenetic, and individual variation may affect this character. It is clear that basal tyrannosauroids such as *Dilong* and *Guanlong* have the traditional caudally facing occiput of theropods, and that many of the largest and most derived tyrannosaurids (*Alioramus*, *Daspletosaurus*, *Tarbosaurus*, *Tyrannosaurus*) possess the derived caudoventral condition. The remaining uncertainty concerns the proper scores for *Albertosaurus* and *Gorgosaurus*, and this should be clarified with the discovery and description of new braincase material (especially of adult individuals).

Character 148. Supraoccipital, contribution to the dorsal rim of the foramen magnum: forms entire rim (0); makes limited contribution to rim via triangular ventral process (1); completely excluded from rim (2).

In most theropods the supraoccipital forms most, or all, of the dorsal margin of the foramen magnum. Tyrannosauroids are united by a synapomorphic condition in which the supraoccipital contribution to the foramen rim is greatly reduced. This condition is also seen in some distant outgroup taxa (e.g., *Allosaurus*: Madsen, 1976), but more closely related coelurosaurian outgroups have the traditional theropod condition of a large supraoccipital contribution (e.g., ornithomimosaurs: Makovicky and Norell, 1998; dromaeosaurids: Barsbold and Osmólska, 1999; troodontids: Norell et al., 2009).

In most tyrannosauroids the supraoccipital tapers ventrally into a small triangular process that barely makes contact with the dorsal rim of the foramen magnum. This condition is seen in *Xiongguanlong* (Li et al., 2010), *Albertosaurus* (Currie, 2003), *Gorgosaurus* (Currie, 2003; Witmer and Ridgely, 2009), *Alioramus* (Bever et al., 2011), *Daspletosaurus* (Currie, 2003), *Tarbosaurus* (Hurum and Sabath, 2003), and *Tyrannosaurus* (Brochu, 2003). A similar condition is likely present in *Teratophoneus* (BYU 8120/9396): in this taxon, the supraoccipital clearly contributed to the dorsal midline of the foramen magnum, but the precise width of its contribution cannot be determined. Two basal tyrannosauroids, *Guanlong* (IVPP V14531) and *Dilong* (IVPP V14243), exhibit a further unique condition in which the supraoccipital is completely excluded from the foramen magnum (fig. 33). Previous authors have often stated that this condition—the complete exclusion of the supraoccipital from the foramen magnum—is a synapomorphy of Tyrannosauroidea (e.g., Currie et al., 2003: char. 12; Xu et al., 2006). The more proper synapomorphic character for Tyrannosauroidea is a reduced supraoccipital contribution, and complete exclusion is either a synapomorphy of *Dilong* and *Guanlong*, was independently derived in *Dilong* and *Guanlong*, or was primitive for tyrannosauroids as a whole and later modified into the reduced condition of tyrannosauroids more derived than *Dilong* and *Guanlong*.

Character 149. Supraoccipital, form of dorsal margin: smoothly convex and undivided (0); divided into two processes (''forked'') (1).

There has been some confusion in the literature regarding this character, as well as a similar character describing the absence or presence of paired ''tablike'' processes of the supraoccipital in occipital view. Bakker et al. (1988), who first described the tablike processes, noted that these structures were present in all tyrannosaurids. Subsequently, Holtz (2001: char. 8) and Currie et al. (2003:

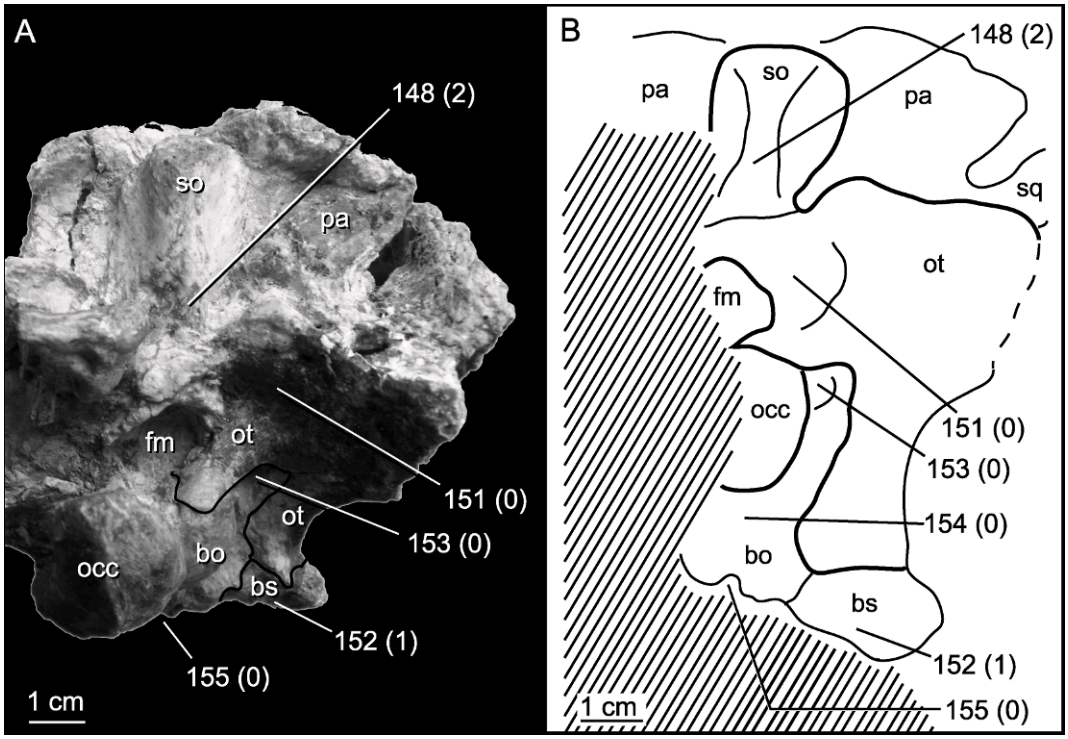

Fig. 33. Photograph (**A**) and line drawing (**B**) of the occlusal surface of the braincase of *Guanlong wucaii* (IVPP V14531). The line drawing was made with the rostrum angled downward relative to the photograph in order to more clearly show the basal tubera. Numbers refer to the character and character states listed in the Discussion. See appendix 1 for anatomical abbreviations.

char. 71) both considered the presence of the tablike processes to be synapomorphies of Tyrannosauridae (their analyses were published before basal tyrannosauroids such as *Guanlong* and *Dilong* were known). Carr and Williamson (2010: char. 172) also utilized this character, which they recovered as a tyrannosauroid synapomorphy, but then introduced a separate character: absence or presence of a forked supraoccipital (char. 170). The forked condition was scored as present only in the derived tyrannosaurines *Daspletosaurus*, *Tarbosaurus*, and *Tyrannosaurus*. Note that in the published version of the Carr and Williamson (2010) dataset the scores for characters 170 and 172 are switched in the data matrix (i.e., the proper scores for the tablike processes character for all taxa are listed in the data matrix as character 170, and the proper scores for the forked supraoccipital character are listed as character 172).

The analysis of Brusatte et al. (2010a) included only a single character relating to these features of the supraoccipital, because at the time some of the authors felt that these two character states were equivalent (i.e., that the bifurcation of the supraoccipital into two forks produced the tablike processes). However, recent observations by one of us (T.D.C.) reveal that the two characters are distinct from each other. The two characters can clearly be distinguished from each other on well-preserved tyrannosauroid specimens, and some taxa (such as *Alioramus altai*) possess the tablike processes but lack a forked supraoccipital. Therefore, we describe each of these characters separately here and will incorporate a second character, relating to the tablike processes, into later versions of our tyrannosauroid phylogenetic dataset.

BIFURCATED SUPRAOCCIPITAL: In most theropods, including most tyrannosauroids, the supraoccipital is an ovoid or wedge-

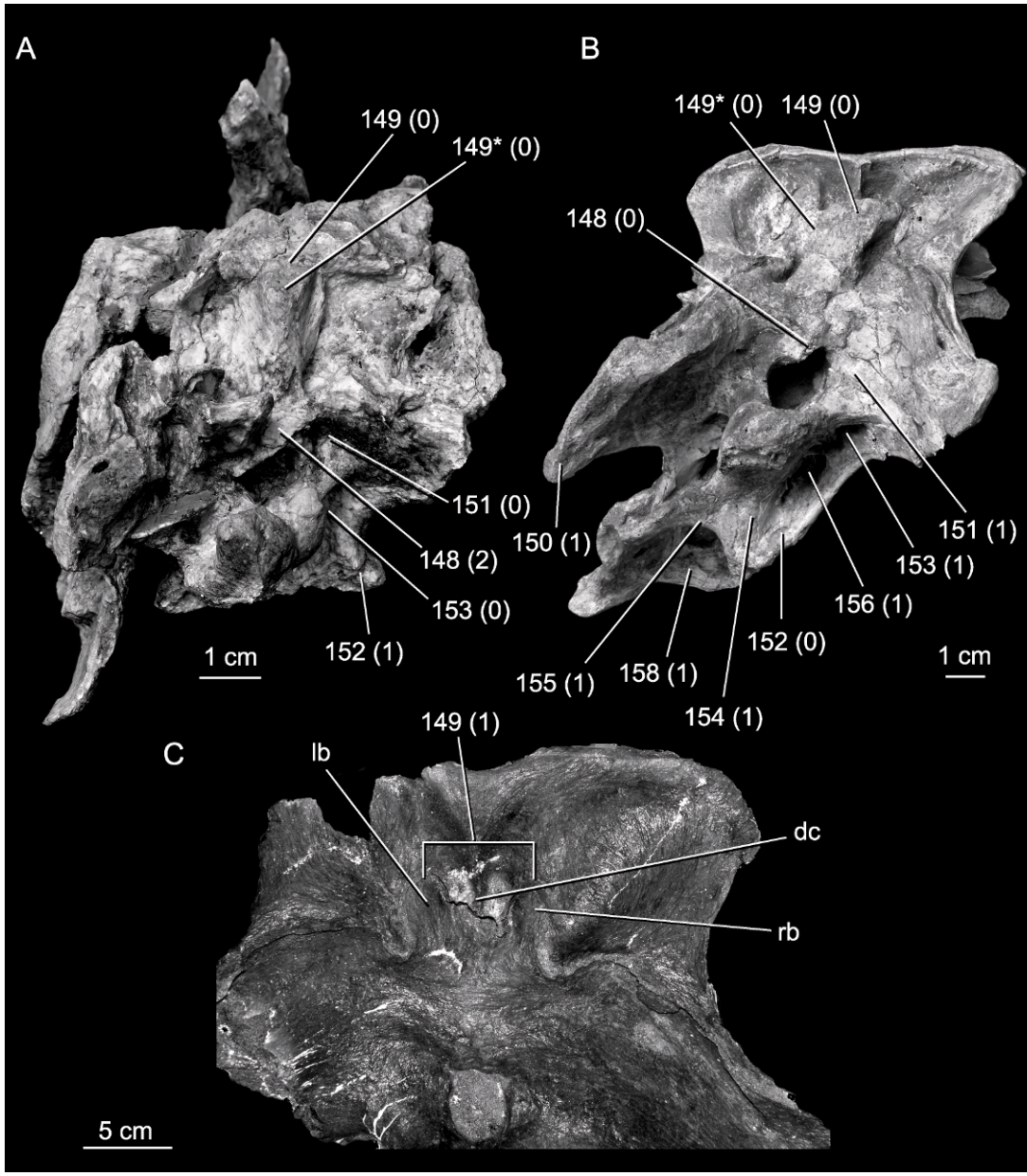

Fig. 34. Photographs of the occipital region of the braincase in (**A**) *Guanlong wucaii* (IVPP V14531), (**B**) *Alioramus altai* (IGM 100/1844), and (**C**) *Tyrannosaurus rex* (MOR 1125). The dorsal part of the occiput of *Guanlong* is in caudal view, but because of crushing, the ventral portion of the occiput (occipital condyle and basal tubera) is deflected somewhat ventrally and therefore viewed at an angle. The depressed center of the suproccipital/parietal suture (dc) causes the right and left bifurcations of the supraoccipital (rb and lb, respectively) to stick out as caudally projecting tabs. ''149*'' refers to the absence (0) or presence (1) of the caudally projecting tabs. Other numbers refer to the character and character states listed in the Discussion.

shaped element with a straight or convex dorsal margin (fig. 34A, B). This is the case in *Alioramus* (IGM 100/1844) as well as *Guanlong* (IVPP V14531), *Dilong* (IVPP V14243), *Xiongguanlong* (Li et al., 2010), *Albertosaurus* (Currie, 2003), *Gorgosaurus* (Currie, 2003; Witmer and Ridgely, 2009; ROM 1427), and *Teratophoneus* (Carr et al., 2011). In three derived tyrannosaurines—*Daspletosaurus*, *Tarbosaurus*, and *Tyrannosaurus*—the dorsal end of the supraoccipital is divided into two processes, the so-called forked condition (Osborn, 1912; Molnar, 1991; Brochu, 2003; Currie, 2003; Hurum and Sabath, 2003; fig. 34C).

TABLIKE PROCESSES: In most theropods, including the basal tyrannosauroids *Guanlong* (IVPP V14531), *Dilong* (IVPP V14243), and *Xiongguanlong* (Li et al., 2010), the dorsal margin of the supraoccipital is a flat plate that abuts (sits directly behind) the posterior surface of the parietal (fig. 34A). As first noted by Bakker et al. (1988), this is not the condition in more derived tyrannosauroids. In these taxa, the dorsal margin of the supraoccipital is not flat and does not sit directly against the parietal, but rather is folded (like a vertical fold in a partially drawn curtain) and curves posteriorly to overlie the remainder of the supraoccipital (like a quiff hairstyle) (fig. 34B, C). The posterior surface of the "quiff" is depressed at its center, and as a result, the left and right sides both appear as discrete tablike processes that project posteriorly. Therefore, these "tabs" are symmetrical along the dorsoventral midline of the supraoccipital. This morphology is present in *Bistahieversor* (NMMNH P-27469), *Albertosaurus* (Currie, 2003), *Gorgosaurus* (Currie, 2003; Witmer and Ridgely, 2009; ROM 1427), *Alioramus* (IGM 100/1844), *Daspletosaurus* (Currie, 2003), *Tarbosaurus* (Hurum and Sabath, 2003), and *Tyrannosaurus* (Bakker et al., 1988; Brochu, 2003; MOR 1125).

Character 150. Otoccipital (exoccipital-opisthotic), paroccipital process, ventral flange at distal end: absent (0); present (1).

This was a new character established by Brusatte et al. (2010a) to codify the derived presence of a ventrally expansive flange at the distal end of the paroccipital process in a subclade of tyrannosauroids (fig. 34B). The flange, which often takes the form of a discrete lobelike structure, is absent in the nontyrannosaurid tyrannosauroid *Xiongguanlong* (Li et al., 2010), present in the nontyrannosaurid *Bistahieversor*, and present in all known tyrannosaurids (*Albertosaurus*, *Daspletosaurus*, *Gorgosaurus*: Currie, 2003; *Alioramus*: IGM 100/1844; *Tarbosaurus*: Hurum and Sabath, 2003; *Teratophoneus*: Carr et al., 2011; *Tyrannosaurus*: Osborn, 1912, Brochu, 2003).

Character 151. Otoccipital (exoccipital-opisthotic), paroccipital process, deep fossa on posterior surface dorsolateral to the foramen magnum: present (0); absent (1).

This character, established by Brusatte et al. (2010a), encapsulates the derived presence of a deep, smooth fossa on the posterior surface of the paroccipital process, immediately dorsolateral to the foramen magnum (fig. 34B). This feature is absent in *Guanlong* (IVPP V14531; figs. 33, 34A) and *Dilong* (IVPP V14243), but it is present in *Xiongguanlong*, *Bistahieversor*, *Albertosaurus*, *Gorgosaurus*, *Alioramus*, *Teratophoneus*, *Daspletosaurus*, *Tarbosaurus*, and *Tyrannosaurus* (based on the citations provided in the character description above). This fossa does not bear any noticeable pneumatic foramina in any of the aforementioned taxa, and therefore does not appear to be associated with any of the pneumatic sinuses of the braincase, but it may conceivably be related to the cervical air sac system. Alternatively, it may be a muscle attachment site, although Snively and Russell (2007), in their study of tyrannosaurid neck muscles, did not reconstruct a muscle as attaching in this region.

Character 152. Otoccipital (exoccipital-opisthotic), crista tuberalis (= metotic strut of many authors, but see our description of terminology above), extent in caudal view: limited, mediolateral width across opposing cristae (measured at their dorsoventral midpoint) less than one-half the dorsoventral depth of the braincase from the dorsal tip of the supraoccipital to the ventral tip of the basal tubera (0); extensive, width greater than one-half the braincase depth (1).

In another new character, Brusatte et al. (2010a) scored *Guanlong* (IVPP V14531) and *Dilong* (IVPP V14243) as possessing the derived condition of a wide crista tuberalis

in occipital view (figs. 33, 34A). All other tyrannosauroids with known braincases were scored for the primitive condition of a narrow width across the cristae (fig. 34B). As discussed above, the great exposure of each crista tuberalis, which extends widely lateral, is due to the presence of pronounced ''corners'' at the lateroventral edge of each basal tuber. It is unclear, however, whether the conditions in *Guanlong* and *Dilong* are truly homologous. In *Guanlong* the ''corner'' is formed entirely by the basisphenoid, in the form of an ovoid process that is located immediately lateral to, and confluent with, the basal tuber in occipital view. In *Dilong*, on the other hand, the ''corner'' is formed entirely from a novel process of the basioccipital and located above the ventral level of the basal tuber, thus producing a notch between the ''corner'' and the tuber. Furthermore, if homologous between *Dilong* and *Guanlong*, it is unclear whether the wide condition is a synapomorphy of these taxa or a tyrannosauroid plesiomorphy lost in more derived taxa. The latter is suggested by the presence of wide cristae tuberalis in a close outgroup, ornithomimosaurs, although in these coelurosaurs the width of the cristae is caused by especially wide basal tubera and not additional corner-like contributions from the basioccipital or basisphenoid (Makovicky and Norell, 1998).

Per our interpretation, the corners at the lateroventral edge of each basal tuber at least could be homologous, despite variation in the bones comprising them. In this case, the bones forming this corner would be considered an additional character. Brusatte et al. (2010a) did not employ this character because each condition (i.e., a corner comprised of either basisphenoid or basioccipital) is currently known only in a single taxon each, and thus this character is phylogenetically uninformative at this time. Future discoveries, however, may reveal that other taxa share the basisphenoid or basioccipital condition with *Guanlong* or *Dilong*, respectively. When or if this happens, an additional character would then be warranted.

Character 153. Otoccipital (exoccipital-opisthotic), fossa for cranial nerves X–XII: shallow (0); deep (1).

This new character in the Brusatte et al. (2010a) dataset differentiates between shallow and deep paracondylar pockets—the fossae on the occipital surface of the braincase, below the pedicels linking the occipital condyle to the otoccipital, that house foramina for cranial nerves X–XII and the jugular vein. It is difficult to quantify what is meant by ''shallow'' and ''deep.'' However, the difference between the slightly inset fossae of basal tyrannosauroids (*Guanlong*, *Dilong*, and *Xiongguanlong*; figs. 33, 34A) and the deep, funnellike fossae of tyrannosauroids (*Albertosaurus*, *Gorgosaurus*, *Alioramus*, *Daspletosaurus*, *Tarbosaurus*, *Tyrannosaurus*; figs. 15, 34B) is stark. Brusatte et al. (2010a) scored this character as uncertain for *Bistahieversor* and *Teratophoneus*, but reassessments of both generally show that they too possess the derived state (T.D.C., personal obs.).

Character 154. Basioccipital, basal tubera, dorsoventral depth: less than (0) or greater than (1) depth of occipital condyle.

The basal tubera (here defined as the portion of the braincase extending below the occipital condyle as a sheet) of basal tyrannosauroids such as *Guanlong* (IVPP V14531), *Dilong* (IVPP V14243), and *Xiongguanlong* (Li et al., 2010) are short, vertical sheets that project only slightly below the occipital condyle (fig. 33). In contrast, the tubera of *Albertosaurus* (Currie, 2003), *Alioramus* (IGM 100/1844), *Daspletosaurus* (Currie, 2003), *Tarbosaurus* (Hurum and Sabath, 2003), and *Tyrannosaurus* (Osborn, 1912; Molnar, 1991; Brochu, 2003) are much larger and more ventrally extensive, with dorsoventral dimensions greater than that of the corresponding occipital condyle (fig. 34B). This distinction was first codified in a phylogenetic dataset by Brusatte et al. (2010a), who provided the above scores for the aforementioned taxa. However, Brusatte et al. (2010a) considered *Gorgosaurus* to possess the primitive state of short basal tubera, but we here note that this is incorrect (e.g., ROM 1247 has tubera that are clearly dorsoventrally deeper than the occipital condyle). We also note that both *Bistahieversor* (NMMNH P-27469) and *Teratophoneus* (BYU 8120/9396), which were scored as uncertain by Brusatte et al. (2010a), possess the derived state of deep basal tubera.

Character 155. Basioccipital, basal tubera, concave notch ventrally between opposing

tubera, dorsoventral depth: shallow, less than 40% of the depth of the tubera (0); deep, approximately 50% of the depth of the tubera (1).

In most theropods the left and right basal tubera are separated along their ventral margins by a concave notch (i.e., the ventral margin of the lamina formed by the conjoined tubera is concave). This is true of all tyrannosauroids, and as first noted by Brusatte et al. (2010a), there is phylogenetically informative variation in the depth of this notch. The basal tyrannosauroids *Guanlong* (IVPP V14531), *Proceratosaurus* (Rauhut et al., 2010), and *Xiongguanlong* (Li et al., 2010) have shallow notches, whose dorsoventral depth is less than half of the depth of the tuberal processes. In *Guanlong*, for instance, the notch is only approximately 10% of the depth of the tubera (fig. 33). More derived tyrannosauroids, however, have deeper notches that are approximately half of depth of the tubera (fig. 34B). These taxa include all tyrannosaurids with well-known braincases (*Albertosaurus*, *Gorgosaurus*, *Daspletosaurus*: Currie, 2003; *Alioramus*: IGM 100/1844; *Tarbosaurus*: Hurum and Sabath, 2003; *Tyrannosaurus*: Osborn, 1912, Molnar, 1991, Brochu, 2003), as well as the nontyrannosaurid *Bistahieversor* (Carr and Williamson, 2010).

Character 156. Basioccipital, subcondylar recess, depth of pneumatic fossae on posterior surface of basal tubera: absent or shallow (0); deep (1).

This character was first codified in a phylogenetic analysis by Carr and Williamson (2010: char. 166), who combined both the absence of subcondylar recesses and deep subcondylar recesses in a composite single state, while shallow recesses were considered a separate (derived) state. Brusatte et al. (2010a) modified this character construction to explicitly distinguish between shallow recesses, which are present as slightly inset fossae on the posterior surface of the basal tubera, from deep recesses, which are present as invasive, funnellike fossae that often have large pneumatic foramina at their centers. Some theropods do not appear to have a subcondylar recess based on external morphology, as they possess no clear fossae or pneumatic foramina. However, as most theropods have not been CT scanned, it is unclear whether the lack of external fossae truly reflects the lack of a subcondylar recess. Furthermore, in the absence of CT data, it is often uncertain whether shallow fossae are truly pneumatic or may be related to muscle attachment (Kurzanov, 1976; Rauhut, 2004). Therefore, taking into account this uncertainty, Brusatte et al. (2010a) combined the absent and shallow state into a single character, in order to minimize assumptions (because it is always straightforward to differentiate a deep funnellike recess from the shallow recess/no recess condition). As more theropod braincases are subject to CT scans, it will be possible to separate the absent and shallow states, and create a multistate ordered character.

Brusatte et al. (2010a) scored *Guanlong* (IVPP V14531), *Proceratosaurus* (Rauhut et al., 2010), *Dilong* (IVPP V14243), and *Xiongguanlong* (Li et al., 2010) for the primitive absent/shallow state. Most large tyrannosaurids, on the other hand, possess the derived funnellike state, including *Albertosaurus*, *Gorgosaurus*, *Daspletosaurus* (Currie, 2003), and *Alioramus* (IGM 100/1844; fig. 34B). Although scored as uncertain by Brusatte et al. (2010a), *Bistahieversor* (NMMNH P-27469) and *Teratophoneus* (BYU 8120/9396) also possess the funnellike state. *Tarbosaurus* and *Tyrannosaurus*, however, possess only very shallow fossae on the caudal surfaces of their basal tubera, although CT data shows that, at least in *Tyrannosaurus*, these fossae are associated with an internal pneumatic recess (Witmer and Ridgely, 2009). Therefore, based on character optimization on the phylogeny of Brusatte et al. (2010a), shallow or absent recesses were primitive for Tyrannosauroidea, deeper recesses evolved at or near the base of Tyrannosauridae, and then a reversal to shallower recesses occurred in the *Tarbosaurus* + *Tyrannosaurus* sister group. The ontogenetic change, from a deep fossa in juvenile *Tyrannosaurus* (CMNH 7541) to the shallow condition in adults is consistent with the phylogenetic trend.

Character 157. Basisphenoid, basipterygoid recess (lateral pneumatic opening on the lateral surface of the braincase above the basipterygoid process, associated with the rostral tympanic recess): absent or present as

shallow pneumatic fossa (0); present as a large rectangular fenestra (1).

Many theropods have pneumatic foramina and fossae on the lateral surface of the basisphenoid and, as described by Rauhut (2004), sometimes pneumaticity in this region is manifested as large depressions or fenestrae that are often referred to as the ''basipterygoid recess.'' As described above, our CT data shows that the ''basipterygoid recess'' of *Alioramus* (which takes the form of a large, rectangular fenestra penetrating the lateral surface of the basisphenoid, immediately above the basipterygoid process) communicates internally with the rostral tympanic recess, and therefore we consider it part of the larger rostral tympanic system.

Carr and Williamson (2010: char. 158) utilized a character referring to the absence or presence of ''pneumatic recess(es) above (the) basipterygoid process in lateral view.'' However, because so many theropods possess pneumaticity in this region, and (as discussed above with the subcondylar recess) it is often difficult to tell whether a taxon with no external pneumatic features or with shallow depressions truly possessed an internal basipterygoid recess leading into the rostral tympanic recess, Brusatte et al. (2010a) restructured this character. They differentiated between the shallow (or absent) lateral fossae of most theropods and the discrete, rectangular, windowlike openings that are present only in *Alioramus* (IGM 100/1844) and *Daspletosaurus* (Currie, 2003: fig. 26) among tyrannosauroids. Subsequent observation has also revealed that *Bistahieversor* (NMMNH P-25049) possesses the windowlike condition as well. Based on character optimization, this feature may have evolved independently in these three tyrannosaurids.

It is worth noting, however, that all known *Alioramus*, *Bistahieversor*, and *Daspletosaurus* specimens with the windowlike condition are juveniles. On the other hand, adult specimens of *Daspletosaurus* (CMN 8506) and *Bistahieversor* (NMMNH P27469) do not possess the windowlike condition, but rather have a smaller recess that is more typical for theropods (adult specimens of *Alioramus* are currently unknown). It appears, therefore, as if the transition from a large fenestra to a small recess occurred during ontogeny in several tyrannosauroids, and this may be a more general transformation characteristic of one or more clades of tyrannosauroids.

Character 158. Basisphenoid, basisphenoid recess, orientation of central axis (when the skull is held with the frontals lying horizontally): vertical, recess obscured in caudal view (0); caudoventral, recess partially visible in caudal view (1); extremely caudoventral, recess compressed rostrocaudally and widely visible in caudal view, and basipterygoid processes located beneath the basal tubera (2).

Authors have long noted that the orientation of the basisphenoid recess differs among theropods. The recess, which is located between the basal tubera and basipterygoid processes on the ventral surface of the braincase, faces completely ventrally in many theropods, such that it is not visible when the skull is seen in caudal view. Currie et al. (2003: char. 7) considered a modified condition, a recess that faces almost equally caudally and ventrally, to be a synapomorphy of tyrannosauroids, and later authors followed suit by distinguishing between a ventrally facing and caudoventrally facing recess in their character statements (e.g., Sereno et al., 2009: char. 50; Carr and Williamson, 2010: char. 163).

Brusatte et al. (2010a) modified this character to add a second derived state, thus transforming the character into an ordered multistate. They scored all tyrannosauroids as possessing a synapomorphic derived condition of a caudoventrally facing recess (fig. 34B), and furthermore united three derived tyrannosaurines as sharing a further modified condition in which the recess is oriented at such an extreme caudoventral degree that it is widely visible in caudal view (*Tarbosaurus*: Hurum and Sabath, 2003; *Teratophoneus*: Carr et al., 2011; *Tyrannosaurus*: Osborn 1912, Brochu, 2003). In these three taxa, the basisphenoid recess is rostrocaudally compressed and the basipterygoid processes are located almost immediately below the basal tubera, a reorientation that serves to widely expose the recess in caudal view. Brusatte et al. (2010a) considered this an ordered character because the three conditions form a logical geometric sequence

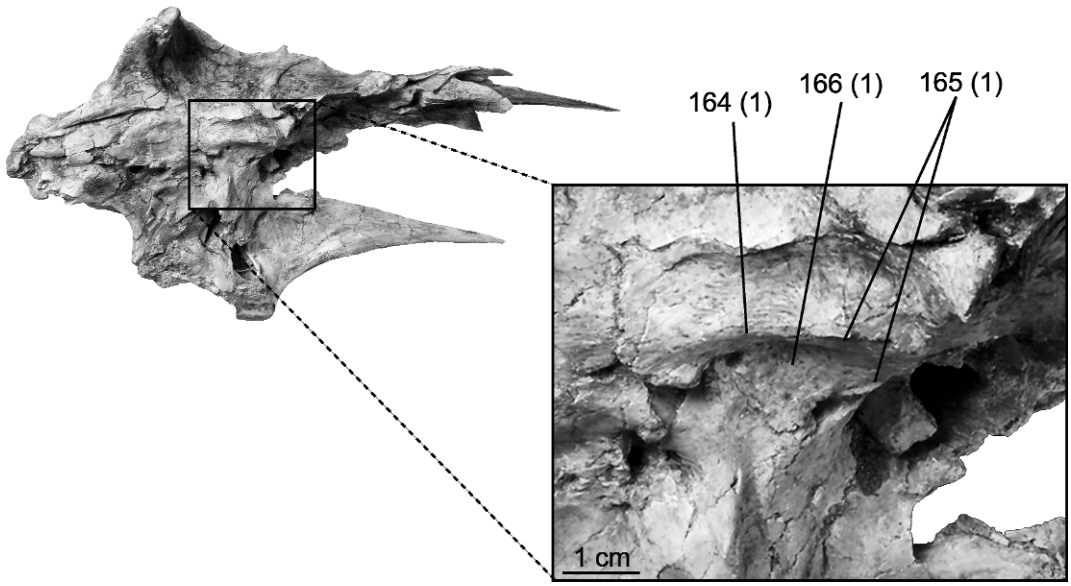

Fig. 35. Right lateral surface of the braincase of *Alioramus* (IGM 100/1844). Numbers refer to the character and character states listed in the Discussion.

(ventral-caudoventral-caudal, and by not ordering this character the caudoventral and caudal condition would not be united as a derived similarity (see Brazeau, 2011, for an explanation of the necessity of this type of coding scheme).

Character 159. Basisphenoid, basisphenoid recess, inflation of the ceiling of the recess: absent (0); present (1).

In ventral view, the ceiling of the recess refers to its dorsally concave interior surface. In some large tyrannosauroids, including *Bistahieversor* (NMMNH P-27469), *Daspletosaurus* (CMN 8506), *Raptorex* (LH PV18), and *Alioramus altai* (IGM 100/1844), the ceiling extends deeply upward as a funnellike cavity, far dorsal to the pneumatic foramina that penetrate the rostral wall of the recess. This condition is different in *Albertosaurus* (CMN 5600) and in *Gorgosaurus* (ROM 1247), where the ceiling is not a deep funnel, but is low. This condition is the result of inflation of the rostral wall of the recess, which fills out the rostral half of the recess (reducing the space) and orients the pneumatic foramina partly ventrally such that the openings face each other. In effect, the recess is less capacious than the condition that is seen in taxa where the recess is not inflated. The caudal orientation of the pneumatic foramina in *Tyrannosaurus* (TMP 1981.006.0001) indicates that it does not have the inflated condition, nor does *Tarbosaurus* (Hurum and Sabath, 2003), *Teratophoneus* (Carr et al., 2011), *Xiongguanlong* (Li et al., 2010), *Guanlong* (IVPP V14531), *Dilong* (IVPP V14243), and *Proceratosaurus* (Rauhut et al., 2010).

Character 160. Basisphenoid, basisphenoid recess, shape in ventral view: funnellike, expands in mediolateral width caudally (0); ovoid or circular, no caudal expansion (1).

In many theropods the basisphenoid recess expands in mediolateral width as it extends caudally, such that it has a funnellike shape in ventral view (fig. 35A). This is the case in the basal tyrannosauroids *Guanlong* (IVPP V14531) and *Proceratosaurus* (NHMUK R 4860), as well as *Raptorex* (Sereno et al., 2009). In more derived tyrannosauroids, however, the recess is approximately circular or ovoid in ventral view (or caudal view in *Tarbosaurus* and *Tyrannosaurus*), with no marked caudal expansion (fig. 35B). This condition is scored as present in *Bistahieversor* (Carr and Williamson, 2010), *Albertosaurus*, *Gorgosaurus*, *Daspletosaurus* (Currie, 2003), *Alioramus* (IGM 100/1844), *Tarbosaurus* (Hurum and Sabath, 2003), and

Tyrannosaurus (Brochu, 2003). The distinction between a funnellike and ovoid recess was codified as a phylogenetic character by Brusatte et al. (2010a).

Character 161. Basisphenoid, shape of basicranium (rectangle defined by positions of both basal tubera and both basipterygoid processes): rostroventrally longer than mediolaterally wide (0); wider than long (1). Measurements are taken at the center of the basicranium and are taken across the basicranium walls (i.e., they also include the length/width of the walls).

As codified by Currie et al. (2003: char. 8), and later followed by Sereno et al. (2009: char. 49) and Carr and Williamson (2010: char. 167), tyrannosauroids differ in the length : width ratio of the basicranium, which is most noticeable when specimens are seen in ventral view. Brusatte et al. (2010a) also included this character, and scored the basal tyrannosauroids *Guanlong* (IVPP V14531) and *Dilong* (IVPP V14243) for the primitive longer-than-wide condition and more derived tyrannosauroids for the wider-than-long condition. These latter taxa include *Xiongguanlong* (Li et al., 2010), *Albertosaurus*, *Gorgosaurus* (ROM 1247), *Daspletosaurus* (Currie, 2003), *Alioramus* (IGM 100/1844), *Tarbosaurus* (Hurum and Sabath, 2003), *Teratophoneus* (Carr et al., 2011), and *Tyrannosaurus* (Brochu, 2003). A few of these scores differ from previous studies. Currie et al. (2003) and Sereno et al. (2009) scored *Gorgosaurus* for the primitive state, but some specimens show that it has a basicranium that is wider than long (e.g., ROM 1247; TMP 91.36.500). Sereno et al. (2009) also scored *Guanlong* for the derived wider-than-long state, but the holotype (IVPP V14531) shows that this is not the case (fig. 35A).

Character 162. Parasphenoid, shape of rostrum: rostrocaudally expanded, ventral margin is a smooth concave arch (0); dorsoventrally expanded, ventral margin is nearly vertical posteriorly and then abruptly transitions to a horizontal trend anteriorly (1).

In this new character, Brusatte et al. (2010a) differentiated two general morphologies of the parasphenoid rostrum among tyrannosauroids. *Guanlong* (IVPP V14531), *Alioramus* (IGM 100/1844), and *Raptorex* (Sereno et al., 2009) have a primitive condition, also seen in outgroups, in which the rostrum is rostrocaudally elongate, with a ventral margin that transcribes a single, smoothly convex arch. Other tyrannosauroids, however, have a proportionally shorter but deeper rostrum, with a ventral margin whose caudal partion trends vertically in its posterior part and then rapidly changes to a horizontal trend more rostrally. Taxa possessing this morphology include *Bistahieversor* (Carr and Williamson, 2010), *Albertosaurus*, *Gorgosaurus*, *Daspletosaurus* (Currie, 2003), *Tarbosaurus* (Hurum and Sabath, 2003), and *Tyrannosaurus* (Brochu, 2003). Because the holotypes of *Alioramus altai* and *Raptorex* are both immature, it is possible (perhaps likely) that the shape of the parasphenoid rostrum is ontogenetically controlled, with younger individuals retaining the primitive condition. Testing this hypothesis awaits future discoveries, especially of more mature individuals of *Alioramus*. It is interesting to note, however, that a seemingly intermediate condition between the primitive and derived states is seen in juvenile *Tyrannosaurus* (CMNH 7541; Witmer and Ridgely, 2009), and possibly also *Tarbosaurus* (MPC-D 107/7; Tsuihiji et al., 2011), where the rostrum is positioned relatively close to the basipterygoid processes. At the very least, these specimens indicate that the shape of the rostrum changed during postnatal ontogeny, as the condition in the juveniles is different than that in adult *Tyrannosaurus* and *Tarbosaurus* (see above).

Character 163. Prootic, dorsal tympanic recess: present (0); absent (1).

Some theropods possess a pneumatic recess on the prootic (and often the parietal), which continues into an internal cavity that is often called the ''dorsal tympanic recess'' (although it may not be homologous to that of extant birds). This feature is present in tyrannosauroid outgroups, including oviraptorosaurs and maniraptorans (Rauhut, 2004), as well as the basal tyrannosauroid *Guanlong* (IVPP V14531). All other tyrannosauroids with well-preserved braincases, however, lack this feature. These taxa include *Bistahieversor* (Carr and Williamson, 2010), *Albertosaurus*, *Gorgosaurus*, *Daspletosaurus* (Currie, 2003), *Alioramus* (IGM 100/1844),

Tarbosaurus (Hurum and Sabath, 2003), *Teratophoneus* (Carr et al., 2011), and *Tyrannosaurus* (Brochu, 2003). Therefore, if this recess is truly homologous among theropods, then a clade of derived tyrannosauroids is united by the loss of the recess.

Character 164. Laterosphenoid, antotic crest separating lateral wall of braincase from orbital and temporal spaces: absent or indistinct (0); present and robust and rugose (1).

Carr and Williamson (2010: chars. 150, 153) utilized two characters that we here consider equivalent to a single character used by Brusatte et al. (2010a), which concerns the morphology of the antotic crest of the laterosphenoid. This ridge of bone separates the lateral wall of the braincase (prootic, laterosphenoid, otoccipital) from the orbital and temporal spaces, which would have been filled with the eyeball and jaw adductor muscles, respectively. The crest is absent or subtle (taking the form of a thin ridge) in many theropods, including *Guanlong* (IVPP V14531), *Bistahieversor* (Carr and Williamson, 2010), *Albertosaurus*, and *Gorgosaurus* (Currie, 2003). Some tyrannosaurines, however, exhibit a modified condition in which the crest is especially prominent, rugose, and swollen (Russell, 1970). These include *Alioramus* (IGM 100/1844; fig. 36), *Daspletosaurus* (Currie, 2003), *Tarbosaurus* (Hurum and Sabath, 2003), and *Tyrannosaurus* (Osborn, 1912; Brochu, 2003).

Character 165. Laterosphenoid, antotic crest, form: single structure (0); bifurcates ventrally (1).

A further character regarding the antotic crest, first utilized by Brusatte et al. (2010a), concerns the shape of this structure. In most theropods, including *Guanlong* (IVPP V14531), the antotic crest is a single structure across its entire length. In more derived tyrannosauroids, however, it bifurcates ventrally (fig. 36). These tyrannosauroids include *Bistahieversor* (Carr and Williamson, 2010), *Albertosaurus*, *Gorgosaurus*, *Daspletosaurus* (Currie, 2003), *Alioramus* (IGM 100/1844), *Tarbosaurus* (Hurum and Sabath, 2003), and *Tyrannosaurus* (Osborn, 1912; Brochu, 2003).

Character 166. Laterosphenoid, fossa on the lateral surface that houses the head of the epipterygoid: absent or shallow (0); present, deep, and rugose (1).

The head of the epipterygoid contacts the lateral surface of the laterosphenoid (and sometimes the prootic) in theropods, and usually this contact is marked by a flat surface or subtle depression on the lateral side of the braincase. This is the case in tyrannosauroid outgroups (e.g., *Allosaurus*: Madsen, 1976; maniraptorans: Norell et al., 2006), as well as *Guanlong* (IVPP V14531). Many derived tyrannosauroids, however, exhibit a deep and rugose contact surface, between the bifurcated portions of the antotic crest (fig. 36). These taxa include *Bistahieversor* (Carr and Williamson, 2010), *Albertosaurus*, *Gorgosaurus*, *Daspletosaurus* (Currie, 2003), *Alioramus* (IGM 100/1844), *Tarbosaurus* (Hurum and Sabath, 2003), and *Tyrannosaurus* (Osborn, 1912; Brochu, 2003). Because the epipterygoid articulation is associated with the antotic crest, and because the distribution of character scores for this and the previous character are identical, it is possible that the two characters (165, 166) are correlated. Further testing awaits the description of more specimens.

Character 167. Ossified sphenethmoid and mesethmoid (when not fossilized, these can be inferred by the presence of scars on the ventral surface of the frontal): absent (0); present (1).

As discussed above, ossified sphenethmoid and mesethmoid bones (which cup the olfactory bulbs and tracts) are present in only a select few theropods (Ali et al., 2008). They are absent in *Guanlong* (IVPP V14531) and *Raptorex* (Sereno et al., 2009), both of which also lack the associated attachment scars on the ventral surface of the frontal. Several more derived tyrannosauroids do possess ossified sphenethmoid and mesethmoid bones, or their presence can be inferred by the presence of frontal scars. Among these taxa are *Bistahieversor* (Carr and Williamson, 2010), *Albertosaurus*, *Gorgosaurus*, *Daspletosaurus* (Currie, 2003), *Alioramus* (IGM 100/1844), *Tarbosaurus* (Hurum and Sabath, 2003), and *Tyrannosaurus* (Osborn, 1912; Brochu, 2003; Ali et al., 2008).

CONCLUSIONS

In paleontology, and especially vertebrate paleontology, our progressive understanding

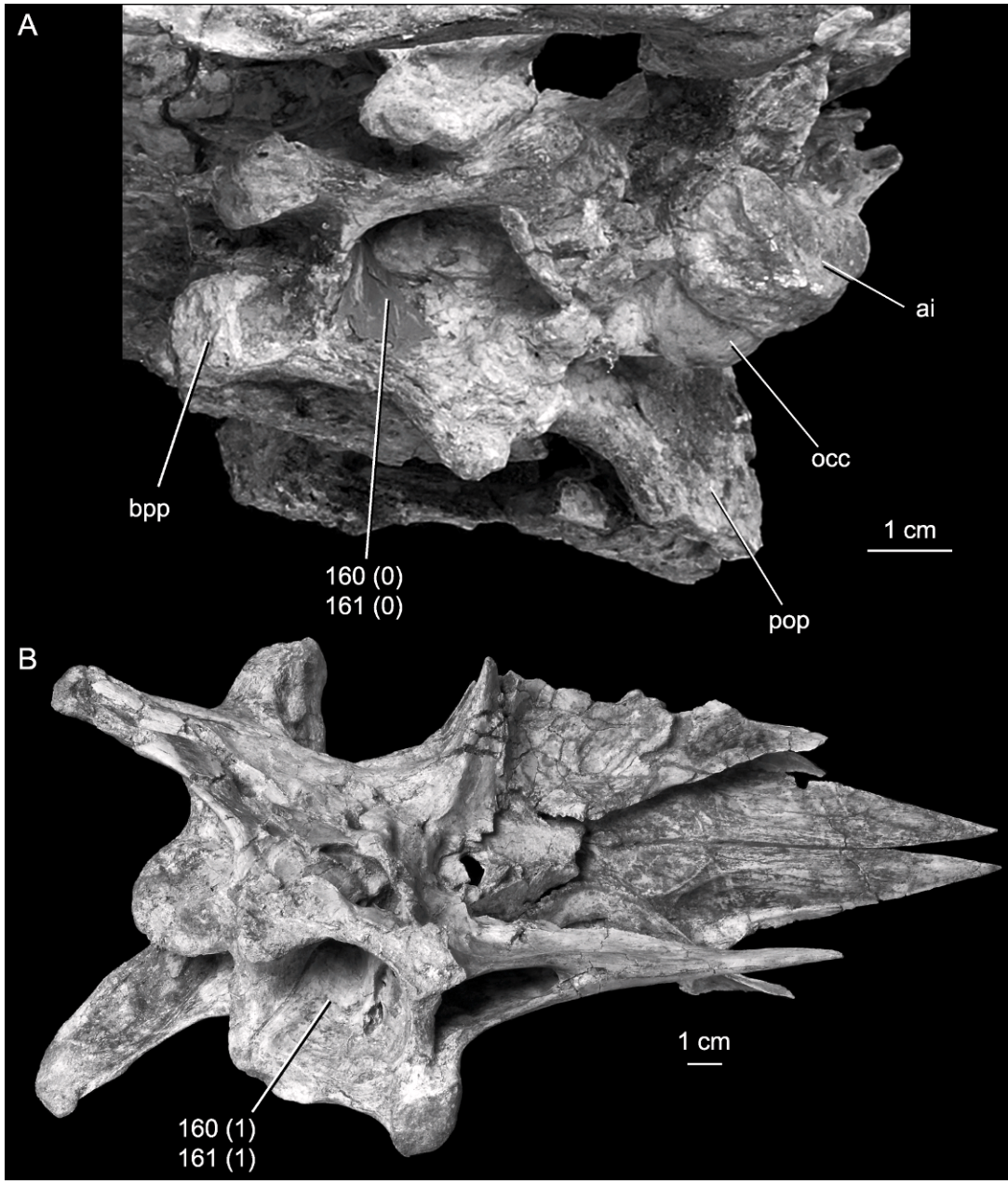

Fig. 36. Ventral surface of the basicranium in (**A**) *Guanlong wucaii* (IVPP V14531) and (**B**) *Alioramus altai* (IGM 100/1844). The rostral end of the braincase is to the left for *Guanlong* and to the right for *Alioramus*.

of systematics and paleobiology is fueled by two enterprises: the discovery of new fossil material and the development of new technologies that allows specimens to be studied in different ways. There is no better example of this dynamic than the detailed braincase description of the holotype of *Alioramus altai* provided here. While it is truly a remarkable specimen, our research efforts were greatly facilitated by the use of high-resolution CT

data, which among other things, allowed us to study in detail the complex anatomy of the various endocranial spaces, including that which housed the brain. These spaces are a potentially rich source of information for understanding everything from sensory capabilities, to behavior, to phylogenetic relationships.

The comparative context needed to transform these potentialities to a full realization remains elusive and will require many more of the type of labor-intensive descriptions presented here. Within Tyrannosauridae, the availability of appropriate comparative data is actually becoming quite dense, which allowed us to evaulate the phylogenetic distribution of numerous internal braincase features within this important clade. Similar datasets are needed for more nontyrannosaurid tyrannosauroids before these internal characters can be fully integrated with those external braincase characters that have been used both traditionally and contemporaneously to decipher tyrannosauroid phylogeny and diagnoses.

ACKNOWLEDGMENTS

We thank Julia Clarke for finding the specimen and all the members of the 2001 American Museum of Natural History–Mongolian Academy of Sciences Paleontological Expedition for collecting it. We thank Amy Davidson for continually providing preparation of the highest quality. Mick Ellison is thanked for producing most of the specimen photographs. CT scanning was facilitated by Justin Sipla (University of Texas at El Paso) and was performed by Matt Colbert (University of Texas at Austin, High-Resolution Computed Tomography facility [UTCT]). Jessie Maisano (UTCT) helped us post our images and movies on the DigiMorph website (www.digimorph.org). The manuscript benefited from the critical remarks of Bhart-Anjan Bhullar and an anonymous reviewer. Support for this project came from the Division of Paleontology at the American Museum of Natural History, New York College of Osteopathic Medicine, Carthage College, and the Institute for Vertebrate Paleontology and Paleoanthropology. S.L.B. is supported by a National Science Foundation Graduate Research Fellowship (Columbia University) and an NSF Doctoral Dissertation Improvement Grant (NSF DEB 1110357).

REFERENCES

Abdala, F., D.A. Flores, and N.P. Giannini. 2001. Postweaning ontogeny of the skull of *Didelphis albiventris*. Journal of Mammalogy 82: 190–200.

Ali, F., D.K. Zelenitsky, F. Therrien, and D.B. Weishampel. 2008. Homology of the "ethmoid complex" of tyrannosaurids and its implications for the reconstruction of the olfactory apparatus of non-avian theropods. Journal of Vertebrate Paleontology 28: 123–133.

Allain, R. 2002. Discovery of megalosaur (Dinosauria, Theropoda) in the Middle Bathonian of Normandy (France) and its implications for the phylogeny of basal Tetanurae. Journal of Vertebrate Paleontology 22: 548–563.

Alonso, P.D., A.C. Milner, R.A. Ketcham, M.J. Cookson, and T.B. Rowe. 2004. The avian nature of the brain and inner ear of *Archaeopteryx*. Nature 430: 666–669.

Bakker, R.T., M. Williams, and P.J. Currie. 1988. *Nanotyrannus*, a new genus of pygmy tyrannosaur, from the latest Cretaceous of Montana. Hunteria 1 (5): 1–30.

Baird, I.R. 1970. The anatomy of the reptilian ear. *In* C. Gans and T.S. Parsons (editors), Biology of the Reptilia. Vol. 2. Morphology B, 193–275. London: Academic Press.

Balanoff, A.M., X. Xu, Y. Kobayashi, Y. Matsufune, and M.A. Norell. 2009. Cranial osteology of the theropod dinosaur *Incisivosaurus gauthieri* (Theropoda: Oviraptorosauria). American Museum Novitates 3651: 1–35.

Barsbold, R., and H. Osmólska. 1999. The skull of *Velociraptor* (Theropoda) from the Late Cretaceous of Mongolia. Acta Palaeontologica Polonica 44: 189–212.

Baumel, J.J., and L.M. Witmer. 1993. Osteologia. *In* J.J. Baumel (editor), Handbook of avian anatomy: nomina anatomica avium. Publications of the Nuttall Ornithological Club 23: 133–188.

Bellairs, A.D'A., and A.M. Kamal. 1981. The chondrocranium and the development of the skull in recent reptiles. *In* C. Gans and T.S. Parsons (editors), Biology of the Reptilia. Vol. 11. Morphology F: 1–263. London: Academic Press.

Bever, G.S. 2008. Comparative growth in the postnatal skull of the extant North American turtle *Pseudemys texana* (Testudinoidea: Emydidae). Acta Zoologica 89: 107–131.

Bever, G.S. 2009. Postnatal ontogeny of the skull in the extant North American turtle *Ster-*

notherus odoratus (Cryptodira: Kinosternidae). Bulletin of the American Museum of Natural History 330: 1–97.

Bever, G.S., and M.A. Norell. 2009. The perinate skull of *Byronosaurus* (Troodontidae) with observations on the cranial ontogeny of paravian theropods. American Museum Novitates 3657: 1–51.

Bever, G.S., C.J. Bell, and J.A. Maisano. 2005. The ossified braincase and cephalic osteoderms of *Shinisaurus crocodilirus* (Squamata, Shinisauridae). Palaeontologia Electronica 8 (1): 4A: 36 pp.

Bever, G.S., S.L. Brusatte, A.M. Balanoff, and M.A. Norell. 2011. Variation, variability, and the origin of the avian endocranium: insights from *Alioramus altai*. PLoS One 6 (8): e23393.

Bhullar, B.-A.S. 2012. A phylogenetic approach to ontogeny and heterochrony in the fossil record: cranial evolution and development in anguimorphan lizards (Reptilia: Squamata). Journal of Experimental Zoology, Molecular and Developmental Evolution 318: 521–530.

Bhullar, B.-A.S., et al. 2012. Birds have paedomorphic dinosaur skulls. Nature 487: 223–226.

Bhullar, B.-A.S., and G.S. Bever. 2009. An archosaur-like laterosphenoid in early turtles (Reptilia: Pantestudines). Breviora 518: 1–11.

Brazeau, M.D. 2011. Problematic character coding methods in morphology and their effects. Biological Journal of the Linnean Society 104: 489–498.

Brochu, C.A. 2000. A digitally rendered endocast for *Tyrannosaurus rex*. Journal of Vertebrate Paleontology 20: 1–6.

Brochu, C.A. 2003. Osteology of *Tyrannosaurus rex*: insights from a nearly complete skeleton and high-resolution computed tomographic analysis of the skull. Journal of Vertebrate Paleontology Memoir 7: 1–138.

Brusatte, S.L., and P.C. Sereno. 2007. A new species of *Carcharodontosaurus* (Dinosauria: Theropoda) from the Cenomanian of Niger and a revision of the genus. Journal of Vertebrate Paleontology 27: 902–916.

Brusatte, S.L., and P.C. Sereno. 2008. Phylogeny of Allosauroidea (Dinosauria: Theropoda): comparative analysis and resolution. Journal of Systematic Palaeontology 6: 155–182.

Brusatte, S.L., T.D. Carr, and M.A. Norell. 2012. The osteology of *Alioramus*, a gracile and long-snouted tyrannosaurid (Dinosauria: Theropoda) from the Late Cretaceous of Mongolia. Bulletin of the American Museum of Natural History 366: 1–197.

Brusatte, S.L., T.D. Carr, G.M. Erickson, G.S. Bever, and M.A. Norell. 2009. A long-snouted multihorned tyrannosaurid from the Late Cretaceous of Mongolia. Proceedings of the National Academy of Sciences of the United States of America 106: 17261–17266.

Brusatte, S.L., et al. 2010a. Tyrannosaur paleobiology: new research on ancient exemplar organisms. Science 329: 1481–1485.

Brusatte, S.L., D.J. Chure, R.B.J. Benson, and X. Xu. 2010b. The osteology of *Shaochilong maortuensis*, a carcharodontosaurid (Dinosauria: Theropoda) from the Late Cretaceous of Asia. Zootaxa 2334: 1–46.

Brusatte, S.L., R.B.J. Benson, and X. Xu. 2010c. The evolution of large-bodied theropod dinosaurs during the Mesozoic in Asia. Journal of Iberian Geology 36: 275–296.

Carr, T.D. 1999. Craniofacial ontogeny in the Tyrannosauridae (Dinosauria, Coelurosauria). Journal of Vertebrate Paleontology 19: 497–520.

Carr, T.D., and T.E. Williamson. 2004. Diversity of late Maastrichtian Tyrannosauridae (Dinosauria: Theropoda) from western North America. Zoological Journal of the Linnean Society 142: 479–523.

Carr, T.D., and T.E. Williamson. 2010. *Bistahieversor sealeyi*, gen. et sp. nov., a new tyrannosauroid from New Mexico and the origin of deep snouts in Tyrannosauroidea. Journal of Vertebrate Paleontology 30: 1–16.

Carr, T.D., T.E. Williamson, B.B. Britt, and K. Stadtman. 2011. Evidence for high taxonomic and morphologic tyrannosauroid diversity in the Late Cretaceous (Late Campanian) of the American Southwest and a new short-skulled tyrannosaurid from the Kaiparowits Formation of Utah. Naturwissenschaften 98: 241–246.

Charig, A.J., and A.C. Milner. 1997. *Baryonyx walkeri*, a fish-eating dinosaur from the Wealden of Surrey. Bulletin of the Natural History Museum, Geology 53: 11–70.

Chure, D.J., and J.H.J. Madsen. 1996. Variation in aspects of the tympanic pneumatic system in a population of *Allosaurus fragilis* from the Morrison Formation (Upper Jurassic). Journal of Vertebrate Paleontology 16: 63–66.

Chure, D.J., and J.H. Madsen. 1998. An unusual braincase (?*Stokesosaurus clevelandi*) from the Cleveland-Lloyd Dinosaur Quarry, Utah (Morrison Formation; Late Jurassic). Journal of Vertebrate Paleontology 18: 115–125.

Clark, J.M., J. Welman, J.A. Gauthier, and J.M. Parrish. 1993. The laterosphenoid bone of early archosauriforms. Journal of Vertebrate Paleontology 13: 48–57.

Clark, J.M., A. Perle, and M.A. Norell. 1994. The skull of *Erlicosaurus* [sic] *andrewsi*, a Late Cretaceous "segnosaur" (Theropoda: Therizinosauridae) from Mongolia. American Museum Novitates 3115: 1–39.

Coria, R.A., and P.J. Currie. 2002. The braincase of *Gigantosaurus carolinii* (Dinosauria: Theropoda) from the Upper Cretaceous of Argentina. Journal of Vertebrate Paleontology 22: 802–811.

Currie, P.J. 1985. Cranial anatomy of *Stenonychosaurus inequalis* (Saurischia, Theropoda) and its bearing on the origin of birds. Canadian Journal of Earth Sciences 22: 1643–1658.

Currie, P.J. 1995. New information on the anatomy and relationships of *Dromaeosaurus albertensis* (Dinosauria: Theropoda). Journal of Vertebrate Paleontology 15: 576–591.

Currie, P.J. 1997. Braincase anatomy. *In* P.J. Currie and K. Padian (editors), Encyclopedia of dinosaurs, 81–85. San Diego: Academic Press.

Currie, P.J. 2003. Cranial anatomy of tyrannosaurid dinosaurs from the Late Cretaceous of Alberta, Canada. Acta Palaeontologica Polonica 48: 191–226.

Currie, P.J., and X.-J. Zhao. 1993. A new troodontid (Dinosauria, Theropoda) braincase from the Judith River Formation (Campanian) of Alberta. Canadian Journal of Earth Sciences 30: 2231–2247.

Currie, P.J., J.H. Hurum, and K. Sabath. 2003. Skull structure and evolution in tyrannosaurid dinosaurs. Acta Palaeontologica Polonica 48: 227–234.

Elzanowski, A., and P. Wellnhofer. 1996. Cranial morphology of *Archaeopteryx*: evidence from the seventh skeleton. Journal of Vertebrate Paleontology 16: 81–94.

Fowler, D.W., H.N. Woodward, E.A. Freedman, P.L. Larson, and J.R. Horner. 2011. Reanalysis of "*Raptorex kriegsteini*": a juvenile tyrannosaurid dinosaur from Mongolia. PLoS One 6 (6): e21376. [doi:10.1371/journal.pone.0021376]

Franzosa, J., and T. Rowe. 2005. Cranial endocast of the Cretaceous theropod dinosaur *Acrocanthosaurus atokensis*. Journal of Vertebrate Paleontology 25: 859–864.

Gleich, O., R.J. Dooling, and G.A. Manley. 2005. Audiogram, body mass, and basilar papilla length: correlations in birds and predictions for extinct archosaurs. Naturwissenschaften 92: 595–598.

Gower, D.J., and E. Weber. 1998. The braincase of *Euparkeria*, and the evolutionary relationships of birds and crocodilians. Biological Reviews 73: 367–411.

Holliday, C.M., and L.M. Witmer. 2007. Archosaur adductor chamber evolution: integration of musculoskeletal and topological criteria in jaw muscle homology. Journal of Morphology 268: 457–484.

Holliday, C.M., and L.M. Witmer. 2008. Cranial kinesis in dinosaurs: intracranial joints, protractor muscles, and their significance for cranial evolution and function in diapsids. Journal of Vertebrate Paleontology 28: 1073–1088.

Holtz, T.R., Jr. 2001. The phylogeny and taxonomy of Tyrannosauridae. *In* D.H. Tanke and K. Carpenter (editors), Mesozoic vertebrate life, 64–83. Bloomington: Indiana University Press.

Holtz, T.R., Jr. 2004. Tyrannosauroidea. *In* D.B. Weishampel, P. Dodson, and H. Osmólska (editors), The Dinosauria, 2nd ed.: 111–136. Berkeley: University of California Press.

Holtz, T.R., R.E. Molnar, and P.J. Currie. 2004. Basal Tetanurae. *In:* D.B. Weishampel, P. Dodson, and H. Osmólska (editors), The Dinosauria, 2nd ed.: 71–110. Berkeley: University of California Press.

Horner, J.R., and E. Dobb. 1997. Dinosaur lives: unearthing an evolutionary saga. New York: Harper Collins, 256 pp.

Hurum, J.H., and K. Sabath. 2003. Giant theropod dinosaurs from Asia and North America: skulls of *Tarbosaurus bataar* and *Tyrannosaurus rex* compared. Acta Paleontologica Polonica 48: 161–190.

Kirkland, J.I., L.E. Zanno, S.D. Sampson, J.M. Clark, and D.D. Deblieux. 2005. A primitive therizinosauroid dinosaur from the Early Cretaceous of Utah. Nature 435: 84–87.

Knoll, F., and D. Schwarz-Wings. 2009. Palaeoneuroanatomy of *Brachiosaurus*. Annales de Paléontologie 95: 165–175.

Kobayashi, Y., and R. Barsbold. 2005. Reexamination of a primitive ornithomimosaur, *Garudimimus brevipes* Barsbold, 1981 (Dinosauria: Theropoda), from the Late Cretaceous of Mongolia. Canadian Journal of Earth Sciences 42: 1501–1521.

Kurzanov, S.M. 1976. Braincase structure in the carnosaur *Itemirus* n. gen. and some aspects of the cranial anatomy of dinosaurs. Paleontologicheski Zhurnal 1976: 127–137. [in Russian]

Larsson, H.C.E., P.C. Sereno, and J.A. Wilson. 2000. Forebrain enlargement among nonavian theropod dinosaurs. Journal of Vertebrate Paleontology 20: 615–618.

Larsson, H.C.E. 2001. Endocranial anatomy of *Carcharodontosaurus saharicus* (Theropoda: Allosauroidea) and its implications for theropod brain evolution. *In* D.H. Tanke and K. Carpenter (editors), Mesozoic vertebrate life, 19–33. Bloomington: Indiana University Press.

Li, D., M.A. Norell, K.-Q. Gao, N.D. Smith, and P.J. Makovicky. 2010. A longirostrine tyrannosauroid from the Early Cretaceous of China. Proceedings of the Royal Society of London B Biological Sciences 277: 183–190.

Madsen, J.H., Jr. 1976. *Allosaurus fragilis*: a revised osteology. Utah Geological and Mineral Survey Bulletin 109: 1–163.

Madsen, J.H., Jr, and S.P. Welles. 2000. *Ceratosaurus* (Dinosauria, Theropoda) a revised osteology. Utah Geological Survey, Miscellaneous Publication 00-2: 1–80.

Makovicky, P.J., and M.A. Norell. 1998. A partial ornithomimid braincase from Ukhaa Tolgod (Upper Cretaceous, Mongolia). American Museum Novitates 3247: 1–16.

Makovicky, P.J., M.A. Norell, J.M. Clark, and T. Rowe. 2003. Osteology and relationships of *Byronosaurus jaffei* (Theropoda: Troodontidae). American Museum Novitates 3402: 1–32.

Manley, G.A., and C. Köppl. 1998. Phylogenetic development of the cochlea and its innervation. Current Opinion in Neurobiology 8: 468–474.

Molnar, R.E. 1991. The cranial morphology of *Tyrannosaurus rex*. Paleontographica Abteilung A 217: 137–176.

Nesbitt, S.J., et al. 2009. A complete skeleton of a late Triassic saurischian and the early evolution of dinosaurs. Science 326: 1530–1533.

Norell, M.A., et al. 2004. The braincase of *Velociraptor*. *In* P.J. Currie, E.B. Koppelhus, M.A. Shugar, and J.L. Wright (editors), Feathered dragons: studies on the transition from dinosaurs to birds: 133–143. Bloomington: Indiana University Press.

Norell, M.A., et al. 2006. A new dromaeosaurid theropod from Ukhaa Tolgod (Ömnögov, Mongolia). Amerian Museum Novitates 3545: 1–51.

Norell, M.J., et al. 2009. A review of the Mongolian Cretaceous dinosaur *Saurornithoides* (Troodontidae: Theropoda). American Museum Novitates 3654: 1–63.

Osborn, H.F. 1912. Crania of *Tyrannosaurus* and *Allosaurus*. Memoirs of the American Museum of Natural History, New Series 1: 1–30.

Rauhut, O.W.M. 2003. The interrelationships and evolution of basal theropod dinosaurs. Palaeontological Association London, Special Papers in Palaeontology 69: 1–213.

Rauhut, O.W.M. 2004. Braincase structure of the middle Jurassic theropod dinosaur *Piatnitzkysaurus*. Canadian Journal of Earth Sciences 41: 1109–1122.

Rauhut, O.W.M., A.C. Milner, and S. Moore-Fay. 2010. Cranial osteology and phylogenetic position of the theropod dinosaur *Proceratosaurus bradleyi* (Woodward, 1910) from the middle Jurassic of England. Zoological Journal of the Linnean Society 158: 155–195.

Rieppel, O. 1985. The recessus scalae tympani and its bearing on the classification of reptiles. Journal of Herpetology 19: 373–384.

Russell, D.A. 1970. Tyrannosaurs from the Late Cretaceous of western Canada. National Museum of Natural Sciences Publications in Palaeontology 1: 1–34.

Sampson, S.D., and L.M. Witmer. 2007. Craniofacial anatomy of *Majungasaurus crenatissimus* (Theropoda: Abelisauridae) from the Late Cretaceous of Madagascar. *In* S.D. Sampson and D.W. Krause (editors), *Majungasaurus crenatissimus* (Theropoda: Abelisauridae) from the Late Cretaceous of Madagascar. Society of Vertebrate Paleontology Memoir 8: 225–253.

Saveliev, S.V., and V.R. Alifanov. 2007. A new study of the brain of the predatory dinosaur *Tarbosaurus bataar* (Theropoda, Tyrannosauridae). Paleontological Journal 41: 281–289.

Sedlmayer, J.C. 2002. Anatomy, evolution, and functional significance of cephalic vasculature in Archosauria. Ph.D. dissertation, Ohio University, Athens, Ohio. 398 pp.

Sereno, P.C., and S.L. Brusatte. 2008. Basal abelisaurid and carcharodontosaurid theropods from the Lower Cretaceous Elrhaz Formation of Niger. Acta Palaeontologica Polonica 53: 15–46.

Sereno, P.C., et al. 2009. Tyrannosaurid skeletal design first evolved at small body size. Science 326: 418–422.

Snively, E., and A.P. Russell. 2007. Functional variation of neck muscles and their relation to feeding style in Tyrannosauridae and other large theropod dinosaurs. Anatomical Record 290: 934–957.

Sues, H.-D. 1997. On *Chirostenotes*, a Late Cretaceous oviraptorosaur (Dinosauria: Theropoda) from western North America. Journal of Vertebrate Paleontology 17: 698–716.

Sues, H.-D., E. Frey, D.M. Martill, and D.M. Scott. 2002. *Irritator challengeri*, a spinosaurid (Dinosauria: Theropoda) from the lower Cretaceous of Brazil. Journal of Vertebrate Paleontology 22: 535–547.

Tahara, R., and H.C.E. Larsson. 2011. Cranial pneumatic anatomy of *Ornithomimus edmontonicus* (Ornithomimidae: Theropoda). Journal of Vertebrate Paleontology 31: 127–143.

Tsuihiji, T., et al. 2011. Cranial osteology of a juvenile specimen of *Tarbosaurus bataar* (Theropoda, Tyrannosauridae) from the Nemegt Formation (Upper Cretaceous) of Bugin Tsav, Mongolia. Journal of Vertebrate Paleontology 31: 497–517.

Walker, A.D. 1985. The braincase of *Archaeopteryx*. *In* M.K. Hecht, J.H. Ostrom, H. Viohl, and P. Wellnhofer (editors), The beginnings of birds: 123–134. Willibaldsburg: Freunde des Jura-Museums Eichstätt.

Walker, A.D. 1990. A revision of *Sphenosuchus acutus* Haughton, a crocodylomorph reptile from the Elliott Formation (late Triassic or early Jurassic) of South Africa. Philosophical Transactions of the Royal Society of London B Biological Sciences 330: 1–120.

Walsh, S.A., P.M. Barrett, A.C. Milner, G. Manley, and L.M. Witmer. 2009. Inner ear anatomy is a proxy for deducing auditory capability and behaviour in reptiles and birds. Proceedings of the Royal Society of London B Biological Sciences 276: 1355–1360.

Wever, E.G. 1978. The reptile ear, its structure and function. Princeton, NJ: Princeton University Press, 1024 pp.

Witmer, L.M. 1990. The craniofacial air sac system of Mesozoic birds (Aves). Zoological Journal of the Linnean Society 100: 327–378.

Witmer, L.M. 1997. Craniofacial air sinus systems. *In* P.J. Currie and K. Padian (editors), Encyclopedia of dinosaurs: 151–159. San Diego: Academic Press.

Witmer, L.M., and R.C. Ridgely. 2009. New insights into the brain, braincase, and ear region of tyrannosaurs (Dinosauria, Theropoda), with implications for sensory organization and behavior. Anatomical Record 292: 1266–1296.

Witmer, L.M., and R.C. Ridgely. 2010. The Cleveland tyrannosaur skull (*Nanotyrannus* or *Tyrannosaurus*): new findings based on CT scanning, with special reference to the braincase. Kirtlandia 57: 61–81.

Witmer, L.M., S. Chatterjee, J.W. Franzosa, and T.B. Rowe. 2003. Neuroanatomy of flying reptiles and implications for flight, posture and behavior. Nature 425: 950–953.

Xu, X., and X.-C. Wu. 2001. Cranial morphology of *Sinornithosaurus millenii* Xu et al. 1999 (Dinosauria: Theropoda: Dromaeosauridae) from the Yixian Formation of Liaoning, China. Canadian Journal of Earth Sciences 38: 1739–1752.

Xu, X., M.A. Norell, X.-L. Wang, P.J. Makovicky, and X.-C. Wu. 2002. A basal troodontid from the Early Cretaceous of China. Nature 415: 780–784.

Xu, X., et al. 2004. Basal tyrannosauroids from China and evidence for protofeathers in tyrannosauroids. Nature 431: 680–684.

Xu, X., et al. 2006. A basal tyrannosauroid dinosaur from the Late Jurassic of China. Nature 439: 715–718.

Zelenitsky, D.K., F. Therrien, and Y. Kobayashi. 2009. Olfactory acuity in theropods: palaeobiological and evolutionary implications. Proceedings of the Royal Society of London B Biological Sciences 276: 667–673.

APPENDIX 1

Anatomical Abbreviations

ai	atlantal intercentrum
aoc	antotic crest
bo	basioccipital
bpp	basipterygoid process
bpr	basipterygoid recess and cavity (rostral portion of basisphenoid recess)
bs	parabasisphenoid
bsr	basisphenoid recess and cavity (here refers only to caudal portion of basisphenoid recess)
bt	basal tubera
ccr	crista cranii
ch	cerebral hemisphere
chc	cochlear canal
cm	cavum metoticum
cmv	caudal middle cerebral vein canal
cp	cultriform process (parabasisphenoid)
cpp	caudal process of prootic
crc	common crus
csc	caudal semicircular canal
ct	crista tuberalis (otoccipital)
cto	caudal tympanic recess and cavity, within supraoccipital
ctp	caudal tympanic recess and cavity, within paroccipital process
ctra	bony aperture of caudal tympanic recess
cvl	crista ventrolateralis, connecting basipterygoid process with basal tubera
dc	depressed center of supraoccipital
dp	dorsal peak (dural sinus)
ec	endocranial cavity
epf	fossa housing articulation with epipterygoid
fA	fenestra A of rostral tympanic recess
faf	facioacoustic fossa
fB	fenestra B of rostral tympanic recess
fC	fenestra C of rostral tympanic recess
fl	floccular canal
fm	foramen magnum
fpr	fenestra pseudorotunda
fr	frontal
fr/pa	frontoparietal suture
fv	fenestra vestibule
ibtl	interbasipterygoidal lamina, running between basipterygoid processes
ie	inner ear cavities
itl	intertuberal lamina, running between basal tubera
lb	left bifurcation of supraoccipital
lcs	articulation surface with lacrimal
ls	laterosphenoid
lsc	lateral semicircular canal
mcm	medial aperture of cavum metoticum
nc	nuchal crest (parietal)
nco	nasal cavity (olfactory region)
occ	occipital condyle
ocv	orbitocerebral vein canal
ol	optic lobe
or	otic recess
orb	orbit
os	orbitosphenoid
osc	otosphenoidal crest
ot	otoccipital
pa	parietal
pa/pr	parietoprootic suture
pcf	paracondylar fossa
pf	prefrontal
pl	perilymphatic canal
pop	paroccipital process
pos	articulation surface with postorbital
pp	preotic pendant
pr	prootic
prf	prootic fossa housing external openings of $V_{2/3}$ and VII_{pal}
ptf	pituitary fossa
rb	right bifurcation of supraoccipital
rmv	rostral middle cerebral vein canal
rsc	rostral semicircular canal
rst	recessus scalae tympani
rtr	rostral tympanic recess and cavity
sc	sagittal crest
sco	sagittal crest on occipital surface
scr	subcondylar recess and cavity
sl	superficial lamina of prootic
so	supraoccipital
sq	squamosal
ssr	subsellar recess and cavity
st	stapes
ts	transverse sinus
ve	vestibule of inner ear
vs	vascular structure
I (b)	olfactory bulb fossa

I (t)	olfactory tract cavity
II	optic canal
III	oculomotor canal
IV	trochlear canal
V_1	ophthalmic ramus of trigeminal canal
$V_{2/3}$	maxillomandibular ramus of trigeminal canal
VI	abducens canal
VII	facial canals
VIII	vestibulocochlear canal
X	vagal canal
XII	hypoglossal canal

Institutional Abbreviations

AMNH FARB	American Museum of Natural History Fossil Fishes, Amphibians, Reptiles, and Birds, New York, New York
BYU	Brigham Young University, Earth Science Museum, Provo, Utah
CMN	Canadian Museum of Nature, Ottawa
CMNH	Cleveland Museum of Natural History, Cleveland, Ohio
DDM	Dinosaur Discovery Museum, Kenosha, Wisconsin
FMNH PR	Field Museum of Natural History, Chicago, Illinois
IGM	Institute of Geology, Mongolian Academy of Sciences, Ulaan Baator
IVPP	Institute of Vertebrate Paleontology and Paleoanthropology, Beijing, China
LH	Long Hao Institute of Geology and Paleontology, Hohot, Inner Mongolia, China
MOR	Museum of the Rockies, Bozeman, Montana
MPC-D	Mongolian Paleontological Center, Ulaan Baator
NHMUK	Natural History Museum, London
NMMNH	New Mexico Museum of Natural History, Albuquerque, New Mexico
PIN	Paleontological Institute, Russian Academy of Sciences, Moscow
ROM	Royal Ontario Museum, Toronto
RSM	Royal Saskatchewan, Regina, Canada
TMP	Tyrell Museum of Paleontology, Drumheller, Canada
UMNH	Utah Museum of Natural History, Salt Lake City
ZPAL	Institute of Paleobiology, Polish Academy of Sciences, Warsaw